SESM 16-02

Damage and Restoration of Water Supply Systems in an Earthquake Sequence

By

Keith A. Porter

July 2016

Abstract

Damage to potable water supply systems profoundly affects society after earthquakes. For at least 25 years, engineers have performed computerized risk analyses of earthquake damage to water-supply systems to estimate earthquake damage and restoration. A new stochastic simulation model is offered here that employs a fairly traditional loss-estimation approach, but proposes to extend the state of the art in three notable ways: (1) It deals with lifeline interaction by directly modeling how individual repairs are slowed by limitations in so-called upstream lifelines and other prerequisites. (2) It quantifies damage and restoration over the entire earthquake sequence, i.e., considering damage in the mainshock, aftershocks, and afterslip. (3) It offers an empirical model of service restoration as a function of the number of pipeline repairs performed (as opposed to more rigorous, but computationally demanding, hydraulic analysis). A fourth novelty is that it offers a procedure to adjust Hazus-MH estimates of restoration to account for an earthquake sequence, lifeline interaction, and corrects for Hazus' default assumptions about the number of available repair crews.

The model is exercised on two Bay Area water supply systems subjected to a hypothetical but highly realistic earthquake sequence initiating with a M_w 7.0 mainshock on the Hayward Fault in the eastern San Francisco Bay Area, plus 16 aftershocks of M 5 or greater, occurring over 17 months after the mainshock. The model quantifies system damage, recovery, delays due to fuel and other lifeline limitations, and setbacks in restoration because of aftershocks. It estimates the benefit of a fuel-management plan and an accelerated pipe-replacement plan, in terms of accelerated restoration of service. The model is validated several ways for each of the two case-study water supply systems and seems reasonable. One water utility anticipates using it to target vulnerable segments of its system for accelerated pipe replacement.

Acknowledgments

Contents

Index of Figures

Index of Tables

1. Introduction

1.1 How water supply is important in an earthquake

People need potable water for daily life, businesses need water for air conditioning, and water is an input to many natural and manufactured products and processes. Damage to the water supply system can contribute greatly to the life-safety and economic consequences of an earthquake, as illustrated by the economic analyses performed for the 2008 ShakeOut scenario (Rose et al. 2011). In that study, the authors found that water supply interruption in a hypothetical M 7.8 earthquake on the Southern San Andreas Fault could realistically result in $24 billion in business interruption losses, a figure that represents more than one third of the $68 billion in total business interruption losses and 13% of the total of property damage plus business interruption. A potable water supply is crucial to carrying on life in residences, businesses, government, hospitals, and other critical care facilities. Long aware of the importance of water supply and the potential for earthquakes to interrupt water supply, earthquake experts recommend that homes and businesses have enough water to provide for one gallon per person, per day after a major earthquake to last at least 3 days and ideally for 2 weeks.

Loss of water supply in that hypothetical earthquake would also contribute substantially to the fire damage to property, which itself could realistically account for $65 billion of the $113 billion in property losses (Scawthorn 2008). The ShakeOut scenario is not a worst-case earthquake: the rupture it deals with has a mean recurrence interval of 150 years, and it has been 300 years since the last rupture. Furthermore, the fire simulation assumes mild winds rather than the fast, hot, dry, Santa Anas that commonly blow in the fall and notoriously fan wildfires.

These earlier estimates, while particular to the ShakeOut, reflect a general truth: earthquake damage to water supply systems in the United States (and elsewhere) threaten the health, safety, and welfare of the population, possibly more than earthquake damage to any other utility or other element of the built environment in part because repairs are so costly and time consuming. More narrowly, earthquakes pose a nearly existential financial threat to any water supply utility in a seismically active region. If a utility cannot deliver water it cannot collect revenues, which can threaten its ability to make payroll. Every water utility in earthquake country may be at risk.

The Hayward Fault earthquake sequence scenario examines among other things the potential for damage to water supply systems in the San Francisco Bay Area from a large, but not exceedingly rare, M 7.05 earthquake on the Hayward Fault in the eastern Bay Area. Earthquakes damage water supply systems and the damage causes other problems, such as for firefighting. The 1906 San Francisco earthquake damaged so much of that city's potable water supply system that pressure dropped too low for firefighters to fight the fires that eventually destroyed much of the city. The moment-magnitude (M_w) 6.9 1989 Loma Prieta earthquake caused at least 761 breaks to water mains and services in pipelines of various materials (Lund and Schiff 1991). The loss of firefighting water supply in the San Francisco Marina District contributed to the fire that damaged seven structures, destroying four buildings containing 33 apartments and flats (Scawthorn et al. 1991). Cast iron, steel, ductile iron, plastic and copper pipes all broke both within and outside areas of liquefaction and other ground failure. The M_w 6.0 2014 South Napa earthquake caused 163 pipeline breaks in the City of Napa (SPA Risk LLC 2014).

The largest total number of breaks and the highest break rate (breaks per mile) in the 1989 earthquake occurred in cast iron pipe subjected to liquefaction-induced ground failure, but other materials also broke, including ductile iron, PVC, and steel. Pipe broke in 1989 in places that were not known to have experienced ground failure, so that damage has been attributed to ground strain associated with wave passage, especially Rayleigh surface waves. There was no observed liquefaction damage to buried pipeline in Napa in the 2014 earthquake, reinforcing the idea that wave passage alone can damage buried pipe. Even the modest M_w 4.0 Piedmont, California earthquake of 17 Aug 2015 caused 9 breaks to buried cast iron water supply pipe in the San Francisco East Bay (Bay City News 18 Aug 2015).

Repairs to an earthquake-damaged water supply system can take months or more. Each break can take as little as two hours to repair, but large numbers of breaks and larger pipes can take much longer. The 30-inch water main that broke near the UCLA campus at 3:30 PM on Tuesday July 29, 2014, took almost 5 days, until 11:00 AM Sunday, August 3 to repair (LADWP 2014). During an earthquake sequence, with many simultaneous breaks, repairs take longer for many reasons. Some of these are:

1. When a pressure zone loses pressure because of many breaks, it can be necessary to repair breaks closer to the source (i.e., nearer the tank, reservoir, etc.) before one discovers breaks farther from the source.
2. Similarly, it may be necessary to repair damage to a pumping plant, reservoir, or regulator before damage in the downstream pipeline network can be addressed.
3. Water districts have an upper limit to their ability to field and manage multiple repair crews operating in parallel, even when the crews are from outside contractors or from water districts that provide mutual aid.
4. Limited supplies of repair resources such as spare pipe, clamps, fuel, and repair crews.
5. Damage to other systems—electrical and gas, for example—can hinder pipeline repair, and in some cases those repairs can cause pipeline damage. Coordination with other agencies can conceivably idle repair crews.
6. Aftershocks can hinder repair efforts because they pose an ongoing safety threat to repair crews. They can also cause new damage or aggravate earlier breaks.

1.2 Study objectives

In this work, I attempt to depict a realistic outcome of the damage and restoration of water supply in the Hayward Fault earthquake sequence. I review available models of earthquake-induced pipeline damage and repair, propose one for use in the scenario earthquake sequence, and apply it to the water supply systems of the San Jose Water Company and the East Bay Municipal Utility District. These two systems were chosen because they are strongly shaken, are affected by the mainshock and by aftershocks, and were willing to share their system maps. The maps were shared under strict requirements of confidentiality, so map details are not available here.

This study supplements conventional loss estimation by examining the detailed activities involved in discovering and repairing water pipeline damage. It identifies steps in the repair process that

rely on other lifelines, to inform a new model of the effects of lifeline interaction to delay water service repairs and restoration.

This study focuses on damage and repair of buried water pipe, which tends to dominate the effort to restore water supply. It considers damage resulting from wave passage, liquefaction, landsliding, and fault offset. It ignores earthquake damage to other elements in the water-supply system, including raw water aqueducts, tanks, tunnels, canals, valves, and reservoirs. The decision to focus this study on buried pipelines without including other critical facilities such as tanks, reservoirs, tunnels, etc., seems reasonable, since a majority of water utilities have implemented seismic improvement programs (SIP) that, for the most part, focused on seismically retrofitting their tanks, reservoirs, etc. but not their old distribution pipelines. As such, old distribution pipelines, as an asset class, present the most significant seismic vulnerability for most water utilities, since for the most part smaller diameter distribution mains were not replaced with seismic-resistant mains because it simply wasn't economically feasible to replace them all as part of a SIP.

This study does not address restoration of water utilities' customer base or the change in demand for water as homes and businesses relocate because of building damage or other reasons.

1.3 Organization of report

This section has summarized the nature of the problem and presented the study objectives. Section 2 presents relevant literature. The methodology and rationale for its selection are presented in Section 3. Section 4 presents a case study using the San Jose Water Company's water supply buried pipeline system. Section 5 presents a second case study of the East Bay Municipal Utility District's water supply buried pipeline system. Section 6 presents a simplified analysis that adjusts a Hazus-MH-based analysis of water supply damage and restoration to account for lifeline interaction and the earthquake sequence, and corrects the analysis for Hazus-MH's default assumptions about available water-supply repair crews. Section 7 contains conclusions about water supply damage and restoration. Section 8 contains references cited.

2. Literature review

2.1 A panel approach to estimating water supply impacts

Before proposing a model to estimate water-supply pipeline restoration considering an earthquake sequence and lifeline interaction, let us first consider some key aspects of prior art. The ShakeOut Scenario (Jones et al. 2008) assessed earth-science impacts, physical damage, and socioeconomic impacts of a hypothetical M7.8 southern San Andreas Fault earthquake. Among many detailed studies were special studies of 12 lifelines, 7 of which were performed by panels of employees of the utilities at risk. The panel process is described in detail in Porter and Sherrill (2011). Briefly, panels meet for several hours (generally 4 hours in the case of ShakeOut). Panelists are presented with the scenario's earth science impacts and previously estimated damage to supposedly upstream lifelines—lifelines whose damage would seem to affect the damage or repair to the lifeline in question, but not vice versa. They then hypothesize a realistic outcome of the earthquake on damage and service restoration, identifying research needs and mitigation options. Panels' discussion and initial findings are documented in brief memos, which are then circulated to the

panelists. Panelists are asked to review the memos and asked to reconsider lifeline interaction in light of damage to supposedly downstream lifelines as well as upstream ones. The process iterates until panelists are satisfied with their estimates of damage and restoration. In practice in ShakeOut and ARkStorm, only one iteration was used and only two or so panelists from each panel actually reviewed and revised the write-ups. However, the panel process worked reasonably well. Panelists were well qualified and seemed to fairly assess realistic earthquake impacts and restoration. They gained insight into lifeline interaction, mutual-aid needs, communication capabilities, and backup supplies.

Figure 1 presents the restoration timeline that the water-supply panel estimated for strongly shaken (MMI VIII+) geographic areas. See Porter and Sherrill (2011) for electric power restoration curves in ShakeOut and Porter et al. (2010) for various restoration curves and modes of lifeline interaction in the ARkStorm scenario.
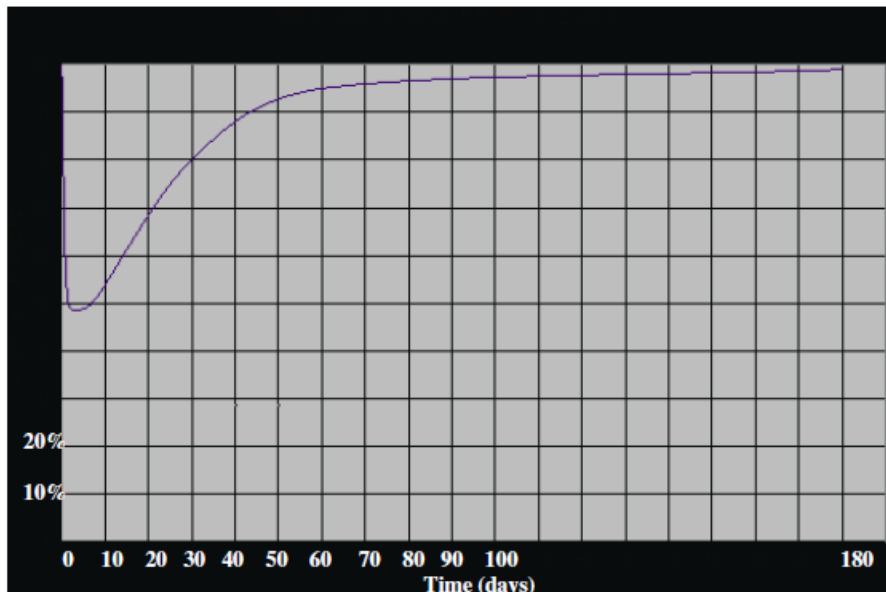
Figure 1. ShakeOut water restoration in MMI VIII or higher, where the vertical axis denotes fraction of customers receiving service (Jones et al. 2008)

2.2 Analytical approaches to estimating water supply impacts

Analytical approaches to estimating water supply impacts typically involve acquiring a map of the system, identifying component materials and sizes, associating each with one or more vulnerability functions or fragility functions (depending on the desired output), estimating ground motion and ground failure severity in one or more scenarios, estimating mean damage and sometimes uncertainty in damage with reference to the vulnerability functions, and sometimes estimating repair costs and duration of loss of function.

FEMA 224 (1991), Scawthorn et al. (1992), Hazus-MH (NIBS and FEMA 2012), MAEViz (Mid-America Earthquake Center 2006), and Marconi (Prashar et al. 2012) all use such an approach. The last three implement their methodologies in software, as do many others. In the case of Hazus-MH, the software assumes that a water main exists under each street, and that 80% of pipes are

brittle (such as cast iron) and 20% are ductile (such as ductile iron). MAEViz and Marconi allow the user to specify the location and characteristics of each pipe segment. Neither Hazus-MH, MAEViz, nor Marconi performs hydraulic analysis. MAEViz and Marconi estimate damage. Hazus-MH estimates damage and estimates repair costs and system restoration time using methods described later.

Khater and Grigoriu (1989) describe an analytical model of water supply damage and serviceability that does perform hydraulic analysis. Coded in software called GISALLE, it involves three tasks: (i) generate damage states for water system components consistent with the seismic intensity at the site; (ii) perform hydraulic analysis for simulated damage state of the system; and (iii) develop statistics on the available flow for postulated levels of seismic intensity.

Some of the available software such as MAEViz and UILLIS (Javanbarg and Scawthorn 2012) have the ability to treat lifeline interaction: how damage or loss of function in one lifeline system affect the functionality or restoration of another. For example, loss of power and limitations in fuel supply can affect the functionality of a water supply system or delay repairs. These programs use a system-of-systems approach to modeling the lifelines. That is, they model two or more lifelines in the same framework, relating the condition of an element of one lifeline to the condition of an element in another.

2.3 Damageability of buried pipe

2.3.1 Vulnerability and fragility functions

There is a very large body of literature on the damageability of buried pipe, only some of which is presented here. As used here, a vulnerability function relates the degree of damage, in this case, number of breaks per unit length of pipeline, as a function of the degree of environmental excitation such as peak ground velocity. A fragility function by contrast measures the probability of reaching or exceeding some undesirable state conditioned on the degree of environmental excitation. The terminology is not universal but will be consistently applied here.

In the present context, vulnerability functions are most useful for estimating the number of breaks in a pipeline network subjected to ground shaking (usually referred to as wave passage in the pipeline literature), landsliding, and liquefaction. But at a fault crossing, a fragility function is more useful: here, we are interested in the probability that a pipeline requires repair at the point where it crosses the fault, as a function of the fault offset and possibly as a function of the angle at which the pipeline crosses the fault. Both vulnerability functions and fragility functions are commonly conditioned on the pipeline's engineering attributes, such as material, diameter, connections at joints, and sometimes soil conditions.

2.3.2 Hazus-MH, M. O'Rourke and Ayala (1993), and Honneger and Eguchi (1992)

Hazus-MH (2012) currently uses a vulnerability function for pipeline subjected to wave passage by O'Rourke and Ayala (1993) and one for pipe in liquefied soil from Honegger and Eguchi (1992). The median rates of repairs per km of pipeline for these two relationships are given by Equations (1) and (2) respectively.

$$\hat{R} = 0.0001 \cdot K \cdot PGV^{2.25} \tag{1}$$

$$\bar{R} = P_L \cdot K \cdot PGD^{0.56} \tag{2}$$

where P_L denotes the probability of liquefaction, $K = 1.0$ for asbestos cement, concrete, and cast iron pipe, $K = 0.3$ for steel, ductile iron, and PVC, PGV denotes peak ground velocity measured in cm/sec, and PGD denotes permanent ground deformation—the absolute distance a point on the ground permanently moves due landsliding, fault offset, or liquefaction-induced ground failure—measured in inches. Equation (1) draws on a number of observed breaks in asbestos cement, concrete, cast iron, and prestressed concrete pipe in four US and two Mexican earthquakes, with diameters between 3 and 72 inches, experiencing ground motion up to 50 cm/sec of peak ground velocity. (The authors do not publish the number of breaks or the lengths of pipe.) Its data implies a coefficient of variation in the ratio of observed to estimated break rate of 0.76, and a ratio of mean repair rate to median repair rate of 1.22.

The work by Honneger and Eguchi reflects an unknown quantity of pipe and number of breaks. Their data mostly come from four earthquakes: 1923 Kanto (Japan), 1971 San Fernando, 1976 Tangshan (China), and 1985 Michaocan (Mexico). Pipe diameters range from 4 inches to 48 inches. Materials included cast iron, concrete, precast concrete, and steel.

2.3.3 Eidinger (2001)

More recently, Eidinger (2001) proposed two vulnerability functions: one for wave passage (i.e., ground shaking absent liquefaction) and one for permanent ground deformation (i.e., in the presence of liquefaction or landslide-induced ground displacement). Equations (3) and (5) present Eidinger's recommended vulnerability functions.

In the equations, $R_w(PGV,p)$ and $R_l(PGD,p)$ denote repair rate per 1000 linear feet of pipe associated with nonexceedance probability p, as a result of wave passage and liquefaction respectively. For example, the median repair rate is estimated using $p = 0.5$. PGV refers to geometric mean horizontal peak ground velocity in inches per second, PGD denotes permanent ground displacement relative to pre-earthquake location, measured in inches, and $\Phi^{-1}(p)$ denotes the inverse standard normal cumulative distribution function evaluated at p.

For the reader who is unfamiliar with probability distributions, the standard normal distribution is the familiar bell-shaped curve that represents how likely are various possible values of an uncertain quantity. Uncertain or random variables can take on a variety of probability distributions; the normal distribution is one of many. It has a peak (the expected or mean value and also the value with 50% probability of not being exceeded, called the median) at 0. Its standard deviation (a measure of how wide the bell is, and therefore how uncertain is the random quantity) is 1.0. Its cumulative distribution function is an S-shaped curve that tells the probability that a sample of a quantity with a standard normal distribution takes on a value less than or equal to any given quantity between $-\infty$ and ∞. The inverse of the standard normal cumulative distribution function is the value of the uncertain quantity that has a specified probability of not being exceeded. Most statistics textbooks provide more information about probability distributions; see for example Ang and Tang (1975) or Benjamin and Cornell

The quantities K_1 and K_2 are factors to account for pipe material, joints, soil corrosivity, and pipe diameter: either small (4 to 12 in diameter) or large (16 inch diameter or greater). See Table 1 for their values. Eidinger (2001) does not provide values for some combinations so they appear blank in the table. The authors acknowledge that permanent ground displacement produces break rates two orders of magnitude greater than wave passage, and that break rate in failed ground is fairly insensitive to PGD.

The terms $\exp(\beta \cdot \Phi^{-1}(p))$ in equations (3) and (5) reflect that the equations treat the repair rate as uncertain and lognormally distributed conditioned on the value of PGV or PGD. (Lognormal is like normal, except that the natural logarithm of the uncertain quantity in question is normally distributed. A lognormal variable can take on any positive value, but not zero or a negative number. Its peak—its most likely value—is the same as its median value, and the bell shape is skewed to the right.) Setting p to 0.5 sets the exp term to 1.0 and makes $R(p)$ produce the median (not the mean) break rate. The mean break rate would be substantially higher than the median. Equations (4) and (6) provide the mean (average) break rate, given Eidinger's values of β shown in Equations (3) and (5) and Eidinger's assumption of lognormality. The interested reader who is unfamiliar with lognormally distributed variables can refer to any of several common textbooks, e.g., Ang and Tang (1975). The interested reader who is unfamiliar with vulnerability functions can refer to Porter (2015) for a short primer.

Equation (3) gives Eidinger's (2001) vulnerability function for wave passage, drawn from 81 sources reporting 3350 repairs recorded in 12 earthquakes. The plurality of data come from the 1994 Northridge earthquake. The data reflect 38 data points regarding damage to cast iron, 13 to steel, 10 to asbestos cement, 9 to ductile iron and 2 to concrete. Data reflect PGV values between 2 and 52 cm/sec.

$$R_w\left(PGV, p\right) = K_1 \cdot 0.00187 \cdot PGV \cdot \exp\left(1.15 \cdot \Phi^{-1}\left(p\right)\right) \tag{3}$$

$$\bar{R}_w\left(PGV\right) = K_1 \cdot 0.003623 \cdot PGV \tag{4}$$

Equation (5) gives Eidinger's (2001) vulnerability function for permanent ground deformation, drawn from 42 data points from 4 earthquakes between the 1906 San Francisco earthquake and the 1989 Loma Prieta earthquake. The plurality of data points come from the 1983 Nihonkai-Chubu earthquake. The plurality of pipe material is asbestos cement (20 data points) followed by cast iron (17 data points), and a mixture of cast iron and steel—presumably meaning that the material was one or the other, but it is not known which (5 data points). None of the data appear to reflect ductile iron. They reflect PGD values between 0 and 110 inches.

$$R_l\left(PGD, p\right) = K_2 \cdot 1.06 \cdot PGD^{0.319} \cdot \exp\left(0.74 \cdot \Phi^{-1}\left(p\right)\right) \tag{5}$$

$$\bar{R}_l\left(PGD\right) = K_2 \cdot 1.39 \cdot PGD^{0.319} \tag{6}$$

Table 1. Eidinger (2001) pipe vulnerability factors K₁ and K₂

ID	Pipe material	Joint type	Soils	Diam.	K₁	K₂
1	Cast iron	Cement	All	Small	1.0	1.0
2	Cast iron	Cement	Corrosive	Small	1.4	1.0
3	Cast iron	Cement	Non-corrosive	Small	0.7	1.0
4	Cast iron	Rubber gasket	All	Small	0.8	0.8
5	Cast iron	Mechanical restrained	All	Small	*0.7¹*	0.7
6	Welded steel	Lap arc welded	All	Small	0.6	0.15
7	Welded steel	Lap arc welded	Corrosive	Small	0.9	0.15
8	Welded steel	Lap arc welded	Non-corrosive	Small	0.3	0.15
9	Welded steel	Lap arc welded	All	Large	0.15	0.15
10	Welded steel	Rubber gasket	All	Small	0.7	0.7
11	Welded steel	Screwed	All	Small	1.3	*1.3¹*
12	Welded steel	Riveted	All	Small	1.3	*1.3¹*
13	Asbestos cement	Rubber gasket	All	Small	0.5	0.8
14	Asbestos cement	Cement	All	Small	1.0	1.0
15	Concrete w stl cyl.	Lap arc weld	All	Large	0.7	0.6
16	Concrete w stl cyl.	Cement	All	Large	1.0	1.0
17	Concrete w stl cyl.	Rubber gasket	All	Large	0.8	0.7
18	PVC	Rubber gasket	All	Small	0.5	0.8
19	Ductile iron	Rubber gasket	All	Small	0.5	0.5

¹ Assumed here because no K-value is offered by the source

Eidinger (2001) also proposed models for damage to pipe that crosses a fault, one for continuous pipelines, Equation (6), and one for segmented pipe, Equation (6). In the equations, PGD denotes mean offset (in inches) over the entire length of the fault, presumably at the fault trace rather than averaged over the area of the fault, and presumably considering coseismic slip and afterslip.

$$\bar{P} = 0.70 \cdot \frac{PGD}{60\,in}$$

$$\leq 0.95$$

(6)

$$\bar{P} = 0 \qquad PGD < 1\,in$$
$$= 0.5 \qquad 1\,in \leq PGD \leq 12\,in$$
$$= 0.8 \qquad 12\,in < PGD \leq 24\,in$$
$$= 0.95 \qquad 24\,in < PGD$$

(6)

2.3.4 T. O'Rourke et al. (2014)

O'Rourke et al. (2014) offer vulnerability functions for the median repair rate per km of asbestos cement or cast iron pipes subjected to wave passage. They draw on data about 2051 repairs in 3400 km of pipe in the 22 Feb 2011 Christchurch earthquake and the 13 Jun 2011 Christchurch earthquake. The majority of pipe length in the database was asbestos cement, but the data also included cast iron, PVC, modified PVC, and unnamed other materials. The data were drawn from locations with PGV between 10 and 80 cm/sec. Their vulnerability functions are given by:

$$\log_{10}\left(R_{AC}\right) = 2.83 \cdot \log_{10}\left(GMPGV\right) - 5 \tag{7}$$

$$\log_{10}\left(R_{CI}\right) = 2.38 \cdot \log_{10}\left(GMPGV\right) - 4.52 \tag{8}$$

where R_{AC} denotes the median repairs per km of asbestos cement pipe, R_{CI} is the analogous value for cast iron pipe, and according to the authors, "GMPGV is the mean of the natural logs of the two maximum horizontal peak ground velocity (PGV) values taken from ground motion recordings available from GNS Science ... at each station." Despite that definition of GMPGV, the authors seem actually to mean the geometric mean of the peak ground velocity values in cm/sec of the two horizontal orthogonal components. (The inverse of the natural logarithm of the mean of the natural logarithms of two quantities equals their geometric mean.) They offer vulnerability functions for pipe subjected to liquefaction, where the ground deformation is measured in terms of (a) the larger principal component of ground strain in the horizontal plane, and (b) the rotation of the axis of the pipe about a horizontal axis normal to the axis of the pipe, which the authors call angular distortion—essentially a differential permanent vertical displacement of two points on the pipe axis, divided by the distance between the two points.

2.3.5 M. O'Rourke (2003)

There does not appear to exist any empirical relationship between fault offset and probability of pipeline damage. A few authors offer analytical formulations between offset and stress or strain in a pipeline that crosses the fault. O'Rourke (2003) summarizes some of these, considering under two conditions that depend on the geometry of the pipeline at the fault crossing: a combination of bending and axial tension, and a combination of bending and axial compression. For the former, he illustrates a relationship between tolerable fault offset as a function of distance between points at which the pipeline is anchored on either side of the fault (to which he refers as unanchor length in Figure 2A) and the angle β subtended by the fault and the pipeline, in which the offset puts the pipeline in tension. The figure is merely an illustration for a particular pipe material and diameter. He offers a second analytical relationship (Figure 2B) for segmented pipe subject to fault offset, again for fault-crossing geometry where offset puts the pipe into tension.
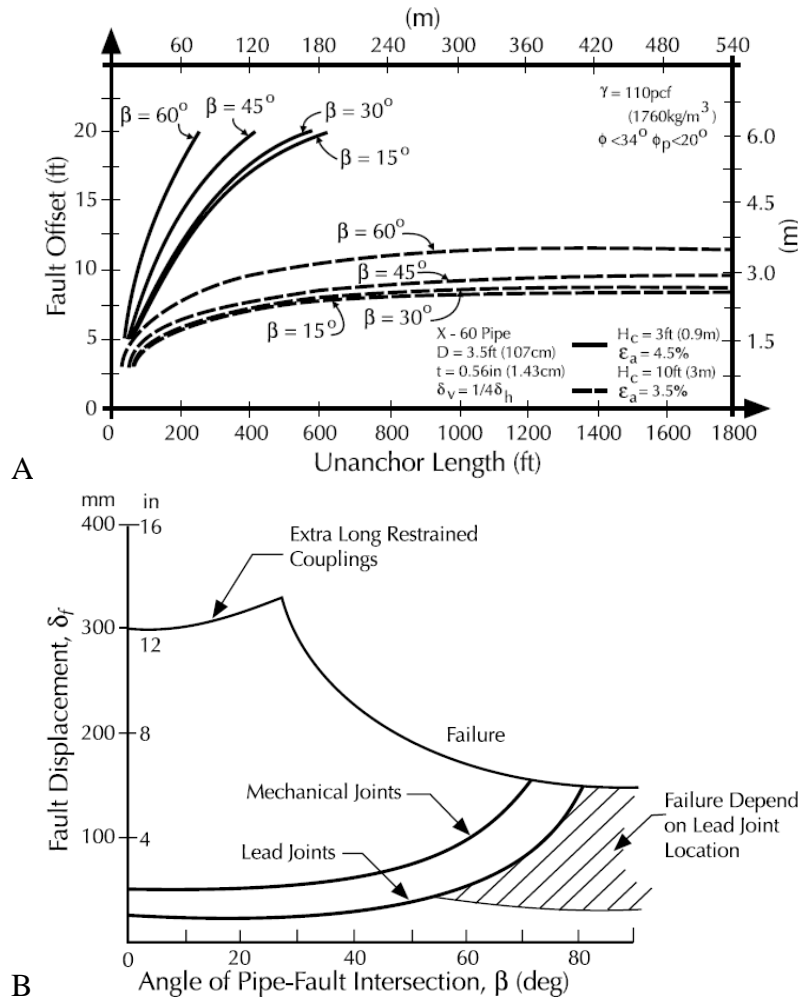
Figure 2. A. Tolerable fault offset vs. unanchor length in continuous pipe (O'Rourke 2003, citing Kennedy et al., 1977), and B. Tolerable fault offset versus pipe-fault intersection angle in segmented pipe (O'Rourke 2003, citing O'Rourke and Trautmann, 1981)

2.4 Tasks and methods to repair leaks and breaks

The city of Winnipeg (2014) offers a list of tasks to repair a water main break, written for the general public. The tasks are shown in chronological order in the left-hand column of Table 2. The task list is generally consistent with a more detailed checklist created by the American Water Works Association (2008) although it omits lists of tools, equipment, disinfecting chemicals, documentation, and testing materials. Column 2 of the table lists my interpretation of rate-limiting factors, that is, prerequisites for each task. The rate-limiting factors are mostly potential impacts from other lifelines, that is, lifeline interactions. If they are unavailable, repairs cannot proceed or they proceed more slowly—that is, their rate is limited. These items include communications, electricity, fuel, site safety (i.e., no fire or hazardous material release), roadway access, repair crews, and repair supplies (replacement pipe, replacement fittings, clamps, and paving materials). Regarding crew availability, public and private water agencies plan to provide mutual assistance for emergencies; see CalWARN (2008) for example. Crews may have to travel from great distances, hundreds of miles or more, so their availability can change over time. Table 2 probably omits tasks that are unnecessary or trivial for day-to-day repairs but become significant in a large

earthquake. For example, a water agency may also have to arrange repair contracts with contractors, track and prioritize repairs, and manage an unusually large number of repair crews operating simultaneously.

Table 2. Water pipeline repair tasks

Tasks	Rate-limiting factors
1. Receive a notice from our 311 Centre about a water main break.	Communications, electricity
2. Dispatch a crew to the location.	Fuel, site safety (e.g., no fire), roadway access, crew availability
3. Control the leak to reduce the risk to public safety, and private and public property. We do this by finding and closing valves.	
4. Contact other utilities to make sure that we can dig without damaging other services or endangering staff or the public.	Communications
5. Pinpoint the location of the leak using an electronic leak detector.	
6. Dig down to the water main and confirm the cause of the leak.	Fuel
7. Repair the water main. Depending on the type of break, we may apply a repair clamp or replace a length of pipe.	Pipe, fitting, or repair hardware such as clamps
8. Open valves to turn the water main back on, flush the water main and sample water quality.	
9. Backfill to temporarily restore the excavated area.	Fuel
10. Permanently restore the sod or pavement in the excavated area.	Pavement material

Lund and Schiff (1991) surveyed pipeline utilities, asking them to provide detailed information about each pipeline failure they repaired after the 1989 Loma Prieta earthquake. See Figure 3 for the survey instrument. The resulting database includes information about 862 pipeline failures among 65 water, sewer, drainage, and gas agencies. The data may be useful for estimating repair times, so I extracted the following statistics from the database.

- *Burial depth.* Among 67 records with reported burial depth, the average was 4.0 feet and the standard deviation was 2.2 ft.
- *Break or leak.* Among the failures where the respondent indicated whether the failure was a break or a leak, it was more common for the pipeline to break (336 failures) than to leak (140 failures).
- *Pipe failure modes.* Among pipe failures, the most common were circumferential cracks (99), followed by splits (43) and corrosion (33). Only one blowout was reported.
- *Joint failure modes.* Almost as common as pipe failures were joint failures: 102 pulled, 29 cracks at joints, 25 gasket failures, and 12 other joint failures.

- ***Fitting failure modes.*** There were a variety of fitting failures: 57 threaded couplings, 9 elbows, 6 offsets, 4 hydrants, 3 tees, and 45 miscellaneous other fitting failures.
- ***Repair methods.*** The most common repair method was to replace the damaged element (185 replacements), more than twice the number of clamps installed (77), followed by mechanical couplings (50), epoxy glue (16), and miscellaneous others such as flex couplings and pressure grout.

American Society of Civil Engineers
Technical Council on Lifeline Earthquake Engineering

Pipeline Damage Check Sheet

Location of Damage _____.

Pipe Description

Size _____, Thickness _____, Material _____, Lining _____,
       Coating _____, Date of Installation _____

Type of Joints _____, Burial Depth _____,
       Bedding Material _____,Type of Backfill _____

Ground Water Present _____, Depth to Water Surface _____

Damage

Impact on Flow: Break (flow disrupted) _____
                 or Leak (flow continued) _____

Pipe Failure: Circumferential (round crack) _____,
       Change in Pressure (blowout) _____, Longitudinal (split) _____,
       Corrosion _____, Other (describe)_____

Joint Failure: Cracked _____ Pulled ___, Compression ___, Gasket ___,
       Other (describe) _____

Fitting Failure: Elbow ___,Tee ___, Cross ___,Offset ___,Flange ___, Flange ___,
       Hydrant ___, Other (describe) _____

Repair Method: Repair Clamp ___, Butt Strap ___, Welded ___, Replaced pipe or
fitting ___, Other (describe) _____

Supervisor _____   Date _____

Comments _____
_____
_____

LL 8-8-90

Figure 3. Lund and Schiff (1991) pipeline damage survey instrument

2.5 Time to repair pipe leaks and breaks

To repair damaged water supply pipe, the repair crew must locate the damage, usually eliminate pressure in the pipe by closing an upstream valve, excavate the damaged element (usually with a backhoe), perform the repair, reopen the upstream valve, backfill the excavation, and repave any

driving surface over the location of the repair. Pipe damage can be repaired by replacing the damaged element, by welding over the crack, or by installing repair hardware: generally either a clamp that is mechanically secured over the damage or a closure ring called a butt strap that is welded to the outside of the pipe over the damage. The time required to perform the repair depends on several issues:

- How long it takes people to report the damage to the utility or otherwise for the utility to become aware of and locate the damage, which itself depends on power and communication;
- Site accessibility;
- Availability of crews and equipment;
- Availability of fuel and consumable repair material;
- Pipe burial depth;
- Groundwater presence and depth;
- Diameter, material, and jointing of the pipe;
- Impact on flow (break or leak);
- Nature of the damaged element: whether to pipe, joint, or fitting;
- If pipe, whether circumferential crack, longitudinal split, corrosion, etc.;
- If joint, whether a crack, pull-out, compression failure, gasket failure, etc.;
- If fitting, the nature of the fitting (elbow, tee, cross, offset, etc.);

Schiff (1988) offers repair times for 21 individual water pipe repairs after the 1987 Whittier Narrows earthquake, mostly of cracks and breaks in 4 to 8-inch steel and cast iron mains. Repair times were reported by the Whittier water distribution superintendent. Times varied between 1 and 16 hours, as shown in Table 3. Schiff reports that water pressure in Whittier dropped to 50 psi from the normal 80 to 100 psi as a result of 40 breaks in 133 miles of pipe (or 0.06 breaks per 1000 lf of pipe).

Table 3. Repair times for water supply pipeline damage in the 1987 Whittier Narrows Earthquake (Schiff 1988)

Ref.* No.	Location	Estimated Repair Time	Pipe Material & Diameter	Installa- tion Date	Type Failure and Comments
	Whittier (Sources: Manny Magana, Jim Johns via Craig Taylor)				
	MAIN SHOCK				
1	La Cuarta & Whittier Blvd	3-4 hrs.	4" CI	1920	Blow-Out -- 3'-4' Section
2	Citrus @ Beverly Dr.	16 (dn3-4 day)	6"	1932	Circum. Crack
3	11741 S. Circle Dr.	3-4	4" CI	1929	Circum. Crack
4	Bronte @ Bacon	4-5	6" CI	1956	Blow-Out -- Pressure Hole
5	Beverly Blvd(Citris& Pick.)	12	24" RC	1930	Beam Crack
6	Painter @Broadway	Leak surfaced from Painter and Beverly and again after the aftershock.			
7	Dorland @ Magnolia	5	6" CI	1938	Circum. Crack
8	Painter @ Sunset	1	3/4 "Steel	Old	
9	Greenleaf @ Orange Dr.	16	Leak surfaced likely from Orange & Friend (See No. 10)		
10	Orange @ Friends	16	16" RC	1930	Circum. Crack -- Leak entered aban doned, uncapped steel pipe
11	13502 Beverly Blvd.	4	6" CI	1927	Joint pullout -- Likely a flair joint
12	8041 Michigan	3-4	4" Steel	Very Old	Blowout Hole developed
13	12101 Rideout Way	2-3	2" Steel	Old	Blowout -- 2'-3' section service line
14	South Cirle @ North Cirle	4-6	6" CI	1929	Circum. Crack
15	Panorama above Orange Dr	20	24" RC	1967	Leaks at caulked collars
	AFTERSHOCK				
16	11630 Whittier	8	6" X 8" CI		Shear -- T sheared at flange
17	8053 Michigan	6 with #18	4" Steel	Very Old	Blow-out -- Hole a few Ft. away
18	Near #17	See #17	4" Steel	Very Old	Blow-Out Same as #17
19	5630 Omelia Rd		8" CI	1938	Cracked Bell
20	Painter & Beverly Blvd.	8	6" X 8" CI	1935	T sheared at flange
21	14245 Bronte	6-8		1948	Service cork pulled from main
22	Greenleaf Booster Station	8	16" CI	1930	Lead caulk forced out of bell; leak
23	Near 14245 Bronte	5	6" CI	1948	Blow-Out
24	11630 Whittier	6	6" X *" CI	See #16.	This may be from soil settlement associated with #16
25	12906 Orange Dr	1	1" Steel		Corroded -- Service line split

East Bay Municipal Utility District (2014) reports on its mutual assistance to the City of Napa after the 24 Aug 2014 M 6.0 South Napa earthquake. EBMUD crews performed 56 repairs in approximately 252 crew-hours, for an average duration of 4.5 hours per repair. It should be noted that this average duration for completing repairs does not reflect the time it took for the City of Napa or its contractors to complete the excavation and backfill (EBMUD crews focused on repair work, and did not complete excavation/backfill/paving-related work).

Tabucchi et al. (2010) elicited opinion from personnel at the Los Angeles Department of Water and Power on repair productivity. They propose a model with triangular probability distributions for each of several repair operations. Each distribution is characterized by a minimum value (the left end of the triangle), a modal value (the peak of the triangle, which is the most likely value), and a maximum value (the right end of the triangle). Table 4 repeats LADWP's estimates.

Distribution-system leak and break repairs are estimated to require no less than 3 hours and no more than 12 hours with modes of 4 to 6 hours.

Event	Minimum	Mode	Maximum
Inspect a			
Trunk or distribution damage location	0.5 h	0.5 h	1 h
Pump station	1 h	1 h	2 h
Regulator station	1 h	1 h	2 h
Tank	1 h	1 h	2 h
Small reservoir	2 h	2 h	3 h
Rerouting operation on a trunk line by			
Trunk redundancy (major)[a]	3–6 h	6–12 h	8–24 h
Trunk redundancy (minor)[a]	3 h	4 h	8 h
Connecting to MWD [a]	3–4 h	6 h	8–12 h
Connecting to well[a]	4–6 h	6–8 h	8–12 h
Using a fire truck[a]	1–2 d	2–3 d	3–4 d
Isolate distribution damage at one demand node	1 h	2 h	4 h
Repair a			
Distribution leak	3 h	4 h	6 h
Distribution break	4 h	6 h	12 h
Trunk leak	4 d	4 d	6 d
Trunk break	6 d	8 d	10 d
Travel a distance D (km)	$D/25$ h	$D/40$ h	$D/80$ h

Note: h, hours; d, days.
[a] Major trunk lines are the pipelines that are the sources for each of the 13 LADWP subsystems; minor trunk lines are the remaining ones. MWD is the Metropolitan Water District. Task durations for major trunk line rerouting operations vary by specific trunk line, as listed in Tabucchi and Davidson (2008).

Hazus-MH (NIBS and FEMA 2012) employs four restoration times: two each for large and small diameter pipes (20 inch diameter and above is large, 12 inches or less is small) times two to distinguish between breaks and leaks. See Table 5.

Table 5. Hazus-MH (2012) estimates of repair time per pipe repair

Class	Diameter from: [in]	Diameter to: [in]	# Fixed Breaks per Day per Worker	# Fixed Leaks per Day per Worker	# Available Workers	Priority
a	60	300	0.33	0.66	User-specified	1 (Highest)
b	36	60	0.33	0.66	User-specified	2
c	20	36	0.33	0.66	User-specified	3
d	12	20	0.50	1.0	User-specified	4
e	8	12	0.50	1.0	User-specified	5 (Lowest)
u	Unknown diameter	or for Default Data Analysis	0.50	1.0	User-specified	6 (lowest)

Seligson et al. (1991) offer an empirical relationship for time required to restore water service as a function of number of pipeline breaks per square mile, based on evidence from the 1971 San Fernando and 1987 Whittier earthquakes. In Equation (9), B denotes breaks per square mile and d denotes number of days of water supply outage:

$$d = 2.18 + 2.51 \cdot \ln B \qquad B > 0.42$$
$$= 0 \qquad B \le 0.42 \qquad (9)$$

2.6 Serviceability of water supply

As previously noted, some analytical models are capable of modeling the serviceability of a damaged water supply system using hydraulic or connectivity analysis (e.g., Khater and Grigoriu 1989). As in the case of the closely related LLEQE software, the Applied Technology Council (1991) noted that such systems can be data intensive and computationally demanding. What can be done to estimate water supply serviceability without a hydraulic model?

Isoyama and Katayama (1982) propose to measure a quantity they call serviceability as the probability that the demand at a system node (such as a customer service connection) is fully satisfied, or in the aggregate, the average fraction of nodes in the entire system whose demand is fully satisfied. Demand seems to mean the pre-earthquake consumption plus post-earthquake leakage.

Markov et al. (1994) propose to measure serviceability via a serviceability index S_S defined as the ratio of the total available flow to the total required flow, which is similar but not identical to Isoyama and Katayama's serviceability. If demand at 10 nodes were fully satisfied and demand at 10 other nodes were partially satisfied, the two measures of serviceability would take on different

values: 0.5 in the case of Isoyama and Katayama (1982) and somewhat higher in the case of Markov et al. (1992).

The developers of the Hazus-MH water system use data from Isoyama and Katayama (1982) and Markov et al. (1994), along with unpublished work by G&E Engineering Systems to propose to estimate the serviceability index $s(r)$ as a function of break rate (breaks, not leaks, per km of service main pipe) using Equation (10). They seem to use the serviceability index to measure the fraction of customers receiving *any* water service, since the software expresses loss of serviceability in terms of "households without water."

$$s(r) = 1 - \Phi\left(\frac{\ln\left((r/L)/q\right)}{b}\right) \tag{10}$$

In Equation (10), ln denotes natural logarithm, r/L denotes the average break rate (r main breaks per L km of pipe), q and b are model parameters, and Φ is the standard normal cumulative distribution function (the y-value of the S-shaped curve in x-y space that depicts the probability that an uncertain quantity with standard normal distribution will take on a value less than or equal to x). Hazus-MH employs values of $q = 0.1$ and $b = 0.85$, respectively, fitting the curve to Isoyama and Katayama's modeling of Tokyo's water supply system, Markov et al.'s modeling of the San Francisco Auxiliary Water Supply System (a dedicated firefighting system), and G&E's unpublished analyses of East Bay Municipal Utility District's water supply system. Hazus' serviceability model is illustrated in Figure 4, in the curve labeled "NIBS."
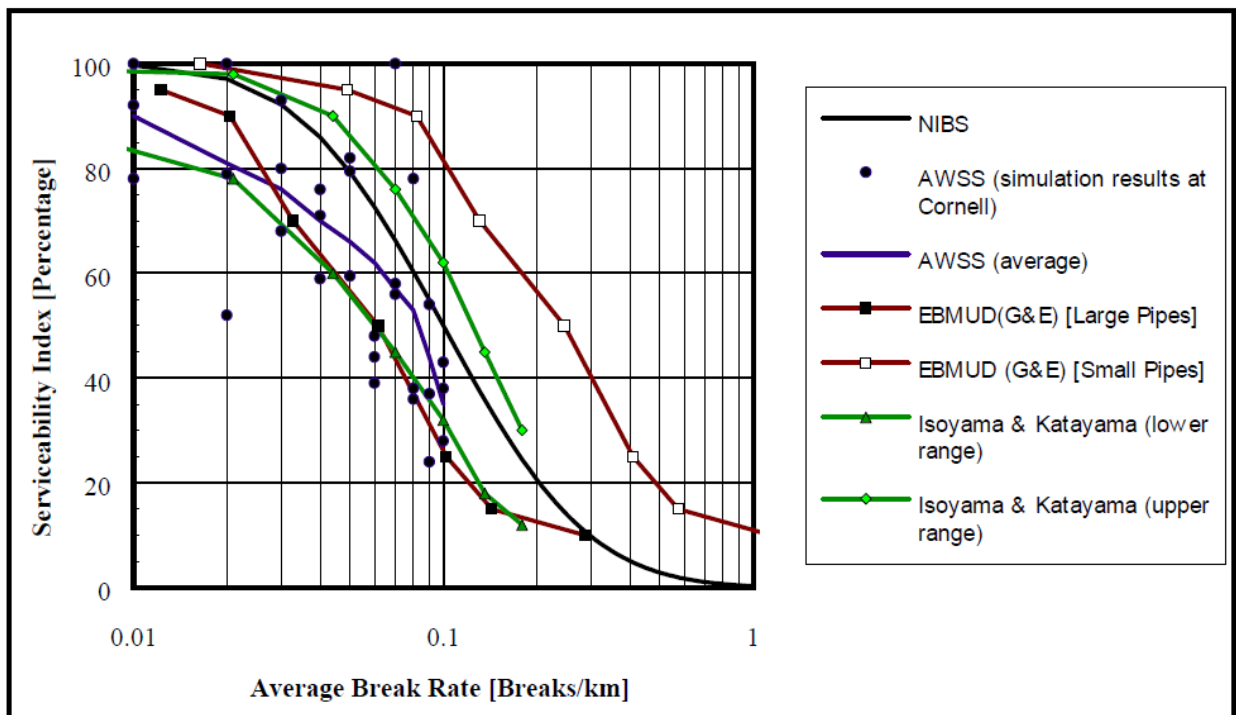
Figure 4. Hazus-MH model of serviceability. Hazus uses the curve labeled "NIBS."

Thus, the Hazus-MH serviceability index might measure:

- The fraction of service connections receiving pre-earthquake flows, regardless of the degree of post-earthquake flow received at other service connections, which would seem to be consistent with Isoyama and Katayama's (1982) serviceability.
- The fraction of pre-earthquake flow being delivered after the earthquake, consistent with Markov et al. (1994); or
- The fraction of service connections receiving *any* water, as the Hazus-MH reports indicate.

Lund et al. (2005), citing Kobe Municipal Waterworks Bureau's M. Matsushita, present a restoration curve for the Kobe water system after the 1995 Kobe earthquake. Tabucchi and Davidson (2008) offer an analogous plot for the restoration of water service in the San Fernando Valley after the 1994 Northridge earthquake. The two restoration curves are duplicated in Figure 5. Restoration after Northridge appears fairly linear; Kobe less so.
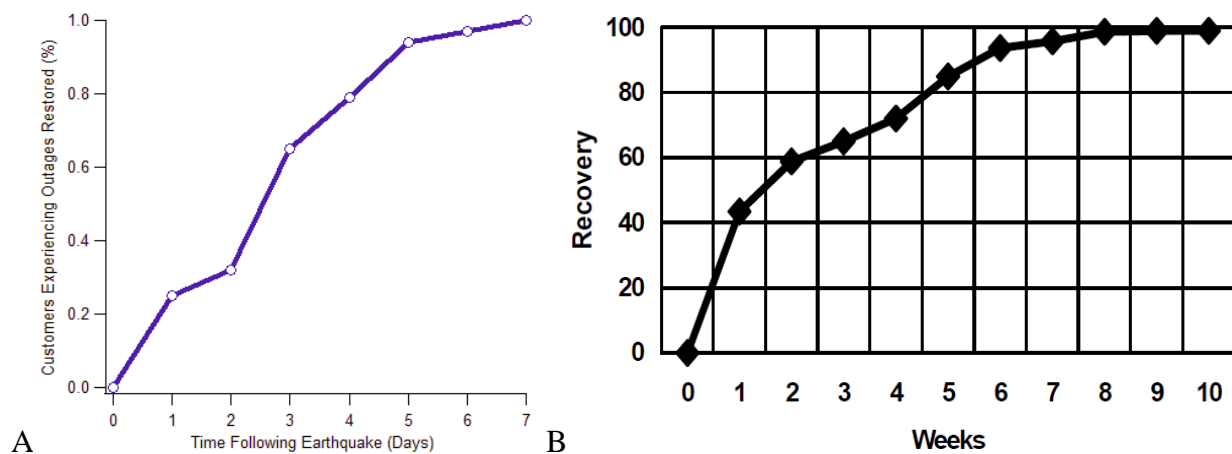
Figure 5. A. Restoration of water service after the 1994 Northridge earthquake and B. After the 1995 Kobe earthquake

2.7 Lifeline interaction

Many authors have characterized lifeline interaction after natural disasters. A few but not all relevant works are summarized here.

For ease of reference, let us recall here some evidence previously noted: Winnipeg (2014) and AWWA (2008) suggest that prerequisites for the repair of buried pipeline include cellular communications and electricity to learn about and coordinate repairs, fuel and roadway access to travel to and perform the repairs, site safety (especially no fires, gas leaks, or electrical hazards), and consumable repair materials including pipe, fittings, repair hardware, and disinfecting chemicals.

Nojima and Kameda (1991) compiled instances of lifeline interaction in the 1989 Loma Prieta earthquake, noting particularly the loss of wastewater treatment because of the loss of electricity, and the degradation of telecommunications resulting from the loss of electricity and difficulty acquiring fuel for central offices' emergency generators as a result of highway problems. See Table 6 for a matrix summarizing lifeline interaction in the earthquake. It shows that water supply was impaired for 18 hours in Santa Cruz because of loss of electric power for pumping. It also shows that electricity failure impaired EBMUD's Lafayette filtration plant and its Oakland Control

Center. Repairs in Santa Cruz were also impaired by delays transporting repair equipment over the damaged Oakland-San Francisco Bay Bridge. In San Francisco and Santa Cruz, overloaded telecommunications impaired repair efforts.

Scawthorn (1993) reviews literature and then-recent disaster experience on lifeline interaction in several disasters (1989 Cajon Pass, 1989 Loma Prieta Earthquake, 1991 Shasta spill, 1991 East Bay Hills fire, and 1992 Hurricanes Andrew and Iniki) to construct a model and analytical methodology for lifeline interaction. He points out that water supply in the 1991 Oakland Hills fire was impaired in part because of breakage of service connections in buildings that collapsed in the fire, and the reliance of water supply on electric power to pumps stations that were required to resupply ridge-top tanks. He suggests characterizing lifeline interactions as either: (a) cross-impact (impact on one lifeline's function due to impairment of service to that lifeline by a second lifeline), collocation (direct damage or impact on one lifeline's function due to failure of another lifeline in a very proximate location), and cascade (increasing impacts on a lifeline due to initial inadequacies, e.g., water supply damage as buildings collapse and sever service connections). In Scawthorn's quantitative model, one characterizes initial damage to a set of lifelines through a vector D of n scalar quantities, each element representing a fraction of customers receiving service for one of n lifelines if there were no interaction, i.e., if only damage to that lifeline mattered. Lifeline interaction is quantified by an $n \times n$ matrix denoted by L, where element $L_{i,j}$ (row i, column j) denotes the fraction of service of lifeline i that is contributed by lifeline j. A higher value of $L_{i,j}$ indicates greater reliance of lifeline i service on lifeline j. A value $L_{ij} = 0$ indicates no interaction. The final functional state of the n lifelines is represented by vector F, whose value is given by Equation (11). Element i of vector F measures the fraction of customers receiving service from lifeline i, where any reduction below $F_i = 1.0$ is a result of initial damage D to all the lifelines and interaction L between them.

$$F = LD \tag{11}$$

Scawthorn offers the model but does not propose particular values for matrix L. Note that, because $0 \leq D_i \leq 1.0$, to ensure that $0 \leq F_i \leq 1.0$, L must be constrained per Equation (12).

$$\sum_{j=1}^{n} L_{ij} = 1.0 \qquad i \in \{1, 2, ... n\} \tag{12}$$

Table 6. Lifeline interaction matrix in the Loma Prieta earthquake (after Nojima and Kameda 1991)

↗	Electricity	Gas	Water	Sewer	Road	Rail	Telephone
Electricity	*	Santa Cruz gas explosion due to electricity comeback (spark ignition). Recovery work arrangement with electric power supply system	Santa Cruz: pump stopped for 18 hrs (gravity flow area survived; no water in pump-based supply area) SF: power failure due to gas leak inspection, no water in pump-based supply area and Marina district. No power for repair work. EBMUD: short-term loss of power at Lafayette filtration plant. Oakland Control Center power loss, no service	SF and Santa Cruz: power failure at pump station	SF and Santa Cruz: traffic jam due to malfunction of traffic signal	SF: BART omitted stops at some stations to save electricity	Capacity diminished by use of storage cells. PBX with no battery, malfunction Pacific Bell: Bush/Pine Office (SF) coolant trouble; no service for 3 hrs. Hollister Office generator failure no service for 3 hrs. GTE: Monte Bello Office (Los Gatos) failure of generator fuel tank; malfunction (6-7 hrs)
Gas	SF & Santa Cruz: gas leak inspection before recovering electricity	*	Santa Cruz: no home treatment. Recovery work arrangement with gas supply system.		SF: road closed due to propane fire (Rte. 80 WB Central Ave)		
Water		Santa Cruz: recovery work arrangement with water supply system	*	Santa Cruz: damage detection by analogy	SF Marina District: road failure due to water leakage		
Sewer			Santa Cruz: suspicion of underground water contamination due to outflow or crude sewage from pipeline	*			
Road			Santa Cruz: no transporting machinery due to bridge damage	Santa Cruz: damage detection by analogy	*	BART riders increased due to Bay Br. Closure (Oct 23: +40 percent)	
Rail						*	
Telephone			SF & Santa Cruz: overload				*

The San Francisco Lifelines Council (2014) adapted the panel process of Porter and Sherrill (2011) to involve Bay Area lifeline operators in qualitatively characterizing the potential effects of lifeline interaction on the post-earthquake functionality of their systems. The authors sought to identify key assets and restoration schemes to prioritize post-disaster restoration and reconstruction activities for San Francisco and ultimately the Bay Area. Through panel discussion with 11 lifeline operators, the authors identified lifeline interaction effects in the context of a hypothetical M 7.9 earthquake on the Northern San Andreas Fault. They propose a qualitative interaction matrix (Table 7) that describes modes of interaction a la Nojima and Kameda (1991) and shows a degree of interaction, with darker shading indicating greater interaction, like a higher value in Scawthorn's (1993) matrix. The authors found that restoring water supply in San Francisco depends significantly on city streets, telecom, and fuel, and to a lesser extent on regional roads, electric power, and the port. The matrix characterizes the mode of each interaction, with five possible modes. Quotations are taken from San Francisco Lifelines Council (2014); interpretations are mine:

- "Functional disaster propagation and cascading interactions from one system to another due to interdependence." This means that a system relies on one or more other systems to operate, each of which can rely on still others. Let us refer to these other systems as "upstream," in the sense that failure of an upstream system flows or cascades down to the system in question and causes its failure. For example, consider water service in a pressure zone that is supplied from tanks whose source is water pumped from lower elevation. Water service in that pressure zone is functionally dependent on electricity, which may be functionally dependent on natural gas. Failure of fuel supplies or electric generation, transmission, or distribution propagates or cascades to cause water supply failure through interdependence.
- "Collocation interaction, meaning physical disaster propagation among lifeline systems." This means that one or more elements of the system in question are located close to one or more elements of another system, and that the other system can fail in such a way that an area around the failure can impair the system in question. For example, fiber optic cable that serves the telecommunication network may be installed in a conduit on a roadway bridge. Excessive displacement of the bridge, for example as a result of settlement of an abutment, can sever the fiber conduit.
- "Restoration interaction, meaning various hindrances in the restoration and recovery stages." This means that one or more elements of the system in question are located close to one or more elements of another system, and that repairs to the other system can damage or hinder the repair of the system in question. For example, consider a water main (the system in question) that is located above a damaged sewer line. Repair to the sewer line could require the temporary removal of or inadvertently lead to damage to the water main.
- "Substitute interaction, meaning one system's disruption influences dependencies on alternative systems." This means that the system in question may have substitutes (alternative systems), and that disruption of one of the alternatives can affect the system in question. For example, damage to the San Francisco-Oakland Bay Bridge in the 1989 Mw

6.9 Loma Prieta earthquake caused a 32% increase in BART ridership during October and November 1989 (San Francisco Bay Area Rapid Transit District 2015).

- "General interaction, meaning between components of the same system." Nojima and Kameda (1991) use a star (*) to mean the same thing. This means that impairment of elements of the system in question can affect other elements of the same system. For example, overturning of electrical switchgear in a pumping station can cause the pumps to fail to operate.

Table 7. The San Francisco Lifelines Council's (2014) lifeline system interdependencies matrix

The overall interaction and dependency on a particular system (read down each column)

Lifeline operators' dependency on other lifeline systems (read across each row)

	Regional Roads	City Streets	Electric Power	Natural Gas	Telecom	Water	Auxiliary Water	Waste-water	Transit	Port	Airport	Fuel
Regional Roads	General	Restoration Substitute	Restoration	Restoration	Restoration	Restoration		Restoration	Substitute		Restoration	Restoration
City Streets	Substitute, Restoration	General	Collocation, Restoration	Collocation, Restoration	Collocation, Restoration	Collocation, Restoration	Collocation, Restoration	Collocation, Restoration	Collocation, Substitute, Restoration	Collocation, Restoration		Restoration
Electric Power	Restoration	Collocation, Restoration	General		Restoration	Collocation, Restoration	Collocation, Restoration	Collocation, Restoration		Collocation	Restoration	Restoration
Natural Gas	Restoration	Functional, Collocation, Restoration	Substitute	General	Restoration	Collocation, Restoration	Collocation, Restoration	Collocation, Restoration		Collocation	Restoration	Restoration
Telecom	Restoration	Collocation, Restoration	Functional, Restoration	Restoration	General	Collocation, Restoration	Collocation, Restoration	Collocation, Restoration			Restoration	Restoration
Water	Restoration	Restoration	Restoration		Restoration	General				Collocation		Restoration
Auxiliary Water	Restoration	Functional, Restoration	Restoration		Restoration	Functional, Restoration	General			Collocation, Restoration		Restoration
Waste-water	Restoration	Collocation, Restoration	Functional, Restoration		Restoration	Functional, Restoration		General		Collocation, Restoration		Restoration
Transit	Substitute, Restoration	Functional, Substitute, Collocation, Restoration	Functional, Restoration		Restoration	Collocation, Restoration	Collocation, Restoration	Collocation, Restoration	Collocation, General	Collocation, Restoration		Functional, Restoration
Port	Restoration	Collocation, Restoration	Collocation, Restoration		Collocation, Restoration	Collocation, Restoration	Collocation	Collocation	Collocation	General		Restoration
Airport	Restoration		Restoration		Restoration	Restoration		Restoration	Collocation, Restoration		General	Functional, Restoration
Fuel	Restoration	Restoration	Functional, Restoration		Restoration	Restoration				Restoration	Restoration	General

2.8 Pipeline damage in afterslip

Several authors have considered lifeline damage due to afterslip, which is fault slip immediately following an earthquake rupture that involves creep much faster than the interseismic rate. According to Aagaard et al. (2012), "Afterslip develops very quickly and can have similar impacts as coseismic slip, with the added complexity that the slip continues for months to years, albeit with a decreasing rate." They discuss afterslip in various Hayward Fault earthquake scenarios, including the one adopted for use here: "Afterslip makes a substantial contribution to the long-term geologic slip and may be responsible for up to 0.5–1.5 m (median plus one standard deviation) of additional slip following an earthquake rupture." The authors offer a power-law expression for afterslip as a function of time t, denoted $D(t)$, as follows:

$$D(t) = A + B \cdot \frac{1}{(1 + T/t)^C} \tag{13}$$

$$A = \frac{1}{1-a}(D_{total} - a \cdot D_{coseismic}) \tag{14}$$

$$B = \frac{-a}{1-a}(D_{total} - D_{coseismic}) \tag{15}$$

$$a = \left(1 + \frac{T}{1\,\mathrm{sec}}\right)^C \tag{16}$$

$$C_{median} = 0.881 - 0.111 \cdot M_w \tag{17}$$

where T is referred to as the afterslip time constant, taken here as 365 days per Aagaard et al. (2012). For example, with $M_w = 7.05$, Equation (17) leads to $C_{median} = 0.0984$. With $T = 365$ days, Equation (16) leads to $a = 5.47$. With $D_{total} = 1.86$m and $D_{coseismic} = 0.83$m, Equations (13), (14), and (15) produce $A = 0.608$m, $B = 1.25$m, and the estimate of slip versus time shown in Figure 6.
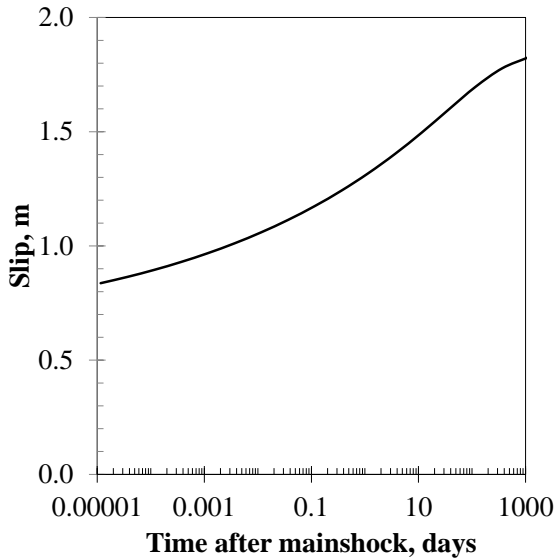
Figure 6. Illustration of afterslip

O'Rourke and Palmer (1996) point out that understanding observations of pipeline damage at fault crossings requires estimating fault slip from the time of pipeline installation to the time of its

excavation for inspection after the earthquake, including pre-seismic slip, coseismic slip, and afterslip.

Treiman and Ponti (2011) suggested that afterslip could realistically account for 40% of the total surface slip in the Coachella Valley resulting from a M 7.8 earthquake on the Southern San Andreas Fault. The afterslip could aggravate damage to the Coachella Canal, railroad, fiber optic cable, electrical lines, gas and oil pipelines, and highways.

Hudnut et al. (2014) measured deformation in a temporarily decommissioned 26-inch diameter gas pipeline that crosses the fault rupture involved in the 2014 South Napa earthquake. They observed that the pipeline was "subtly warped more than 35 cm by fault offset, most of which accumulated as afterslip that is still continuing as of 3 months after the earthquake." They argue that "Lifeline performance in future events, with both coseismic slip and afterslip, deserves additional consideration."

2.9 Measuring loss of resilience

Bruneau et al. (2003) propose to measure the loss of resilience as the area above the curve $Q(t)$, where $Q(t)$ is defined (somewhat vaguely) as the "quality of the infrastructure of a community" They denote a quantity they call "community earthquake loss of resilience" by R and calculate it as in Equation (18):

$$R = \int_0^{t_1} \big(1 - Q(t)\big)\, dt \tag{18}$$

where $t = 0$ and $t = t_1$ denote the times of the initiating event and the time of full restoration, respectively. For brevity, let us refer to R more simply as the loss of resilience. Bruneau et al. do not define $t = 0$ and $t = t_1$ precisely. Let us define $t = 0$ here as the time of the first earthquake in the earthquake sequence under consideration, and let us define t_1 as the time when $Q(t) = 1$ after the last earthquake in the sequence under consideration. Let $Q(t)$ measure the fraction of water customers receiving at least an adequate degree of service at time t, meaning sufficient water flow and pressure at the tap for drinking (even if it needs to be boiled first), bathing, and using toilets. R has units of time, and as applied here can be seen here as the expected value of the time that an arbitrary customer is receives less water than a useful degree of service.

To be clear, a reduction in the loss of resilience indicates a briefer average time that an arbitrary customer lacks adequate service, but I will *not* equate a reduction in the loss of resilience with an increase in resilience. In Bruneau et al.'s terminology, resilience is not a quantity but rather a quality that means "the ability of the system to reduce the chances of a shock, to absorb a shock if it occurs (abrupt reduction of performance) and to recover quickly after a shock (re-establish normal performance)." Resilience is *not* the mathematical complement of the loss of resilience.

3. Methodology

3.1 Overview of the methodology

Using the brief literature review of section 2 as a basis, I propose the following methodology. A lifeline earthquake performance and restoration model typically involves the following analytical elements:

1. Asset definition, in which the system is described in terms of nodes and links. Nodes have a location, flow capacity, sometime a value (e.g., replacement cost), and an asset category that associates the component with one or more relationships between environmental excitation (e.g., severity of shaking) and loss (e.g., in terms of dollars, deaths, downtime, or some combination). Links connect nodes. They have a path, sometime a direction, flow capacity, sometimes a value, and an asset category. The assets in question here are defined in section 4 of this report.

2. Hazard model, relating geographic location to environmental excitation. In the case of earthquake hazard, the hazard model typically includes a mathematical idealization of seismic sources in the region, their locations, the frequency with which they can produce earthquakes of various magnitudes, and one or more ground motion prediction equations to relate earthquake magnitude and location to shaking and other site effects. In the present study, the hazard model is presented elsewhere. Briefly, it is a physics-based model of the San Francisco Bay Area, depicted in Aagaard et al. (2010a, b).

3. Hazard analysis, in which one evaluates the hazard model for one or more realizations of an earthquake. In the present analysis, I use the realization from Aagaard et al. (2010) depicting a M_w 7.05 rupture of the Hayward Fault north and south segments with an epicenter under Oakland. Accompanying the model of shaking from the mainshock are estimates of liquefaction probability, landslide probability, coseismic slip, and afterslip associated with the mainshock, along with shaking in each of a sequence of 16 aftershocks of M 5.0 and greater.

4. Vulnerability model, relating environmental excitation at a particular location to the potentially uncertain loss in each of a set of asset classes. Section 3.2 presents the vulnerability model used here.

5. Damage analysis, in which one evaluates the vulnerability model for each lifeline component at the level of environmental excitation to which the component is subjected. Section 3.3 presents the procedures of the damage analysis.

6. Restoration model, which characterizes the time to restore the damaged components to their pre-disaster condition, and calculates the degree of service at each of many points in time. Section 3.4 presents the restoration model developed and employed here. The present restoration model is new. It includes a new method for quantifying the effects of lifeline interaction. It includes an initial assessment period suggested by engineers of the East Bay Municipal Utility District, along with a period during which repair crews and other resources ramp up from an initial, in-house quantity to one that includes mutual aid.

7. Aftershock analysis, in which one inserts one or more aftershocks into the restoration process, which in a sense restarts the hazard, damage, and restoration analyses with a still-damaged lifeline system.

3.2 Vulnerability model

3.2.1 What is a vulnerability model?

By "vulnerability model" is meant a mathematical formulation of the relationship between loss (usually normalized by quantity, e.g., pipeline breaks per 1,000 ft of pipe) and environmental

excitation (e.g., degree of peak ground velocity). These relationships often apply to classes of components that share common engineering features, e.g., pipe sharing common material, diameter range, joint type, etc. All specimens of the class are assumed to be interchangeable and indistinguishable for purposes of estimating loss. A vulnerability model can be deterministic, providing for example only a mean estimate of loss conditioned on excitation, or probabilistic, providing both a mean value and error term. Let us define some terms:

$y_i(x)$ = the expected value of the degree of loss experienced by a component of class i when subjected to excitation x. One can refer to $y_i(x)$ as the mean vulnerability function for class i.

$\varepsilon_i(x)$ = the error term for class i. The error term can be constant for class i or it can depend on degree of excitation x. The error term has unit mean and usually has some parametric distribution, such as lognormal with a specified standard deviation of the natural logarithm of the error term, referred to here as the logarithmic standard deviation. The vulnerability model can provide mean vulnerability functions and error terms for one or more modes of damage j, such as damage by wave passage and damage by ground failure due to liquefaction, landslide, or fault offset.

$y_{i,j}(x_{i,j})$ = the mean loss to a component i of a specified class in damage mode j when component i is subjected to mode-j excitation $x_{i,j}$, such as the peak ground velocity to which a particular segment of pipe is subjected.

$\varepsilon_{i,j}(x_{i,j})$ = the mode-j vulnerability error term for the class to which component i belongs, when the component is subjected to excitation $x_{i,j}$.

$Y_{i,j}(x_{i,j})$ = the uncertain normalized loss is denoted by (e.g., uncertain total pipeline breaks per 1,000 lf of pipe), where the index i refers to the component class to which component i belongs, j refers to the damage mode under consideration (e.g., pipeline breaks per 1,000 lf of pipe as a result of wave passage), and xi,j is as previously defined.

The uncertain normalized loss is calculated as:

$$Y_{i,j}\left(x_{i,j}\right) = y_{i,j}\left(x_{i,j}\right) \cdot \varepsilon_{i,j}\left(x_{i,j}\right) \tag{19}$$

The vulnerability model comprises the set of functions y and ε, the component classes to which they refer, and the domain of excitations for which the functions are valid.

3.2.2 Selecting a vulnerability model for a pipeline network

Several authors have created and published pipeline vulnerability functions; a few appear in section 2. There are no commonly accepted rating systems for pipeline vulnerability functions, but it seems reasonable to choose among competing vulnerability functions based on at least the following criteria:

- Vulnerability functions reflect diverse conditions: pipe material, diameters, joint systems, age, and corrosivity similar to the conditions where the vulnerability functions will be applied.
- Vulnerability functions are drawn from numerous damage data.
- Vulnerability functions are drawn from ground motion levels reaching as high as those where they will be applied.

- The articles in which the vulnerability functions are presented are respected, highly cited, and frequently used for similar applications, which here means estimating and depicting realistic outcomes of a hypothetical US earthquake.

Table 8. Comparison of criteria for selecting pipeline vulnerability functions

Source	Diverse pipe	Repairs	Max PGV	Max PGD	Citations
M. O'Rourke & Ayala (1993)	Yes	Unknown	50 cm/sec	NA	87
Honneger and Eguchi (1992)	Yes	Unknown	Unknown	Unknown	21
Eidinger (2001)	Yes	3350	52 cm/sec	110 in	18
T. O'Rourke et al. (2014)	Yes	2051	80 cm/sec	N/A	20

O'Rourke et al. (2014) have been more cited in far fewer years than Eidinger (2001), suggesting somewhat greater credibility. Maximum PGV values are greater in the O'Rourke work, suggesting greater applicability in strong shaking. However, Eidinger (2001) draws on a larger data set and his vulnerability functions cover both wave passage and ground failure. For these reasons, it seems the Eidinger vulnerability functions are most suited to the present problem.

Thus, for wave passage, one can use Equation (3) to calculate break rate with probability p of nonexceedance, or alternatively Equation (4) for the mean break rate. There is a problem however applying a liquefaction and landslide model that requires permanent ground displacement, as in Eidinger's model Equations (5) or (6). The problem here is that peak ground displacements are unavailable for the this scenario, only liquefaction probability and landslide probability. How to apply Eidinger's ground-failure model without an estimate of permanent ground displacement, *PGD*?

The solution employed here takes advantage of the fact that Equation (6) is not very sensitive to *PGD*. One can see the limited sensitivity in the small power to which *PGD* is raised, 0.319. At the same time, the logarithmic standard deviation $\beta = 0.74$ in Equation (6), which gives the marginal distribution of break rate, is very large, suggesting the 90th percentile bounds differ by more than an order of magnitude. In this case, the 95th and 5th percentiles of break rate conditioned on *PGD* differ by a factor of 11.4.

So Eidinger's liquefaction equation tells us that an increase in PGD from 1 inch to 10 inches only increases mean break rate by a factor of 2. See Figure 7: for $K_2 = 1$, the break rate for *PGD* = 1 inch and the break rate for *PGD* = 10 inches are 1.4 and 2.9 breaks per 1,000 lf, respectively. At either point, *PGD* = 1 inch or 10 inches, the uncertainty in break rate is much greater, i.e., even if one knew *PGD,* one would still be very uncertain as to break rate. The apparent improvement in accuracy gained by estimating liquefaction-induced or landslide-induced *PGD* would be illusory. That is not to say that it would not be a little better to estimate PGD, it just would not be much better.
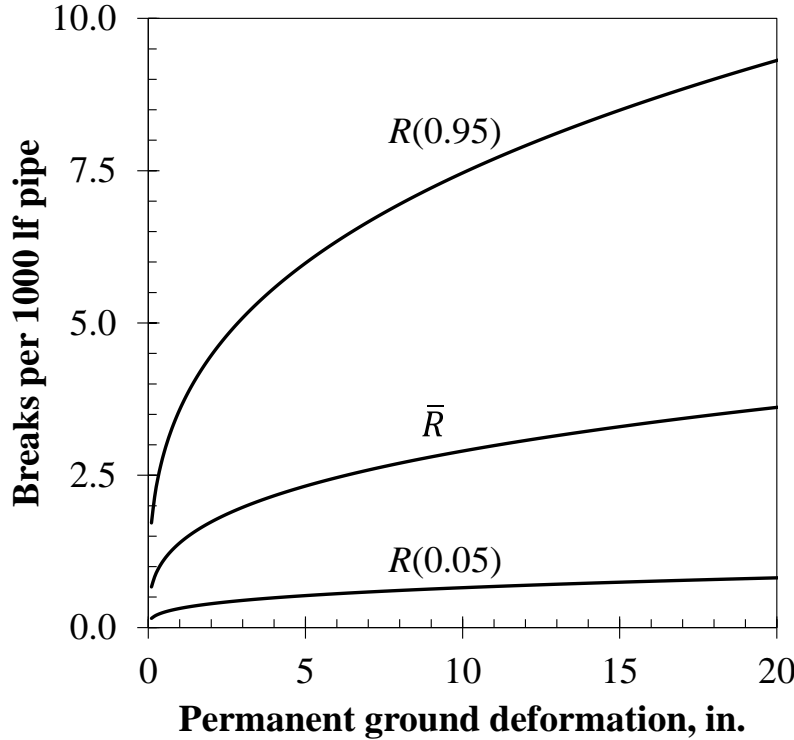
Figure 7. Eidinger (2001) pipe liquefaction vulnerability for $K_2 = 1.0$, mean and 90% bounds

In light of the very high uncertainty in break rate and the relatively modest sensitivity of the vulnerability function to *PGD*, let us assume a reasonable moderate *PGD* associated with liquefaction, say 6 inches, and rewrite Equations (5) and (6) using liquefaction probability, as shown in Equations (21):

$$R_l(P_L, p) = K_2 \cdot P_L \cdot 1.06 \cdot 6^{0.319} \cdot \exp\left(0.74 \cdot \Phi^{-1}(p)\right)$$
$$= 1.88 \cdot K_2 \cdot P_L \cdot \exp\left(0.74 \cdot \Phi^{-1}(p)\right) \tag{20}$$

$$\bar{R}_l(P_L) = K_2 \cdot 1.39 \cdot 6^{0.319} \cdot P_L$$
$$= 2.46 \cdot K_2 \cdot P_L \tag{21}$$

where P_L denotes probability of ground failure, either through liquefaction, landslide, or fault offset. The equation estimates mean break rate per 1,000 linear feet of pipe.

How does one sum break rates from wave passage and ground failure if one uses Eidinger's (2001) model? He says that "wave propagation effects are masked within the more destructive effects of [peak ground displacements]." If one knew where ground failure occurs, one would ignore the wave-passage model so as not to double-count it. The problem here is that Eidinger's empirical model of damage due to liquefaction probably includes some damage that was caused by wave passage. But he does not know which breaks were caused by which peril. In zones of liquefaction, he treats all damage as caused by liquefaction. That is, his empirical relationship for damage in zones of liquefaction include an unknown (but probably small) fraction of damage caused by wave passage.

As a result, one must not double-count wave passage damage by applying both the liquefaction and wave-passage models in zones of liquefaction. To eliminate double-counting, let us modify the wave-passage model of Equations (3) and (4) by multiplying the break rate a factor $(1 - P_L)$, where P_L denotes ground-failure probability. After eliminating double-counting, one can sum the wave-passage and ground-failure models as shown in Equations (22) and (23). In both equations, R denotes break rate in breaks per 1,000 ft of buried pipe, PGV is peak ground velocity in inches per second, and p denotes nonexceedance probability. In Equation (22), R gives break rate with nonexceedance probability p, while Equation (23) gives mean (average) break rate. The coefficients are smaller in Equation (22) than they are in Equation (23) because the median is smaller than the average for a lognormally distributed random variable, and the difference depends on the logarithmic standard deviation.

$$R(PGV, P_L, p) = (1 - P_L) \cdot R_w(PGV, p) + R_L(P_L, p)$$
$$= (1 - P_L) \cdot K_1 \cdot 0.00187 \cdot PGV \cdot \exp(1.15 \cdot \Phi^{-1}(p)) + 1.88 \cdot K_2 \cdot P_L \cdot \exp(0.74 \cdot \Phi^{-1}(p))$$
$$(22)$$
$$\bar{R}(PGV, P_L) = (1 - P_L) \cdot \bar{R}_w(PGV) + \bar{R}_l(P_L)$$
$$= (1 - P_L) \cdot K_1 \cdot 0.003623 \cdot PGV + 2.46 \cdot K_2 \cdot P_L$$
$$(23)$$

For damage resulting from fault offset, one could apply Eidinger's (2001) proposed model. Given the absence of supporting data, the relatively small number of breaks that occur at the fault trace compared with breaks that occur as a result of wave passage and liquefaction, and the desire to model breaks as a function of offset at the location of the pipe rather than average offset over the entire trace, a simpler model is adopted here. Let us assume that any pipe segment that crosses a fault is broken if the fault offset exceeds 4 inches, and use the same threshold regardless of pipe material, jointing, and angle subtended by the fault and pipeline alignment. I treat the fault trace as a collection of line segments rather than as a zone on the surface of the earth with a finite width. The offset therefore is lumped at the line rather than distributed over the width of the zone. Mathematically, let Z_i denote a binary variable to indicate that pipe segment i is damaged by fault offset (1 if true, 0 if false), d denotes the fault offset distance, d_f denotes the threshold of fault offset distance that produces damage, and $I(\cdot)$ is the indicator function (1.0 if the value in parentheses is positive, 0.0 if negative), then

$$Z_i = I(d - d_f) \tag{24}$$

where $d_f = 6$ inches, consistent with the fault offset that Eidinger (2001) equates with a 50 percent failure probability for all segmental pipe. One could use a more refined model such as ASCE (1984), which applies engineering first principles of stress and strain, the engineering characteristics of the pipe and backfill, the geometry of how the pipe crosses the fault, etc. In the context of an earthquake planning scenario in which one cares about the total number of pipe breaks over the entire strongly shaken region, such an analysis seems like excessive effort for a relatively small contributor to overall damage. Furthermore, considering the necessary assumptions about unknown backfill characteristics and probably other model parameters, such an analysis would probably provide illusory precision.

3.3 Damage analysis (number of repairs required)

3.3.1 What is a damage analysis?

A damage analysis applies the vulnerability model and the hazard model to the assets under consideration to estimate degree of damage or loss, e.g., total number of pipeline repairs required when a particular pipeline network is affected by a particular earthquake. Let us employ a common general formulation for number of repairs required for a system of n_i discrete components (e.g., segments of pipe) that can each be uniquely identified with a class of components (e.g., type of pipe).

Each component i has an associated quantity or value V_i (e.g., length of pipeline segment), and is assumed to be subject to damage from up to n_j modes of damage (e.g., wave passage and liquefaction). Each combination of component class and mode of damage is assigned a vulnerability model $y_{i,j}(x_{i,j})$ and $\varepsilon_{i,j}(x_{i,j})$ as previously defined. Let R denote the total uncertain loss (e.g., total number of pipeline breaks). It is estimated as shown in Equation (25).

$$R = \sum_i^{n_i} \sum_j^{n_j} V_i \cdot y_{i,j}\left(x_{i,j}\right) \cdot \varepsilon_{i,j}\left(x_{i,j}\right) \tag{25}$$

Equation (25) assumes that damage to one component or in one model is independent of damage to other components or in other modes. That is, that the degree of damage to component i in mode j is unaffected by damage to a different component, and that if component i is damaged in one mode, it can also be damaged in another mode and that the losses resulting from the two modes of damage simply sum.

In the case of water supply pipelines, one implication of this assumption of independence is that it assumes that repairs are spaced widely enough apart that it makes sense to repair individual breaks or leaks, at least initially, rather than to remove and replace pipe and thus repair two or more breaks with a single repair.

3.3.2 Applying the damage analysis to a water supply system

Applying Equation (25) to water supply pipelines using Eidinger's (2001) vulnerability model, and adding an additional term for fault crossings, one can estimate mean total number of repairs r as shown in Equation (26):

$$
\begin{aligned}
r &= \sum_{i=1}^{n} \bar{R}_w\left(PGV_i\right) \cdot L_i + \sum_{i=1}^{n} \bar{R}_l\left(P_{L,i}\right) \cdot L_i + \sum_{i=1}^{n} I\left(d - d_f\right) \\
&= \sum_{i=1}^{n} \left(1 - P_{L,i}\right) \cdot 0.003623 \cdot K_{1,i} \cdot PGV_i \cdot L_i + \sum_{i=1}^{n} 2.46 \cdot K_{2,i} \cdot P_{L,i} \cdot L_i + \sum_{i=1}^{n} I\left(d - d_f\right)
\end{aligned}
\tag{26}
$$

where i is an index to pipe segments, n is the total number of segments in the network, $K_{1,i}$ and $K_{2,i}$ denote the values of K_1 and K_2 for pipe segment i, $PGVi$ is the peak ground velocity to which segment i is subjected, $P_{L,i}$ denotes the ground-failure probability at pipe segment i, L_i is the length of pipe segment i in thousands of linear feet, $I(\cdot)$ is an indicator function that takes on the value 1.0 if the expression in parentheses is positive, 0.0 if negative, d_i is the fault offset to which a segment of pipe i is subjected, and d_f is the offset at which breakage occurs. Here I propose to take d_f as

deterministically equal to 6 inches (15 cm). Note that as long as pipe segments i are relatively short, less than a few hundred meters, there should be little difference between shaking at the ends, and thus little error introduced by discretizing a pipeline network in this way.

Because the present analysis does not require a probabilistic estimate of loss, let us ignore the error term ε and deal only with the expected value of loss. I use the lower-case r in Equation (26) to indicate a deterministic value rather than the upper-case R of Equation (25) that stands for an uncertain quantity.

To carry out Equation (26), one uses a geographic information to create a table of system components, e.g., a table of pipe segments. Components are listed in rows. For each component, assign an identifier, determine its quantity (e.g., its length), assign it to a class that has one or more vulnerability or fragility functions (e.g., Eidinger's classes that group water supply pipe by material, joint, soil corrosivity, and diameter), and determine its location, e.g., the latitude and longitude of a pipe segment midpoint. Then using the GIS, look up the ground-motion parameter values $x_{i,j}$. Equation (26) can then be calculated for each component (each row) and the losses summed over all rows to calculate the expected value of loss r (e.g., the number of pipeline breaks requiring repairs).

3.3.3 Breaks or leaks?

Lund and Schiff (1991) define leaks and breaks for purposes of compiling damage data. Under their definition, a pipe with a leak continues to function with minimal loss of service while a pipe with a break completely loses function. It seems as if another, equivalent definition is that a pipe break separates a pipe segment into two, and a leak only partially fractures a pipe. Hazus-MH assumes an 80%/20% break/leak ratio for liquefaction, 20%/80% breaks/leaks for wave-passage damage. The authors of the technical manual do not cite a source for their choices.

Lund and Schiff (1991) found that, among all pipeline failures in the 1989 Loma Prieta earthquake where it was known whether the failure was a break or a leak, it was more common for the pipeline to break (336 repairs, 71%) than to leak (140 repairs, 29%). A study by Ballantyne et al. (1990) of pipe damage in 1949 and 1969 Seattle, 1969 Santa Rosa, 1971 San Fernando Valley, 1983 Coalinga, and 1987 Whittier Narrows earthquakes, found that ground failure resulted in a 50%/50% break/leak ratio, and absent ground failure, the ratio was 15%/85% breaks vs leaks. Since the present model allows one to distinguish between repairs associated with ground failure versus wave passage, and since the Ballantyne et al. (1990) are highly regarded and offer their evidence, I employ their ratios.

3.3.4 Degraded vulnerability?

The model presented here applies the same vulnerability functions to the same system map in the aftershocks that it applies to the mainshock. Is it correct to do so? Perhaps we should consider a system that has already been degraded by the mainshock or a large aftershock to be weaker. Perhaps the mainshock causes small undetected leaks or incipient breaks that become large leaks or breaks in an aftershock. But there does not seem to be sufficient research available to support explicitly modeling system degradation—making the mathematical model of the system more vulnerable in aftershocks than before the mainshock. This is a topic deserving of future research.

3.4 Restoration model

3.4.1 What is a lifeline restoration model?

As used here, a restoration model relates the damage (the output of the damage model) to the system's functionality over time, usually depicting its returns to its pre-disaster condition. Functionality can be measured a variety of ways, but in the case of a utility such as a pipeline network, it is common to measure functionality in terms of the number of service connections that receive the lifeline service as a function of time. I do not offer a general mathematical formulation of a lifeline restoration model, but merely list its elements here, and then propose a particular solution for the water supply pipeline system examined here. A lifeline restoration model includes the following elements:

- A model of the level of functionality immediately after the disaster
- A model of the repair resources—crews and supplies—available over time.
- A model of the number of services restored by each repair
- A model of the elapsed time after each repair
- Ideally, a model of lifeline interaction, i.e., accounting for how damage or restoration of other lifelines affects or delays damage or restoration of the lifeline in question.

3.4.2 Number of services lost because of earthquake

A hydraulic or connectivity analysis a la Khater and Grigoriu (1989) or Applied Technology Council (1991) is too demanding for present purposes. Let us use the same simplification as Hazus-MH does. As noted in the section on serviceability of water supply, Hazus interprets the serviceability index, which measures the drop in water pressure as a function of the average number of breaks per km of pipe, as a proxy for the fraction of customers receiving service. Let us employ the serviceability index the same way: immediately after an earthquake, when the number of repairs required is r, L is the number of km of pipe in the system, and M is the total number of customers, then the number of services available immediately after the earthquake is given by M times the serviceability index of Equation (10). Let V_0 denote the number of services available after the earthquake and before repairs begin:

$$V_0 = M \cdot s(r)$$

$$= M \cdot \left(1 - \Phi \left(\frac{\ln\left(\frac{r}{L \cdot q}\right)}{b} \right) \right) \tag{27}$$

where M is the total number of services, r is the number of main breaks (not leaks), L is the length of pipe in the distribution system (km), $q = 0.1$, and $b = 0.85$. The parameter q determines the number of breaks per km (0.1) at which V_0 reaches $0.5M$. The parameter b determines the width of the S-shaped curve in Figure 4. How long does it take to complete n repairs?

3.4.3 Number of services restored by the nth repair

Equation (27) suggest one approach to estimating service as repairs proceed: measure the remaining repairs r as a function of the breaks caused by the earthquake sequence, reduced by the number of repairs, and evaluate services available after n repairs have been completed as shown in Equation (28), to which I will refer as the serviceability-index approach.

$$V(n) = M \cdot \left(1 - \Phi \left(\frac{\ln\left(\frac{r-n}{L \cdot q}\right)}{\beta} \right) \right) \tag{28}$$

Or one could model services as being restored in proportion to the number of breaks remaining, as shown in Equation (29). Let us refer to this equation as the proportional approach.

$$V(n) = V_0 + (M - V_0) \cdot \left(\frac{n}{r} \right) \tag{29}$$

A more general approach is suggested by conversations with engineers of the East Bay Municipal Utility District (EBMUD). They indicated that their repair strategy in an earthquake would be to focus most of EBMUD's resources to repair transmission lines that serve large areas, then smaller diameter distribution lines that serve smaller numbers of customers, etc. The strategy would depend on how portions of the system, which may be impacted by breaks in large diameter pipes, could first be isolated to continue to maintain services to as many customers as possible by re-routing water using a combination of temporary system such as portable pumps, flexible hoses, etc. If one were to plot a restoration curve with fraction of customers receiving service on the y-axis, time after the earthquake on the x-axis, then a plot for EBMUD's strategy would maximize slope as soon as repairs begin. The slope might increase if the number of crews increases, but with constant resources, the slope will decrease as individual repairs restore fewer and fewer services. Equation (30) would have such a form for values of $0 < a < 1$. The smaller the value of a, the more the restoration curve would rise quickly early. Setting $a = 1$ in Equation (30) yields the proportional repair-restoration approach of Equation (29). Let us refer to Equation (30) as the power approach.

$$V(n) = V_0 + (M - V_0) \cdot \left(\frac{n}{r} \right)^a \tag{30}$$

If we assume that repairs after the 1994 and 1995 Northridge and Kobe earthquakes were completed at a constant pace, then the power approach with $a = 0.67$ resembles the observed restoration of water service in the San Fernando Valley after the 1994 Northridge earthquake (Figure 5A), while the power approach with $a = 0.33$ resembles restoration after the Kobe earthquake (Figure 5B). Figure 8 shows the three approaches all on the same plot (with two curves for the power approach, with $a = 0.33$ and $a = 0.67$). The y-axis is normalized by pre-earthquake number of services and the x-axis is normalized by number of pipeline breaks.

Of the three, the power approach matches the two earthquakes the best, proportional next best, and serviceability-index approach the worst. There may be many other reasonable approaches, but considering the three examined here, I will employ the power approach with the more conservative of the two a-parameter values considered here, i.e., $a = 0.67$.
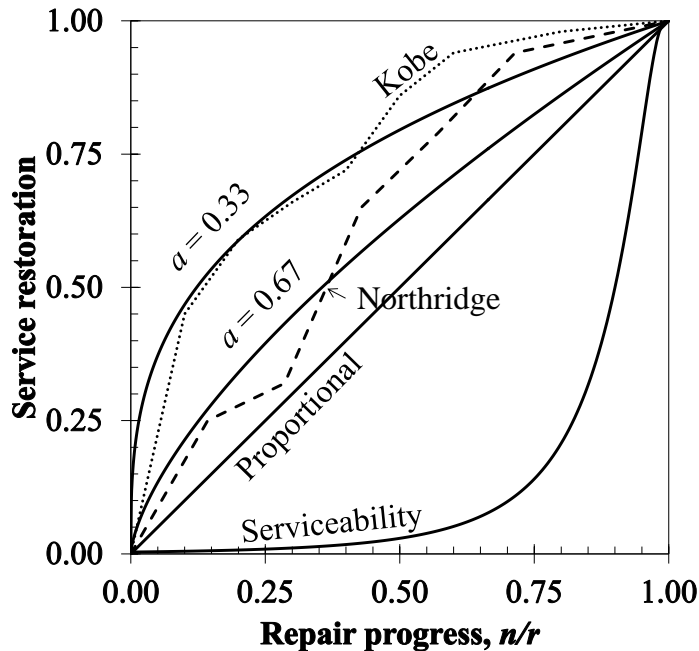
Figure 8. Parametric restoration curves with Kobe and Northridge experience

3.4.4 Repair resources and repair rate with lifeline interaction

Now that we can estimate the number of services available after completing *n* repairs, let us consider how long it takes to perform *n* repairs.

Section 2.5 summarizes a few sources of pipe repair time information: an empirical model of per-break repair time, an empirical model of regional repair time as a function of regional break rate, and expert opinion of per-break repair time that generally agrees with the empirical evidence, albeit slightly lower both in terms of lower mean repair time and narrower confidence bounds. Loss estimation practitioners generally prefer empirical models with explanatory power; for this reason I employ Schiff's (1988) pipeline repair data.

I analyzed the (relatively small) sample and found an average repair time of 7.6 hours and a standard deviation of 5.3 hours. Staff of the San Jose Water Company found that figure to be reasonable (J. Walsh, oral commun., 14 Oct 2015). A lognormal distribution with median repair time of 6.5 hours and logarithmic standard deviation of 0.70 fits the data sufficiently well to satisfy the Lilliefors (1967) goodness of fit test, as shown in Figure 9A. Separating the data for the small-diameter pipe repairs from the data for two large-diameter pipe repairs (24-inch damage instances, requiring 12 and 20 hours, respectively), the small-diameter median and logarithmic standard deviation are 6.1 hours and 0.58, respectively, as illustrated in Figure 9B. Schiff offers too few samples of large-diameter pipe repair time to derive an empirical distribution, so let us assume a median of 16 hours and a logarithmic standard deviation of 0.6.

The LADWP estimates of repair duration for distribution pipelines (Tabuchhi et al. 2010) generally agree with actual earthquake experience reported by Schiff. However they seem to underestimate uncertainty, with lower and upper limits that include only 70 percent of the repairs

reported by Schiff, omitting the lower and upper 15 percent of repair times of Figure 9A. They are also slightly optimistic, with modes at the 20th and 40th percentiles of repair times in Figure 9A.

It is difficult to compare the Hazus repair times with Schiff (1988) or Tabucchi et al. (2010) because the former measures repair time per worker and the latter two measure repair time per repair. However, assuming a crew size of 4, Hazus' per-worker repair times equate with 6 to 18 hours, or the 35th and 90h percentiles of Figure 9A.
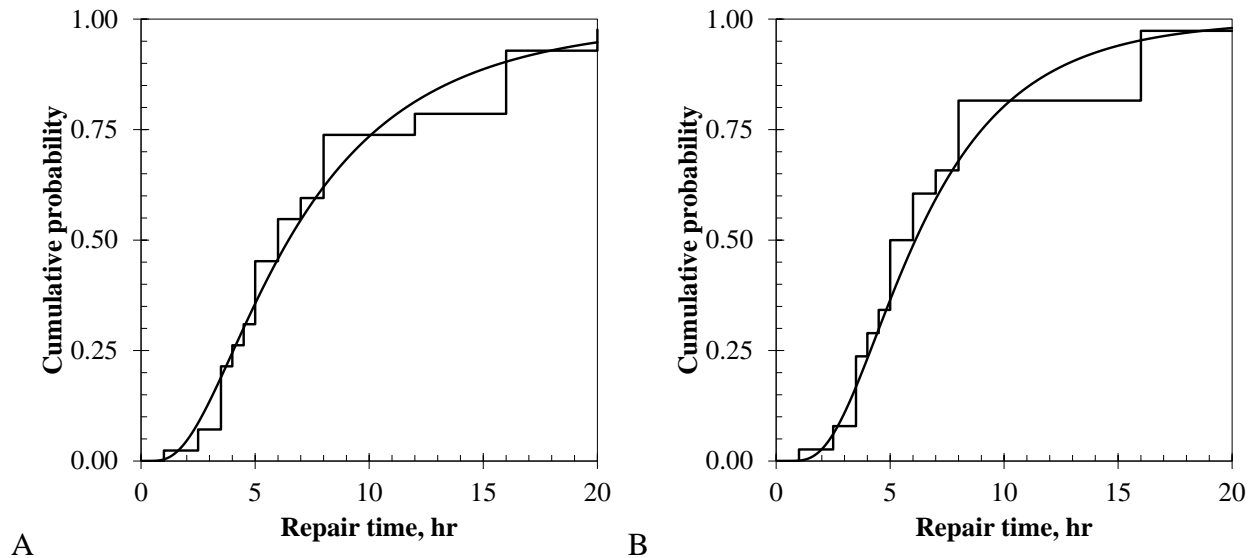
Figure 9. Repair times based on data from Schiff (1988): (A) all repairs (B) excluding repairs to large diameter pipe

For a deterministic model, it seems reasonable to use the mean estimate (7.6 hours per repair per crew, or 0.32 days per repair per crew) for small-diameter pipe repairs (here, assuming crews work 12 hours on, 12 hours off, until repairs are completed.

When will crews become available? As discussed earlier, public and private water agencies plan to provide mutual assistance for emergencies. CalWARN (ND) and East Bay Municipal Utility District (2014) report how three Bay Area water agencies dispatched teams to assist in the repair of water supply pipelines in the City of Napa after the 2014 South Napa earthquake. The assistance took 24 hours to arrive, which suggests a delay in the arrival of mutual aid from across a metropolitan region. Mutual aid in a major metropolitan earthquake would likely come from hundreds, possibly thousands of miles away, and probably take longer to mobilize, arrive, house, and integrate into repair operations. Repair resources ramp up over time, and the larger the disaster, probably the longer the ramp-up time. It may take several days to first assess the extent of damage and locate leaks before actual repairs can be initiated. Let us parameterize this assessment time and time to ramp up crews using a time-dependent model of the number of repair crews available to an agency.

$c(t)$ = number of repair crews operating on the day of time t
$w(t)$ = crew workload, fraction of day that crews work, e.g., 0.5 for 12 hours on and 12 hours off
d_0 = unconstrained repair duration, days per repair for one crew under ideal conditions, i.e., without constraints on materials, coordination, and other prerequisites
= 0.32 days on average

i = an index of rate-limiting factors. In Table 2, there are six such factors: communications, electricity, fuel, site safety (i.e., no fire), roadway access, and repair supplies.

t_0 = time at which the 1st repair is performed

t = time at which the nth repair is performed

$g_i(t)$ = flow of rate-limiting factor i at time t, normalized so that $g_i(t) = 1.0$ indicates unlimited availability, $g_i(t) = 0.5$ indicates that the flow or supply rate of factor i is half of what is normally available, and $g_i(t) = 0$ indicates that factor i is unavailable at time t. If for example there is no limit on fuel, g of fuel is 1.0. If a utility could only fuel half its repair vehicles, its g-value would be 0.5. If completing a phone call to coordinate repairs took twice as long as normal because of communications network congestion, its g-value would be 0.5. If one could not complete a phone call at all, the g-value for communications would be 0. In the case of a rate-limiting factor that is a lifeline with a number of service connections M_i and a number of service connections available at time t denoted by $V_i(t)$, then

$$g_i(t) = \frac{V_i(t)}{M_i} \tag{31}$$

u_i = rate-limiting factor, a constant to indicate the reduction in repair productivity in the absence of a resources required to perform a repair, also called a *u*-factor, and indexed by i. One assigns *u*-factors based on an estimate of the additional time required to carry out one repair if it is necessary to do so without the required resource. It is estimated as

$$u = 1 - \frac{d_0}{d_{impaired}} \tag{32}$$

Where d_0 is the average time required to perform a repair under normal conditions and $d_{impaired}$ is the average time it takes to perform a repair when the required resource required is unavailable. For example, if a repair takes 8 hours normally, but it takes 9 hours in the absence of a required resource, one assigns $u = 1 - 8\ hr/9\ hr = 0.11$. That is, productivity drops by 11% in the absence of the required resource. Thus, $u_i = 1.0$ indicates that resource i is critical to repairs: without it, repairs do not proceed. A *u*-value of 0.5 indicates that repairs proceed by half their normal rate when resource i is unavailable.

Let us denote by $f(t)$ the repair rate (repairs per unit time) at time t of the nth repair and estimate it as:

$$f(t) = \frac{w(t) \cdot c(t) \cdot \left(\prod_i \left(1 - u_i \cdot \left(1 - g_i(t)\right)\right) \right)}{d_0} \tag{33}$$

And let $\tau(n,t)$ denote the amount of time required to perform the nth repair, given that it starts at time t:

$$\tau(n,t) = \frac{1}{f(t)} = \frac{d_0}{w(t) \cdot c(t) \left(\prod_i \left(1 - u_i \cdot \left(1 - g_i(t)\right)\right) \right)} \tag{34}$$

We can now calculate $F(t)$, the total number of repairs completed by time $t+\tau$. It is given by

$$F(t) = 0 \qquad\qquad\qquad\qquad t < t_0$$

$$= \int_{t_0}^{t} f(t)\, dt \qquad\qquad\qquad t \geq t_0$$

$$= \int_{t_0}^{t} \frac{a(t) \cdot c(t) \cdot \left(\prod_i \left(1 - u_i \cdot \left(1 - g_i(t) \right) \right) \right)}{d_0} dt \qquad t \geq t_0 \qquad (35)$$

$$\leq r$$

Recall that $c(t)$ denotes the number of crews working on the day of time t, u_i denotes the importance of rate-limiting factor i (such as another lifeline), $g_i(t)$ denotes the flow of rate-limit factor i at time t (such as the fraction of fuel required that is actually available at time t), d_0 denotes the unconstrained repair duration, and r denotes the total number of repairs.

Equation (33) treats the effect of multiple required resources as multiplicative rather than a simple sum, but conceivably the effect is greater. The loss of only one out of two redundant resources (e.g., commercial power and emergency onsite power) might not hinder repairs at all, while the loss of both might entirely prevent repairs. I acknowledge that such a complication is possible, but for simplicity do not treat it here.

Note that for other lifelines, $F(t)$ might be part of a rate-limiting factor. For example, communication might require water service for evaporative cooling to cool some central offices. Suppose for example that from the perspective of communication, water has a u-value of 0.5 (half of central offices have evaporative cooling) and a g-value equal to the fraction of water services available, i.e.,

$$g_{water}(t) = \frac{V(n)}{M}$$

Water might in turn rely on communications, so a time series of simultaneous equations would have to be solved to find the simultaneous serviceability of multiple lifelines and other resources such as consumable repair supplies over time. Let us refer to the time series of restoration curves that satisfy their mutual restoration rates at all points in time as the equilibrium restoration solution.

3.4.5 Ordering lifelines to avoid circular lifeline interaction

It would be desirable to avoid having to solve simultaneous equations to find the equilibrium restoration solution. Let us introduce a simplification for practicality by constraining the model of lifeline interdependencies so that lifelines do not affect one another in a circle, that is, there are no pairs of lifelines i and j where j depends on i and i depends on j, either directly or through some intermediate lifeline k.

The lifeline interaction matrices presented in section 2.7 do not clearly order the lifelines; there is no sense that the 3rd row is somehow more or less of anything than is the 2nd row. However, to deal with circular interactions let us introduce an order to the lifeline interaction matrix so that lifelines appear in it in an approximate one-way chain of dependence, from so-called upstream lifelines first (upper rows, left-hand columns) to downstream lifelines last (lower rows, right-hand columns). If lifeline j depends on lifeline i, either directly or through an intermediary, but not vice

versa, then let us refer to lifeline *i* as being upstream of lifeline *j*, and order *i* before *j*. In our one-way model, downstream lifelines depend only on upstream lifelines or on none at all, and not vice versa.

This simplification requires compromising the fidelity of the model, because circular interactions probably exist. It takes fuel to repair a road, but to deliver fuel, one must drive over roads. This complication is ignored here for computational simplicity. There may be no right way to perfectly order these resources, and different people may judge the proper order differently. I propose the following order of lifeline repair resources, from upstream to downstream, based on the following rationale:

1. Consumable repair supplies. Without repair supplies, one cannot repair fuel supplies, roads, electricity, communications, water, or wastewater. They are commonly stored and do not spoil or otherwise depend on fuel, roads, electricity, mobile telecommunications, natural gas, water or wastewater.
2. Fuel. Without fuel for repair vehicles, one cannot repair roads, electricity, communications, gas, water, or wastewater. One cannot pump fuel until damaged equipment at fuel depots is repaired, which requires consumables, but repairs do not require roads, electricity, mobile telecommunications, natural gas, water, or wastewater to use. Admittedly without water, one cannot create fuel, but fuel can be transported from somewhere else that has water. One must also use roads to access and to deliver fuel, but the road network is so redundant and it is often easy enough to travel at least slowly over damaged roads that any dependence seems weak.
3. Roads. To repair roads requires consumable repair supplies and fuel, but one can operate roads without electricity, natural gas, water, or wastewater. One can communicate with road repair crews through direct, face-to-face meeting.
4. Electricity. To repair damaged electric generation, transmission and distribution facilities requires consumable repair supplies, fuel, and access via roads. One can repair electric without electricity, natural gas, water, and wastewater. One can communicate with road repair crews through direct, face-to-face meeting.
5. Communication, especially mobile telephones. Damage to central office and cell tower equipment requires consumable repair supplies. Powering then requires electricity or fuel. As with fuel, the dependency of communication on roads is weak but the dependency of roads on communication seems weaker. Operating or repairing central offices and cell towers does not seem to require natural gas, water, or wastewater. An exception is that some central offices may employ evaporative cooling, which requires makeup water.
6. Natural gas. The repair of damaged natural gas pipelines and other components requires consumable repair supplies, fuel, and roads (to a modest extent). Repair of damaged natural gas pipelines seems like a time-critical need that requires rapid communication and coordination, which seems to call for electricity and communication. To operate a natural gas system does not seem to require water or wastewater.
7. Water. The repair of a damaged water system requires consumable repair supplies, fuel, and roads (to a modest extent). To supply water in a pressure zone that relies on pumping requires electricity. Repair of damaged water pipelines seems like a time-critical need that requires rapid communication and coordination, which seems to call for electricity and communication. To operate a water system does not seem to require natural gas, so the order of natural gas and

water is arbitrary. The operate a water system does not seem to require a functioning wastewater system.

8. Wastewater. The repair of a damaged wastewater system requires consumable repair supplies, fuel, and roads (to a modest extent). To treat wastewater and to operate lift stations requires electricity. Coordinating the repair of damaged wastewater pipelines seems to depend to a limited extent on electricity and communication. To operate a wastewater system does not seem to require natural gas, so the relative order of natural gas and wastewater is arbitrary. The operate a wastewater system does not seem to require a functioning water system, so their relative order also seems arbitrary.

3.4.6 Rate-limiting factors for lifeline repairs

In the present formulation, I quantify the effect of the loss of a repair resource by the rate-limiting factor u that measures the reduction in repair productivity (repairs per unit time) when the required resource is unavailable. In the case of water supply, the list of tasks required to repair a pipeline break (Table 2) indicates that the rate-limiting factors include communications, electricity, fuel, site safety (e.g., no fire), roadway access, and consumable repair materials. How much does the loss of each resource slow repairs?

- Consumables. Without replacement pipe and fittings, clamps, etc., repairs do not proceed. Let $u_{consum} = 1.0$

- Fuel is required for a repair crew to travel to the location of the break, operate a backhoe to dig down to the water main, and to backfill the excavated area (tasks 2, 6, and 9 in Table 2). Repairs do not proceed at all without fuel. Let us therefore assign $u_{fuel} = 1 - 8 \text{ hr}/\infty = 1.0$. That is, repair productivity drops by 100% while electricity is unavailable.

- Roads. Damage to roads could delay the initial delivery of additional equipment and crews, but the roadway network is highly redundant. Let $u_{road} = 0.0$.

- In the case of a water supply system that relies entirely on gravity to supply water, electricity is required for receiving notices about breaks (task 1), referring to GIS-based system maps (not shown in Table 2), and powering stoplights that control traffic and facilitate crews traveling from repair to repair. Let us assume that the addition time required to refer to paper maps occurs at headquarters while repairs are ongoing and does not actually slow repair crews, but that travel from repair to repair increases repair duration by 15 minutes: $u_{electr} = 1 - 8 \text{ hr}/8.25 \text{ hr} = 0.03$. That is, repair productivity drops by 3% while electricity is unavailable.

- In the case of a water supply system with pumped pressure zones, repairs may require electricity to provide water in order to locate leaks. For a utility with pumped pressure zones that relies on the commercial electric utility to provide a fraction z of its services (i.e., after accounting for the utility's own emergency generators), let us add the quantity z to u_{electr} as calculated above, i.e., $u_{electr} = 0.03 + z$.

- Communications. Let us treat this solely as cellular communications, and assume that utilities possesses or can quickly acquire portable radios to communicate between their headquarters, repair crews, and a county emergency operations center. Compared with cellular, using a radio to communicate might slow the effort of receiving notices about water main breaks (task 1) and contacting other utilities to coordinate safety (task 4). Using radios might reduce repair productivity slightly, but not enormously. Let us assume that

radio communication would increase the time to perform one repair by say 30 minutes in an 8-hour repair, suggesting $u_{commun.} = 1 - 8\ hr/8.5\ hr = 0.06$ for communications. That is, repair productivity drops by 6% while cellular service is unavailable.

Site safety does not appear in the lifeline interaction matrices of section 2, but seems worth addressing if only to dismiss it. Let us assume that fires alter the order in which repairs are performed but do prevent repairs, and that gas leaks will be shut off in a matter of hours after the earthquake and will not substantially hinder pipeline repairs afterwards. Let $u_{safety} = 0.0$.

Let us tentatively assign the u-values shown in Table 9. The table shows for example that consumables (pipe, clamps, etc.) have a u-value of 1.0 for water supply. By Equation (33), $u = 1$ means that repairs depend so strongly on consumables that without them repairs halt. That is, if at some point in time t, the available supply runs out, $g(t) = 0$ for consumables, and repair rate $f(t)$ goes to 0 until supply is restored.

I have assigned the same u-values to other lifelines that I have proposed for water, with one exception. It seems as if restoring mobile telephone service (under the label of communication) is more dependent on electricity than are water pipeline repairs. Presumably the repair of equipment in central offices and the repair of cell towers requires either on-site generators or commercial power to power the equipment. Cell towers are generally supplied with onsite power in the form of uninterruptible power supply (UPS), sufficient for 4 to 8 hours of service if commercial power is interrupted (S. Daneshkah, oral commun. 4 Nov 2014). In the case of Verizon Wireless, 90% of cell sites in Northern California are also equipped with generators in addition to UPS (T. Serio, oral commun. 14 Jan 2014).

Let us guess that all COs and 1 in 3 cell towers have a generator on site (as in the case of most Verizon towers) and that, telecommunication being a national security priority, carriers can supply fuel to those central offices and towers. Let us guess that repairing the cell towers is what dominates repair efforts for cellular communications. If 33% of cell towers have generators, then the loss of commercial electricity prevents 67% of repairs entirely, and does not hinder the other 33% at all, hence productivity drops by 67%, implying $u = 1 - 0.67 = 0.33$. The u-values are qualitatively consistent with the San Francisco Lifeline Council's (2014) lifeline system interdependency matrix, in that darker shading in Table 7 corresponds to higher numerical values in Table 9.

Table 9. Tentative interdependency u-values

Upstream→ Downstream ↓	Consumables	Fuel	Roads	Electr.	Commun	Nat. gas	Water
Fuel	1.0						
Roads	1.0	1.0					
Electricity	1.0	1.0	0.0				
Communication	1.0	1.0	0.0	0.33			
Natural gas	1.0	1.0	0.0	0.03	0.06		
Water	1.0	1.0	0.0	0.03+z	0.06	0.0	
Wastewater	1.0	1.0	0.0	0.03+z	0.06	0.0	0.0

z denotes the fraction of services in pumped pressure zones

3.4.7 Depicting lifeline interaction with an influence diagram

It can sometimes help to depict the relationships among decisions, uncertain quantities, and value outcomes using an influence diagram. These diagrams, sometimes also called a relevance diagrams, decision diagrams, and decision networks, are graphical representations of a decision situation. They can represent a mathematical model that relates the decisions, uncertain quantities, and uncertain value outcomes with functional relationships. They are commonly used in decision analysis. They tend to be more compact than decision trees, able to show more information in less space. The interested reader is referred for more background on influence diagrams to Howard (1990). The interdependencies implied by Table 9 are depicted in an influence diagram in Figure 10.

In the influence diagram, decisions are depicted in rectangles, uncertain quantities in ovals, and mathematical dependency by arrows. Time generally flows from left to right or from top to bottom in an influence diagram; here time flows from left to right. Each arrow starts at a quantity (a decision or an uncertainty) and points to another quantity. An arrow implies that the second quantity depends to some extent on the first. Where there is no arrow connecting one quantity to another, the implication is that neither quantity depends on the other. For example, there is no arrow from roadway restoration to any of the other lifeline restoration uncertainties. This is not strictly true, at least according to the San Francisco Lifelines Council (2014) and other lifeline interaction matrices, but for practical reasons any such dependency can be ignored because the roadway network is so redundant that it seems unlikely that realistic roadway damage could significantly impair restoration of other lifelines. There is an arrow corresponding to each nonzero quantity in the interdependency matrix of Table 9. The arrow is omitted where the corresponding u-value in Table 9 has a zero value.

The figure omits the dependence of lifeline restoration after aftershock 1 on fuel supply and on consumable repair resources, but the omission is just for clarity. In practice, or at least in the calculations performed here, those dependencies exist.

Figure 11 distills the influence diagram to combine all upstream lifelines together and all downstream lifelines together. The figure also adds value outcomes—the quantities that in the end the analyst cares about, which in the present case is indirect business interruption loss. In the canonical influence diagram, value outcomes are shown as hexagon at the right side of the diagram. Indirect business interruption can be quantified by others as a function of the restoration of the lifelines; that task of disaster economic is not addressed here.
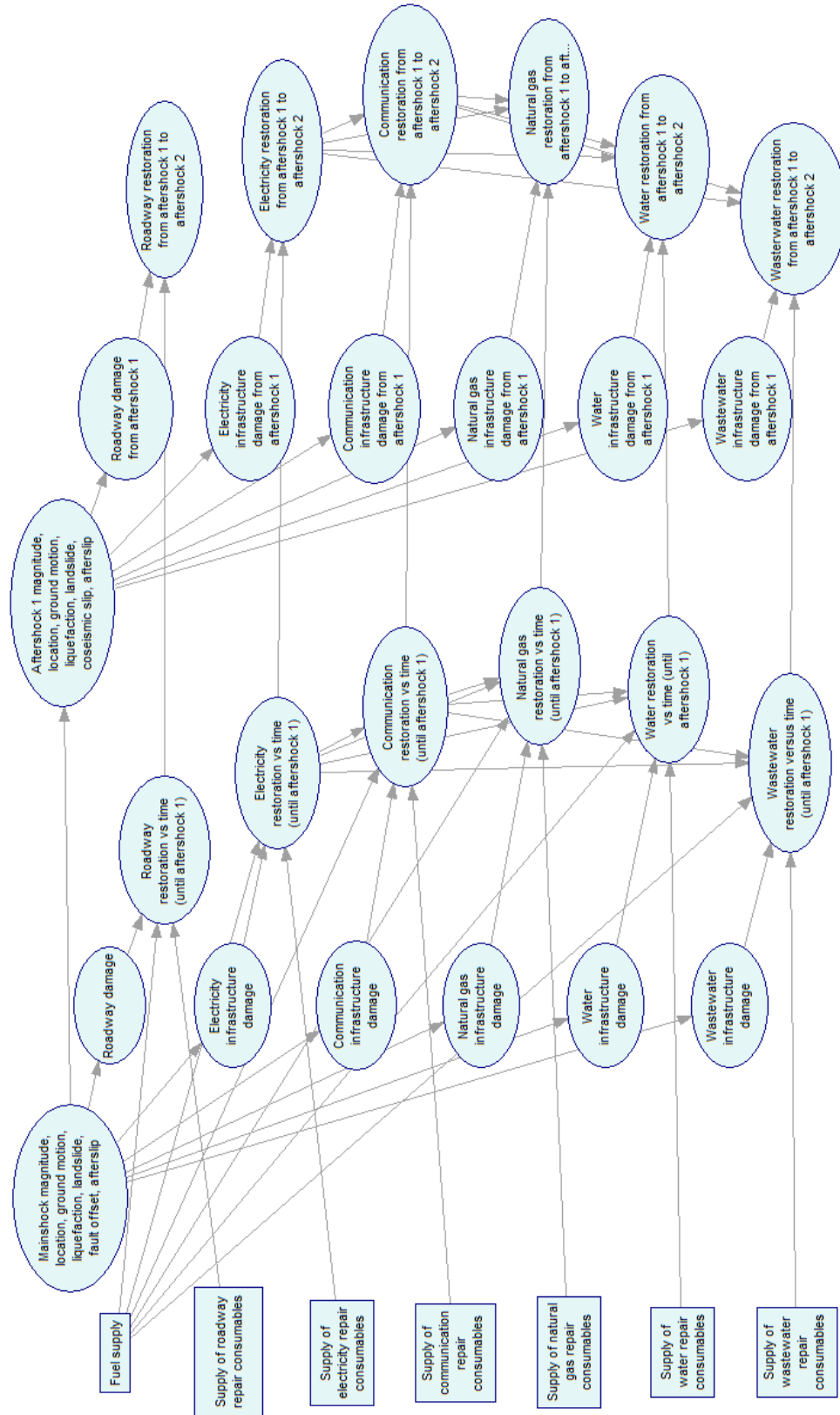
Figure 10. Lifeline interaction influence diagram
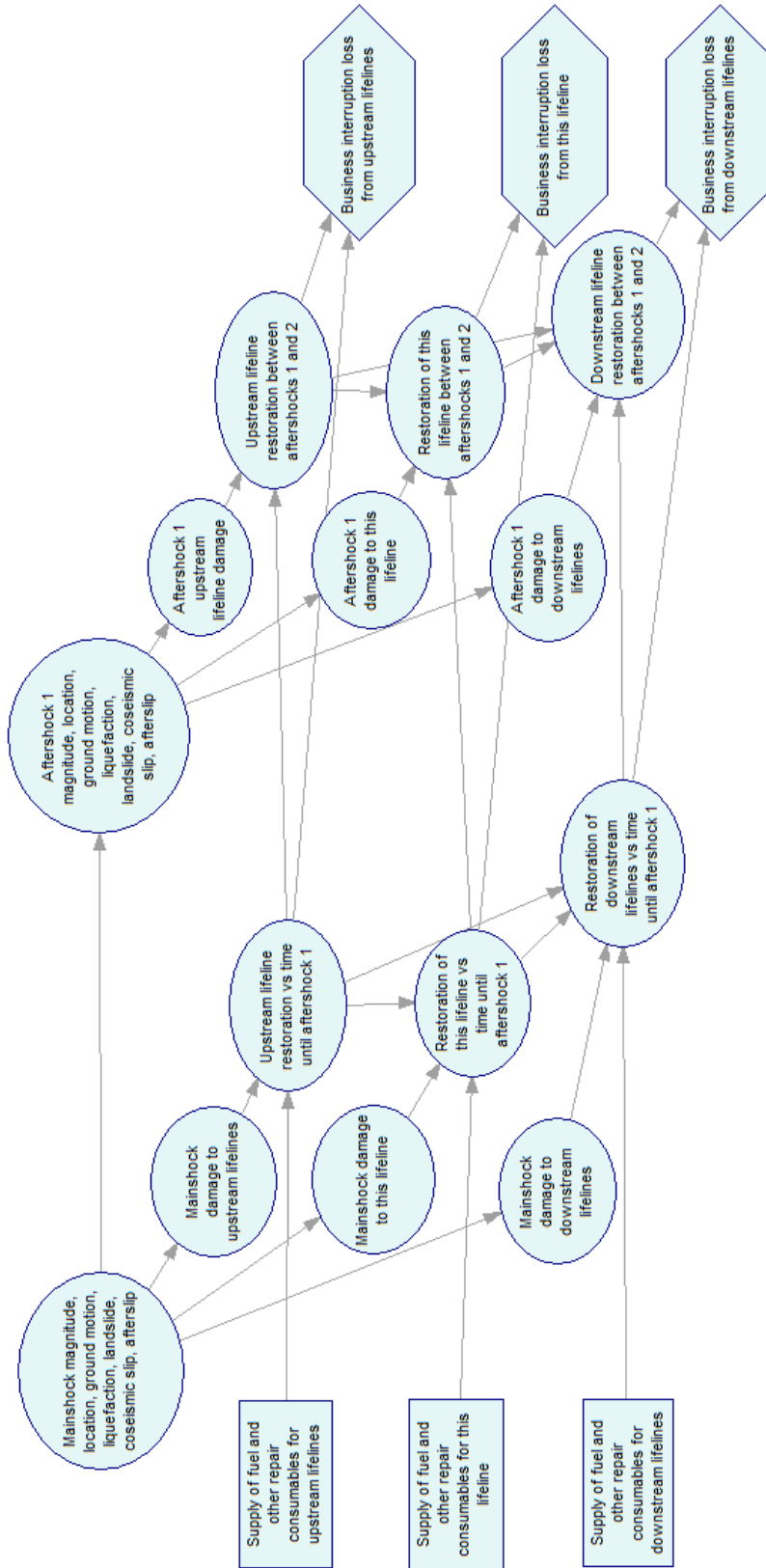
Figure 11. Alternate lifeline interaction influence diagram, showing value outcomes

3.5 Measuring water supply resilience

As proposed by Bruneau et al. (2003), let us view the area above the restoration curve *R* as a measure of the loss of resilience: less area means less impact, faster recovery, or both. Recall that Bruneau et al. (2003) measured *R* as in Equation (36):

$$R = \int_0^{t_1} \left(1 - Q(t)\right) dt \tag{36}$$

where $Q(t)$ denotes the degree of service as a fraction of full service at time *t*, and times $t = 0$ and $t = t_1$ denote the initiating event (the earthquake) and the time of full restoration, respectively. For present purposes, let us measure $Q(t)$ as the fraction of all service connections receiving water at time *t*, whether treated or not, whether at normal pressure or not (which one can call "wet water," as opposed to treated water). Since the present analysis calculates $V(t)$, the number of service connections receiving water at time *t*, one can normalize $V(t)$ by the number of service connections, denoted here by *M*, and substitute:

$$R = \int_0^{t_1} \left(1 - \frac{V(t)}{M}\right) dt \tag{37}$$

R can be seen as the average number of days a service connection loses service. It will be useful to estimate the total economic impact of the loss of resilience, which relates more closely to the number of service-days lost, $R \cdot M$:

$$R \cdot M = \int_0^{t_1} \left(M - V(t)\right) dt \tag{38}$$

Let us measure the benefit of a mitigation option in terms of the reduction in R·M relative to some baseline condition such as as-is conditions:

$$\Delta(R \cdot M) = (R \cdot M)_{baseline} - (R \cdot M)_{what-if} \tag{39}$$

where "what-if" indicates the loss of resilience with the mitigation measure.

Suppose that in some cases, loss of water supply is the sole cause that a home or business loses function, and the home residents or business occupants experience a financial loss as a consequence. (Loss of water service caused 18% of business closures after the 1994 Northridge earthquake, according to Tierney's 1995 survey.) A household might have temporarily move to a hotel until water is restored, or a business might suspend operations until water is restored. What would be the daily cost of lost service?

In the San Francisco Bay Area, moving to a hotel might cost a household on the order of $560 per day including accommodations, meals, and incidental expenses. (San Francisco Bay Area average household size is 2.7 [http://goo.gl/NAOnhZ] and the 2016 GSA per diem rate for Oakland is $209 including lodging, meals, and incidental expenses: 2.7·$209 = $564.) Alameda County contains 140,000 firms (http://goo.gl/b9O19I), which had total sales in 2007 of $81.6 billion, suggesting an average daily business revenues of $1,600. Considering that Alameda County has 545,000 households (http://goo.gl/b9O19I), the average daily cost of loss of function of a household or business establishment can be estimated as the weighted average of $560 and $1,600, or $770. Until an economic analysis is performed, one can take $770 as the average cost of one lost service-day.

3.6 Optional stochastic simulation methodology

3.6.1 Simulation of earthquake excitation

The present work can be applied to an earthquake planning scenario that requires only a single realistic outcome, not best, worst, or mean cases or any particular probabilistic outcome. However, to make the work more generally useful, it is convenient to add features that allow the analyst to treat earthquake damage to a water supply system as stochastic, i.e., uncertain, random.

I will treat the simulation of the earthquake excitation only superficially; the interested reader is referred to Chen and Scawthorn (2003) for methods to generate a stochastic set of earthquakes that are consistent with the seismicity of regional faults, their possible earthquake magnitudes and rupture locations. In the United States, the National Seismic Hazard Mapping Program (e.g., most recently Petersen et al. 2014) can offer a model of seismicity.

For each mainshock rupture in the stochastic set, one generates an earthquake sequence of foreshocks, mainshock, and aftershocks. Ogata (1998) provides a general reference for modeling aftershocks using an epidemic-type aftershock sequence (ETAS). Field et al. (2013) developed an ETAS model for California.

Median ground motion and logarithmic standard deviations of ground motion in each earthquake in the sequence can be calculated using convenient and regionally appropriate ground motion prediction equations. In the case of the Hayward Fault mainshock, I adopted results of a physics-based model by Aagaard et al. (2010a, b), but one can also use less-expensive methods. For example, for shallow crustal earthquakes in active tectonic regimes, one can use the NGA West 2 ground motion prediction equations; see Boore et al. (2014).

Ground motion is uncertain and spatially correlated. Here, uncertain means that ground motion it can be higher or lower than the median predicted by the ground motion prediction equations, potentially many times higher and lower. It is important to treat that variability about the median: ignoring it will tend to bias damage and loss estimates low. One can simulate a properly varying and spatially correlated field of ground motion using Jayaram and Baker (2009).

3.6.2 Simulation of pipeline vulnerability

Vulnerability of buried pipeline is uncertain. To simulate break rate in buried pipe subjected to wave passage, landslide, and liquefaction, one can draw two sample u_1 and u_2 from a U(0,1) uniform distribution (i.e., equally likely to take on any value between 0 and 1), and simulate break rates in buried pipeline by substituting u for the nonexceedance probability p. For example, in the present adaptation of Eidinger's (2001) model, Equation (22), one substitutes u for p as shown in Equations (40) and (41):

$$u_1 \sim u_2 \sim U(0,1) \tag{40}$$

$$R\left(PGV, P_L, u_1, u_2\right) = \left(1 - P_L\right) \cdot K_1 \cdot 0.00187 \cdot PGV \cdot \exp\left(1.15 \cdot \Phi^{-1}\left(u_1\right)\right)$$
$$+1.88 \cdot K_2 \cdot P_L \cdot \exp\left(0.74 \cdot \Phi^{-1}\left(u_2\right)\right) \tag{41}$$

The symbol ~ here means "is a sample taken from the distribution." Equation (40) says, "draw a sample u_1 and another sample u_2 from a U(0,1) distribution." Each assignment can be carried out in a spreadsheet using, for example Microsoft Excel's rand() function, which produces a sample U(0,1) and changes it each time the spreadsheet is recalculated.

The simulation equations assume that vulnerability to wave passage varies independently from vulnerability to ground failure, but that the intra-system vulnerability for each peril is completely correlated. That is, all wave-passage break rates within a system will be uniformly higher or lower than average in a given system, and all ground-failure break rates within a system will be uniformly higher or lower than average in a given system.

3.6.3 Simulation of damage to buried pipeline

Next, simulate the damage to the buried water supply pipeline system. The simulation treats the break rates as uncertain as shown in Equation (41). Let us denote by r_i the simulated break rate in each segment of pipe. The simulation then treats the number of leaks or breaks in any given segment of buried pipe i as distributed with a Poisson distribution whose mean rate r is estimated from Equation (26) for summand i. The Poisson distribution is a discrete probability distribution that expresses the probability of a given number of events occurring in a fixed interval of time or space if these events occur with a known average rate and independently of the time or distance between events. In this case, the events are breaks or leaks and the fixed interval of space is the length of the pipe segment.

So, conditioned on the mainshock shaking and ground failure values (here, PGV and P_L) at each pipe segment's midpoint, and on the vulnerability function assigned to each component (here, K_1, K_2, and L values for each pipeline segment), the simulation assumes that the probability of exactly y breaks on segment i ($y \in \{0, 1, 2, ... \}$) is given by Equation (42). The probability that y or fewer breaks occur is given by Equation (43), which is the cumulative distribution function for the Poisson distribution with rate parameter r_i.

$$P\left[Y_i = y\right] = \frac{r_i^y \exp\left(-r_i\right)}{y!} \tag{42}$$

$$P\left[Y_i \leq y\right] = \sum_{n=0}^{y} \frac{r_i^n \exp\left(-r_i\right)}{n!} \tag{43}$$

$$Y_i = \max\left(y : u_i \leq P\left[Y_i \leq y\right]\right) \tag{44}$$

To simulate a particular number of breaks in segment i, one draws a sample u_i from a uniform distribution $u_i \sim$ U(0,1) and solves Equation (44) for y. The equation inverts the cumulative distribution function of a Poisson distribution with rate r_i at u_i to produce the number of simulated breaks on segment i. I know of no closed-form expression for the value of Y_i in Equation (44), but simulation software such as @Risk can perform the simulation.

Equation (44) does not include breaks at where the pipeline crosses the fault. To deal with pipe breakage at fault offset, let us take d_f from Equation (26) as uncertain. It is common to take fragility functions as approximated by a lognormal cumulative distribution function, so absent a better empirical or analytical model, let us do so here, and assume a median value $\theta = 4$ inches and logarithmic standard deviation $\beta = 0.6$. I propose this particular median value because it seems like a reasonable threshold in light of Eidinger's liquefaction vulnerability function in Figure 7. I propose this particular logarithmic standard deviation because it reflects a relatively large degree of uncertainty, compared with other fragility functions such as those in FEMA P-58 (Applied Technology Council 2012).

To use these fragility parameters to model pipe breaks due to fault offset, for each segment i that crosses the fault, add 0 or 1 pipe breaks per Equation (45). In the equation Z_i denotes either 0 or 1 pipe breaks produced by fault offset at segment i, $I(\cdot)$ is the indicator function (1.0 if the term in parentheses is positive, 0.0 if negative), $\Phi(\cdot)$ is the standard normal cumulative distribution function evaluated at the term in parentheses, d_i is the fault offset distance where the fault intersects pipeline segment i, θ and β are as just defined, and u_i is another sample from a uniform distribution $u_i \sim U(0,1)$. To explain the equation, the Φ term gives the probability that segment i is broken. If u_i is less than that probability, then the simulation says that that segment is broken, that is, that that segment's uncertain capacity to resist fault offset was less than d_i.

$$Z_i = I\left(\Phi\left(\frac{\ln\left(d_i/\theta\right)}{\beta} \right) - u_i \right) \tag{45}$$

Finally, one can sum over all pipeline segments to simulate the total simulated number of breaks W, as in Equation (46):

$$W = \sum_{i=1}^{n}\left(Y_i + Z_i\right) \tag{46}$$

3.6.4 Simulation of restoration

As shown in Figure 9, time to repair a break or leak is uncertain and approximately lognormally distributed. Let us use the parameters derived from Schiff's data for small-diameter pipe and the assumed parameters for large-diameter pipe as recapped in Table 10. Repair duration for a single break can be estimated using Equation (47). In the equation, u_i is a random number drawn from a uniform distribution, $u_i \sim U(0,1)$, and is not the same u_i value as used elsewhere in this section.

Table 10. Uncertain pipe-repair duration

	Median, θ (hr)	Logarithmic standard deviation, β	Basis
Small diam (<20 in)	6.1	0.58	Schiff (1988)
Large diam ($\geq$ 20 in)	16	0.6	Schiff (1988) and judgment

$$d_{0,i} = \theta \cdot \exp\left(\beta \cdot \Phi^{-1}\left(u_i\right)\right) \tag{47}$$

It is problematic to offer a stochastic model for number of services lost as a function of damage (the serviceability index), partly because the use of the serviceability index seems so tenuous to

begin with. Treating it as uncertain with a specified model seems like illusory thoroughness — cutting the baloney too thin. However, until a better model comes along, let us treat the initial level of service V_0 (now an uncertain quantity rather than a deterministic value) as beta-distributed with bounds 0 and 1, mean value given by Equation(48), and coefficient of variation $\delta = 0.5$ (this last by eye from Figure 4). (For the reader who is unfamiliar with the beta distribution, it is a commonly used probability distribution for an uncertain quantity that can take on a value only between two bounds, such as between 0 and 1, and has a specified mean and standard deviation.) The parameters of the beta distribution, denoted here by α and β, can be calculated as shown in Equations (50) and (51). The inverse cumulative distribution function for the beta distribution is approximated by the inverse of the Kumaraswamy cumulative distribution function (Kuramaswamy 1980, Jones 2009), which is easier to calculate. One generates a sample of a uniform distribution $u \sim U(0,1)$ and evaluates the inverse cumulative distribution function of the Kumaraswamy distribution as shown in Equation (52) to produce a sample of the initial level of service V_0.

$$\mu = M \cdot s(r)$$

$$= M \cdot \left(1 - \Phi \left(\frac{\ln\left(\dfrac{r}{L \cdot q}\right)}{b} \right) \right) \tag{48}$$

$$\delta = 0.5 \tag{49}$$

$$\alpha = \frac{(1-\mu)}{\delta^2} - \mu \tag{50}$$

$$\beta = \alpha \cdot \left(\frac{1}{\mu} - 1 \right) \tag{51}$$

$$V_0 = F^{-1}(u) = \left(1 - (1-u)^{1/\beta} \right)^{1/\alpha} \tag{52}$$

The rate-limiting factors of section 3.4.6 can similarly be treated as beta-distributed (which one can approximate using the Kumaraswamy distribution as before) bounded by 0 and 1, with means as proposed in Table 9. Values that are assigned 0 or 1 in the table can be taken as certain, i.e., with coefficient of variation equal to 0. Rate-limiting factors greater than 0.0 and less than 1.0 are uncertain; let us take their coefficient of variation as substantial, say 1.0. That is, let

$\quad u$ = a sample of the (possibly uncertain) rate-limiting factor
$\quad m$ = expected value of the rate-limiting factor, from Table 9
$\quad d$ = assumed coefficient of variation of the rare-limiting factor
$\quad d = 1 \quad m \notin \{0,1\}$ (the symbol $\notin$ means "is not a member of the set listed here")
$\quad \quad = 0 \quad$ otherwise
$\quad v$ = a sample of a uniform distribution bounded by 0 and 1, i.e., $v \sim U(0,1)$. I use v here for the sample uniform variate because u is already in use in this step.

Then,

$$a = \frac{(1-m)}{d^2} - m \quad d \neq 0 \tag{53}$$

$$b = a \cdot \left(\frac{1}{m} - 1\right) \quad d \neq 0 \tag{54}$$

$$u = \left(1 - (1-v)^{1/b}\right)^{1/a} \quad d \neq 0$$
$$= m \quad d = 0, \text{ i.e., } m \in \{0,1\} \tag{55}$$

The symbol $\in$ means "is a member of the set listed here, i.e., inside the curly brackets."

3.7 Accounting for afterslip and aftershocks

Aftershocks produce new damage to a system that may be only partially repaired. To estimate number of required repairs after an aftershock, let us estimate new damage as if it occurred to a pristine system. Add the number of repairs that have not yet been completed, and recommence the calculation of services restored by the nth repair and time required to perform the nth repair.

Afterslip can increase the deformation on a pipeline segment at a fault crossing where the pipeline is already strained by coseismic (and possibly preseismic) slip. One way to model pipeline damage due to afterslip is to treat the pipe as having a fixed capacity to resist deformation.

When the coseismic slip plus afterslip at a point where a pipeline segment crosses the fault reaches that capacity, the pipe breaks. The capacity can be treated as having a deterministic value or a probabilistic value. As discussion in section 2, the capacity in reality depends on the material, pipe diameter, jointing, and sense of deformation, i.e., whether in tension, shear, or compression. For simplicity for present purposes I propose to treat the capacity as having a single scalar quantity for all materials, diameters, etc., per Equation (24) for a deterministic model or Equation (45) for a stochastic model.

3.8 Adjusting Hazus' lifeline restoration model

3.8.1 Why one might need to adjust the restoration curves offered by Hazus-MH

As discussed in section 2, Hazus-MH is FEMA-funded software to perform risk analysis for earthquakes, hurricanes, and floods in the United States. Hazus performs hazard analysis, damage analysis, loss analysis and recovery analysis including repair costs, life-safety impacts, and the duration and economic losses resulting from loss of function. It includes built-in asset definitions for virtually the entire built environment of the US, including lifelines, and encodes other restoration parameters such as the number of workers available to perform repairs. It is a very powerful tool.

In the author's experience, loss-estimation software, not matter how advanced, becomes obsolete soon after its release. Users see that the software's capability extends to X and soon conceive of a new need ΔX that that the software does not satisfy. Hazus-MH is like that. The new need identified here is the ability to treat lifeline interactions and aftershocks. Hazus-MH is currently closed source, so the analyst who wants to add the ability to treat lifeline interaction and

aftershocks cannot do so by changing the source code, although many parameters can be changed. How can one modify the outputs, using principles presented here to do so?

3.8.2 Adjusting Hazus' estimates of lifeline restoration to account for repair crews

Before addressing lifeline interaction and aftershocks, let us consider the situation where a Hazus-MH analysis has already been performed and the user realizes that an important adjustable parameter—the number of workers available to perform repairs—was wrong? The Hazus-MH default value for the number of water-supply pipeline repair workers available in each county appears to be 100 regardless of the size of the county, which may be far from accurate in many cases. If the analyst has a supposedly better estimate of the number of repair workers in a particular county, how can the analyst adjust Hazus's restoration estimate to account for that better estimate of repair crews after the fact? Let us assume that repair progress increases linearly with number of repair crews. It seems uncontroversial to adjust Hazus' estimated restoration curve to account for a different estimate of repair-crew resources as shown in Equation (56):

$$V(\tau) = \int_{t=0}^{\tau} \frac{q(t)}{q_0} \cdot \left(\frac{d\hat{V}(t)}{dt} \right) dt \tag{56}$$

$$\leq M$$

where

$$\frac{d\hat{V}(t_j)}{dt} \approx \frac{\hat{V}(t_{j+1}) - \hat{V}(t_j)}{t_{j+1} - t_j}; \qquad j \in \{1, 2, ...5\}$$

$$\geq \frac{d\hat{V}(t_{j-1})}{dt} \qquad j \in \{2,3,4,5\} \tag{57}$$

Let us also assume

$$\hat{V}(t_6) = M \tag{58}$$

where

$\hat{V}(t_j)$ = Hazus' estimate of the number of service connections with water service at time t_j assuming default values of the number of workers, for the geographic area of interest, e.g., a county

j = an index to points in time after the earthquake, $j \in \{1, 2, ... 6\}$

t_j = time after the earthquake, $t_j \in \{1, 3, 7, 30, 90, 540\}$ days, where t_6, 540 days, is added to Hazus' basic list of 5 points in time (1, 3, 7, 30, 90) days to account for the fact that Hazus-MH might report incomplete restoration at 90 days, and the analyst may need to evaluate restoration after 90 days

$q(t)$ = analyst's estimate of the number of water pipeline repair workers available in the county at time t

q_0 = Hazus default value used in the analysis (e.g., 100)

M = number of service connections in the geographic area of interest (a county)

The inequality in Equation (57) is necessary in case $\hat{V}(t_{j+1}) = M$, i.e., the unadjusted Hazus estimate of restoration is complete in the time between tj and tj+1, which would produce an unrealistically low restoration slope.

Let us refer to $q(t)/q_0$ as the repair-crew availability factor, and let us refer to $V(t)$ as the repair-crew-adjusted estimate of restoration before accounting for lifeline interaction. Equation (56) says that the pace of repairs at time τ is estimated as Hazus' estimate (the derivate gives the rate of restoration, i.e., services restored per unit time), increased by the repair-crew availability factor, i.e., to account for the analyst's estimate of the correct number of repair workers available at time τ, and integrated from time 0 to time t.

For the special case of constant $q(t)$, let us substitute the constant q for $q(t)$. Given constant q and piecewise linear restoration $V(t)$ to go with Hazus' limited set of $\hat{V}(t)$ values, one can evaluate Equation (56) to evaluate the repair-crew-adjusted estimate of restoration before accounting for lifeline interaction as shown in Equation (59):

$$V(t_j) = V(t_1) + \sum_{k=1}^{j-1} \frac{q}{q_0} \cdot \left(\frac{d\hat{V}(t_k)}{dt} \right)(t_{k+1} - t_k) \quad j \in \{1,2,3,4,5\} \tag{59}$$
$$\leq M$$

3.8.3 Accounting for lifeline interaction in Hazus-MH

Hazus-MH's restoration curves do not consider lifeline interaction. As of this writing, Hazus-MH evaluates restoration at five points in time after an earthquake: 1, 3, 7, 30, and 90 days. Let us further modify the restoration rate from Equation (56) as shown in Equation (60):

$$\frac{dV'(t)}{dt} = \frac{dV(t)}{dt} \cdot \prod_{i=1}^{n} \left(1 - u_i \cdot \left(1 - g_i(t)\right)\right) \tag{60}$$

where

$$V'(t) = V(t_0) + \int_{\tau=0}^{t} \frac{dV'(\tau)}{d\tau} d\tau \tag{61}$$

u_i is as previously defined (see Table 9), and

$g_i(t)$ is as defined in Equation (31), i.e., the flow of rate-limiting factor i divided by the pre-earthquake flow. In the case of a lifeline, g is the fraction of service connections in upstream lifeline i receiving service at time t, after accounting for lifeline interaction with *their* upstream lifelines. In the case of consumable repair supplies, g is the flow of repair supplies as a fraction of the amount needed.

The product in Equation (60) is just another factor that modifies the restoration rate, like q/q0 in Equation (59). We can include lifeline interaction by multiplying the restoration rate by this additional factor, as in Equation (62):

$$V'(t_j) = V'(t_1) + \sum_{k=1}^{j-1} \frac{q}{q_0} \cdot \left(\frac{d\hat{V}(t_k)}{dt} \right) \left(\prod_{i=1}^{n} \left(1 - u_i \cdot \left(1 - g_i(t)\right)\right) \right)(t_{k+1} - t_k) \quad j \in \{1,2,3,4,5\} \tag{62}$$
$$\leq M$$

3.8.4 Accounting for aftershocks in Hazus-MH

To adjust Hazus-MH results to account for an aftershock occurs, let us reduce V(t) by the amount of service estimated lost when the virgin system is damaged by aftershock j, i.e.,

$$V''(t) = V'(t) - \left(M - V_j(0)\right) \tag{63}$$

Where M denotes the number of services in the county and $V_j(0)$ denotes the number of service connections receiving lifeline service immediately after the aftershock, as estimated by Hazus-MH for the virgin system, i.e., as if the system were undamaged at the time of the aftershock.

3.9 Mitigation options

Let us consider only two mitigation options: one to reduce a water utility's reliance on commercial fuel, another to reduce the quantity of brittle pipe or pipe running through liquefiable soil. Other mitigation options certainly exist.

3.9.1 Fuel plan

A utility can reduce its reliance on commercial fuel supplies by installing above-ground fuel storage tanks in its service centers. An above-ground storage tank of 3,000 gallons such as shown in Figure 12 would be sufficient for 10 repair crews to operate for a week or more before needing to be refilled. The above-ground fuel tank in Figure 12 has a fuel transfer pump (the red box) that can be powered by a small vehicle-mounted generator that a repair truck can easily carry. An electrical contractor can be dispatched connect a secondary electrical generator to a fuel island in a few hours. If trucks are regularly refilled at the end of each day, the time required to connect a fuel pump to a generator need not affect repair operations. Alternatively, service centers can be equipped with an emergency generator and switchgear to power fuel pumps in the case of commercial electric failure. At least one large California utility carries such a generator on all its repair vehicles and maintains a fuel supply of up to 3,000 gallons or more at its service centers, and has installed emergency generators at several of its service centers.

Figure 12. Above-ground petroleum tank

3.9.2 Pipe replacement

With an aggressive pipe-replacement program, a water utility can realistically replace 1 percent of buried pipe per year, although lower replacement rates are more common. For example, San Francisco plans to replace 1.3 percent of its water distribution pipe (15.5 miles of a its 1,230-mile distribution system) in FY 2016 (https://goo.gl/iRtu4w, https://goo.gl/SmjBwm) With a sustained program that focuses on replacing brittle pipe (e.g., cast iron and asbestos cement), or pipe installed in liquefiable soil, a utility could replace the majority of its brittle or vulnerable system within a few decades.

3.10 Summary of the methodology

To recap, the methodology proposed here models damage and restoration of buried pipelines subject to earthquake shaking (called wave passage) and ground failure (liquefaction, landslide, and surface rupture of the fault). Briefly, its steps are as follows.

1. One acquires maps of ground motion, especially peak ground velocity and ground failure (liquefaction, landslide, and fault offset), for each earthquake of interest. One then carries out the following steps.

2. Equation (26) estimates r, the number of repairs required because of earthquake damage, using basic loss-estimation principles.
3. Equation (27) estimates V_0, the number of service connections that have service available immediately after the earthquake. It assumes that the serviceability index (a measure of water-supply pressure loss as a function of water-supply pipeline breaks per km of pipe) can be used as a proxy to estimate the fraction of services available. It would be desirable to replace this assumption, but doing so seems to require hydraulic modeling that would make the present analysis prohibitively time consuming.
4. Equation (30) estimates $V(n)$, the number of services available after n repairs have been completed. It employs a parametric form for service restoration, one that reflects EBMUD engineers' strategy to perform the most effective repairs (the ones that restore the most services per repair) first, and one that generally agrees with experience in the Kobe and Northridge earthquakes.
5. Equation (35) estimates $F(t)$, the number of services restored by time t. Lifeline interaction is quantified at this stage via a set of time-independent rate-limiting factors u that indicate loss of repair productivity resulting from the loss of each upstream lifeline or other required repair resource. The lifeline interaction model modulates the time-dependent effect of the loss of required resources with a set of time-dependent factors $g(t)$ that measure the flow of each resource at time t. One calculates $F(t)$ for each of many points in time, $t = 0$, Δt, $2\Delta t$, etc., where the datum $t = 0$ refers to the time when the mainshock occurs.
6. To apply these equations to a mainshock, one estimates damage and immediate loss of service. Then estimate the service restoration and time required to perform the service restoration for each repair $n \in \{1, 2, ... r\}$. Finally one relates time to number of services available.
7. To account for aftershocks, repeat tasks 2-6, adding the damage that remains unrepaired as if the remaining damage occurred with the aftershock.
8. To treat the entire model as stochastic (i.e., random, uncertain), simulate pipeline vulnerability using Equation (41), damage using Equation (42), initial loss of service using Equation (52), and the rate limiting factors for each upstream resource using Equation (55). Carry out tasks 2-7 as before, many times. Each time represents one possible outcome. Compile the samples of whichever parameter values are of interest and estimate any moments (mean, variance, etc.) of interest.
9. To account for lifeline interaction in Hazus-MH, apply Equation (61), which adjusts the slope of the Hazus-calculated restoration curve to account for rate-limiting factors among upstream lifelines, and then integrates the adjusted slope to produce a new restoration curve.
10. To account for aftershocks in Hazus-MH, apply Equation (63) after each aftershock, which reduces each lifeline's functionality as estimated by Hazus-MH for the virgin system shaken by the aftershock. One then continues the integration over time using the adjusted mainshock restoration curve of the previous step.

4. Case study 1: San Jose Water Company

4.1 San Jose Water Company asset definition

Let us exercise the proposed methodology on a real water supply system subjected to the hypothetical Hayward Fault earthquake sequence. Let us first consider summary features of the case study system: the San Jose Water Company's water supply system's buried pipeline network.

The following statistics are taken from SJWC (2015). SJWC is 150 years old, serves 225,000 service connections, and employs 345 people. It serves 80% of San Jose, 50% of Cupertino, all of Saratoga, Los Gatos, Monte Sereno, and Campbell, and unincorporated parts of Santa Clara County. Daily demand for drinking water varies from 85 to 165 million gallons, with an average daily demand for drinking water of approximately 120 million gallons. It has 2,400 miles (4,000 km) of water pipes (mains), 105 active wells, a 6,500-acre water shed in Santa Cruz Mountains, 96 distribution reservoirs, two surface-water treatment plants, and performs approximately 370 water quality tests each month.

SJWC provided an ArcGIS map of its water supply system. The system map is shown in Figure 13. The map shows 3,959 km of pipe of various types and lengths. Quantities of pipe are summarized by material in Table 11 and by diameter in Figure 14. In the tables and figures, "Material" presents a code for pipe material, "Count" means the number of segments of that material in the system map, "Miles" and "km" refer to the total length of pipe of that material, "Material description" describes the pipe material, and "Eidinger type" and "ID" refer to the assumed corresponding vulnerability functions by Eidinger (2001) and their associated vulnerability factors K_1 and K_2 from Table 1. Some of SJWC's pipe does not map well to an Eidinger type, especially SJWC's steel pipe, which generally has lead or cement caulk rather than any of the joint types that Eidinger considers.

Some of the material codes do not appear in SJWC's glossary of pipe types, and are probably data-entry errors. I have made a reasonable assumption about the intended meaning, but in any case the total quantities of these questionable materials are small: 30.2 of 2459 miles, or just over 1%.
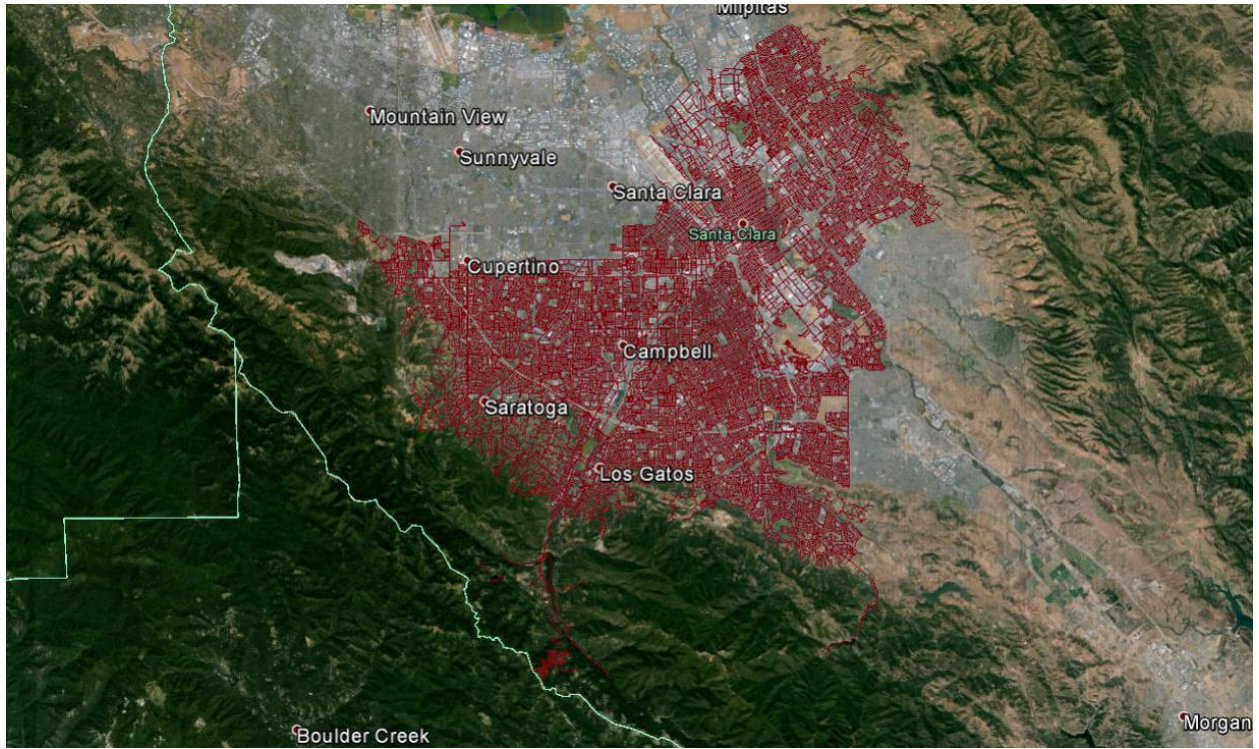
Figure 13. SJWC system map

Table 11. SJWC pipe construction, associated with Eidinger (2001) vulnerability functions

Material	Count	Miles	Km	Material description[1]	Eidinger (2001) type[2]	ID[2]
AC	7144	398.5	641.3	Asbestos cement	Asbestos cement, cement joint	14
BCL	14	0.3	0.4	Bare cement lined steel	Welded steel, rubber gasket	10
CCCL	1110	63.0	101.4	Cement mortar coated and lined steel pipe	Ditto	10
CI	3913	210.7	339.0	Cast iron	Cast iron rubber gasket	4
CL	5	0.0	0.0	*Cement-lined steel*	Welded steel, rubber gasket	10
CU	71	0.9	1.4	Copper	Ditto	10
DCCL	136	4.7	7.6	Dimet coated cement lined steel	Ditto	10
DCIL	1	0.2	0.3	*Ductile iron cement lined*	Ductile iron rubber gasket	19
DFK	1	0.0	0.0	Dipped & fiberglass-Kraft wrapped (asphalt coated) steel	Welded steel, rubber gasket	10
DICL	16962	789.4	1270.4	Ductile iron cement lined	Ductile iron rubber gasket	19
DIMCL	7	0.3	0.5	*Dimet coated cement lined steel*	Welded steel, rubber gasket	10
DS	6	0.3	0.4	*Dimet coated steel*	Ditto	10
FKCL	3643	199.4	320.8	Fiberglass-kraft wrapped cement-lined steel	Ditto	10
GALV	72	0.6	0.9	Galvanized steel	Ditto	10
GG	9	0.0	0.1	Groove and grip steel	Welded steel screwed joint	11
HDPE	14	2.9	4.6	High Density Polyethylene plastic	PVC rubber gasket	18
PB	2	0.1	0.1	Polybutylene plastic	Ditto	18
PE	5	0.3	0.5	Polyethylene plastic	Ditto	18
PP	1	0.0	0.0	Polypropylene plastic	Ditto	18
PVC	857	40.2	64.7	polyvinyl chloride plastic	Ditto	18
RCP	3	0.0	0.0	Reinforced Concrete	Asbestos cement, cement joint	14
S	109	1.7	2.7	Steel	Welded steel, rubber gasket	10
SB	232	3.9	6.3	Standard black steel	Ditto	10
SG	1	0.0	0.0	*Standard galvanized steel*	Ditto	10
SI	114	5.6	9.0	Sheet Iron	Ditto	10
SOMCL	4903	281.8	453.5	Somastic coated cement lined steel	Ditto	10
SS	256	8.1	13.0	Standard screw steel	Welded steel screwed joint	11
TBD	695	29.4	47.3	*Steel*	Welded steel, rubber gasket	14
WI	12	0.3	0.5	Wrought iron	Cast iron, cement joint	1
WS	598	32.0	51.5	Wrapped steel unlined	Welded steel, rubber gasket	10
WSCL	6353	384.5	618.8	Wrapped steel cement lined	Ditto	10
ZCCL	5	0.2	0.3	*Zinc coated cement lined welded steel*	Ditto	10
Total		2,459	3,957			

[1] Descriptions in italics are assumptions

[2] Assumed corresponding vulnerability function from Table 1
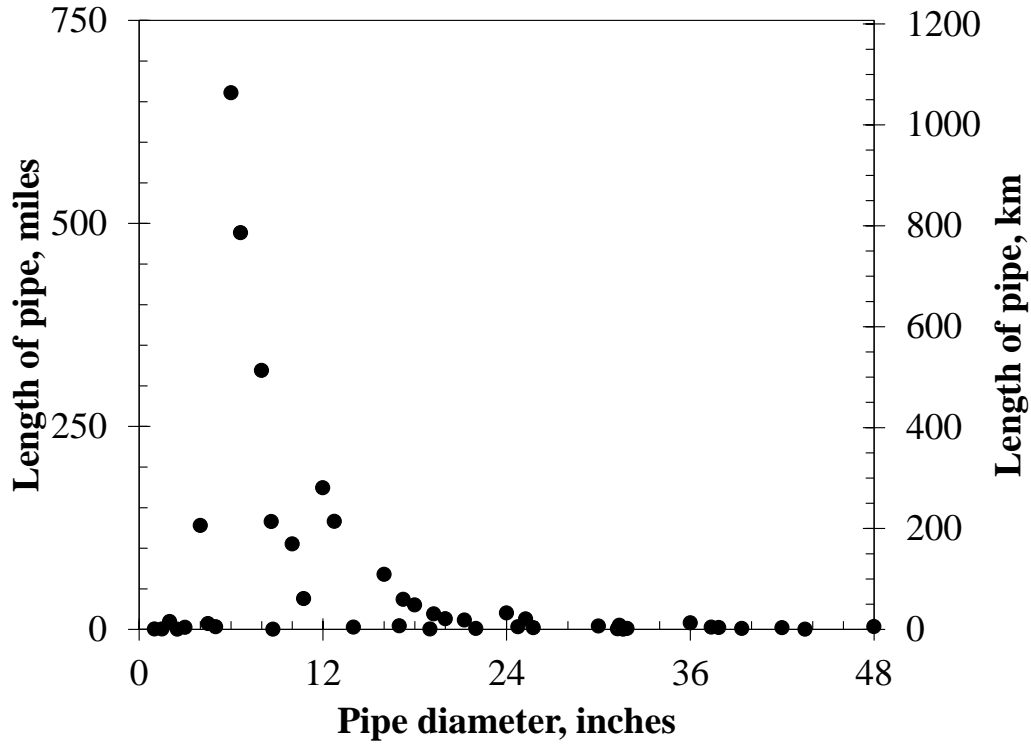
Figure 14. SJWC pipe quantities by diameter

4.2 San Jose Water Company hazard analysis

The Hayward Fault earthquake sequence considered here begins with a M_w 7.0 mainshock on the Hayward Fault, with an epicenter near Oakland, CA and rupturing the north and south segments of the fault from a point under San Pablo Bay at the north end to a point near Hayward CA at the south end. It is followed by a hundreds of aftershocks of magnitude 2.5 or greater. Of these

aftershocks, 16 are of magnitude 5.0 or greater. Table 12 summarizes the day, location, label, and magnitude of each event. In the table, day 1 corresponds to 18 April 2018.

Table 12. Hayward Fault earthquake sequence

Day	Epicenter	Label	Mag
1	Oakland	Mainshock	7.05
1	Union City	uc523	5.23
1	San Pablo	sp504	5.04
12	Fairfield	ff558	5.58
15	Fremont	fr51	5.10
32	Oakland	ok542	5.42
40	Palo Alto	pa62	6.21
40	Menlo Park	mp552	5.52
41	Palo Alto	pa569	5.69
41	Atherton	at511	5.11
67	Palo Alto	pa522	5.22
74	Palo Alto	pa526	5.26
166	Cupertino	cu64	6.40
166	Mountain View	mv598	5.98
166	Sunnyvale	sv535	5.35
166	Santa Clara	sc509	5.09
492	Palo Alto	pa501	5.01

Figure 15, Figure 16, and Figure 17 show the system map overlain with mainshock peak ground velocity, liquefaction probability, and landslide probability, respectively. The mainshock surface rupture does not reach SJWC's system, so it does not appear in the figures. Figure 18 shows peak ground velocity contours in a M 6.4 aftershock that occurs on day 166, i.e., 5 months after the mainshock.
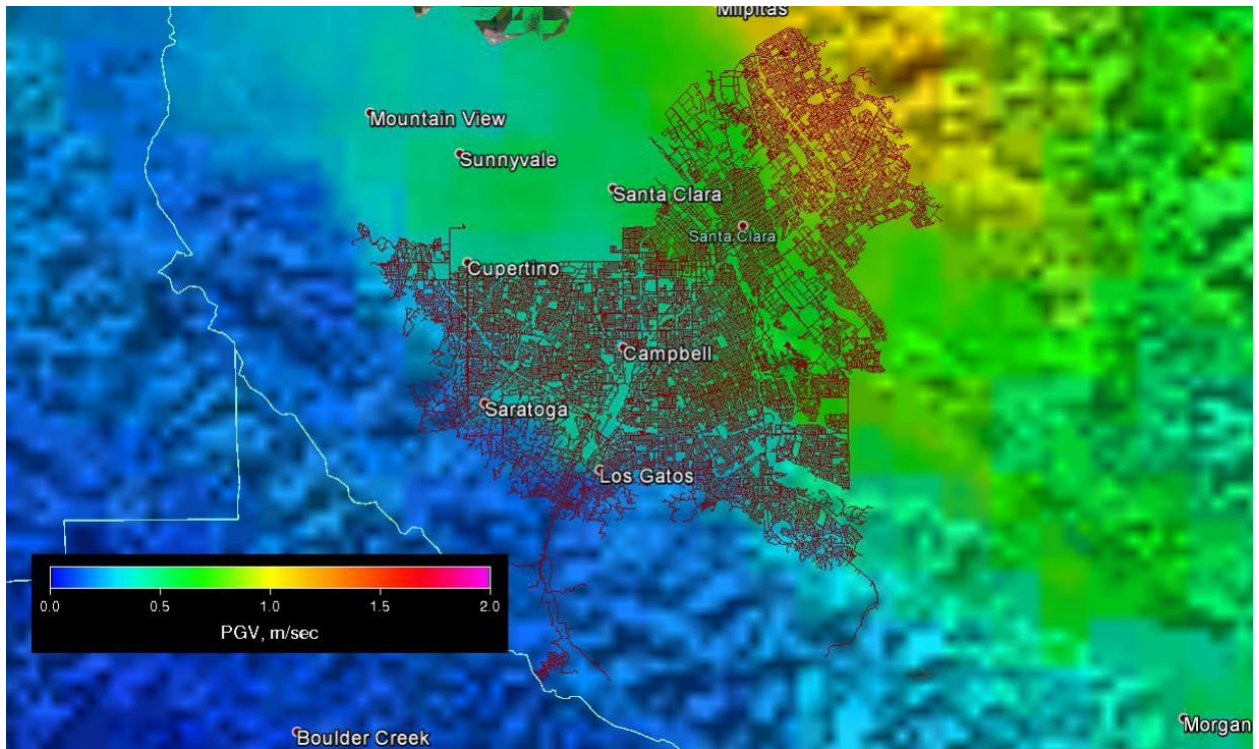
Figure 15. SJWC system map with mainshock peak ground velocity
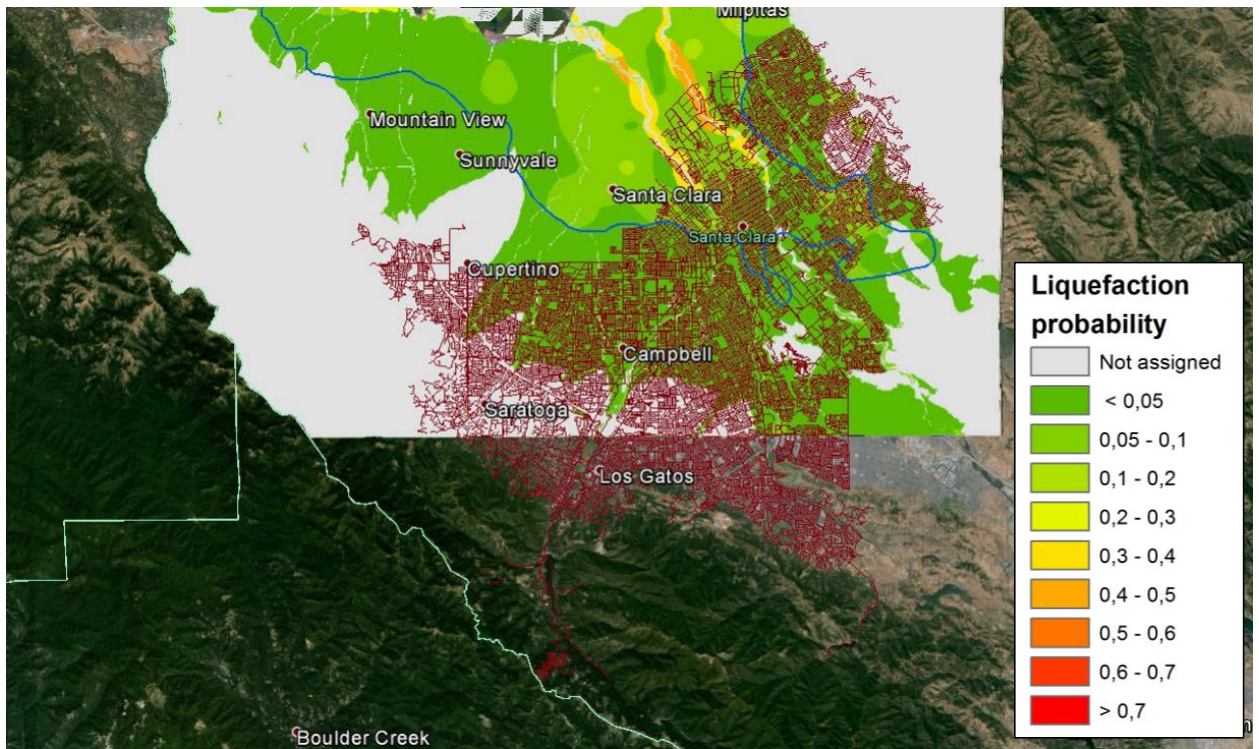
Figure 16. SJWC system map with liquefaction probability
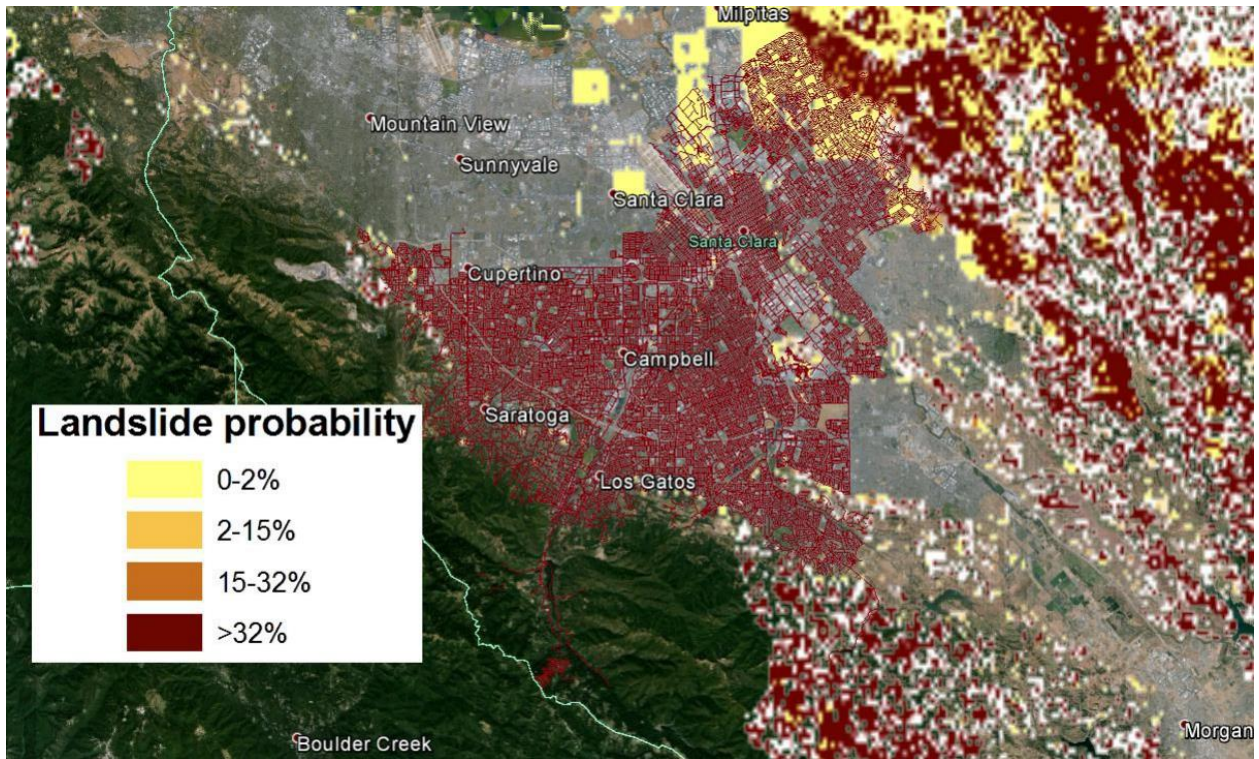
Figure 17. SJWC system map with landslide probability
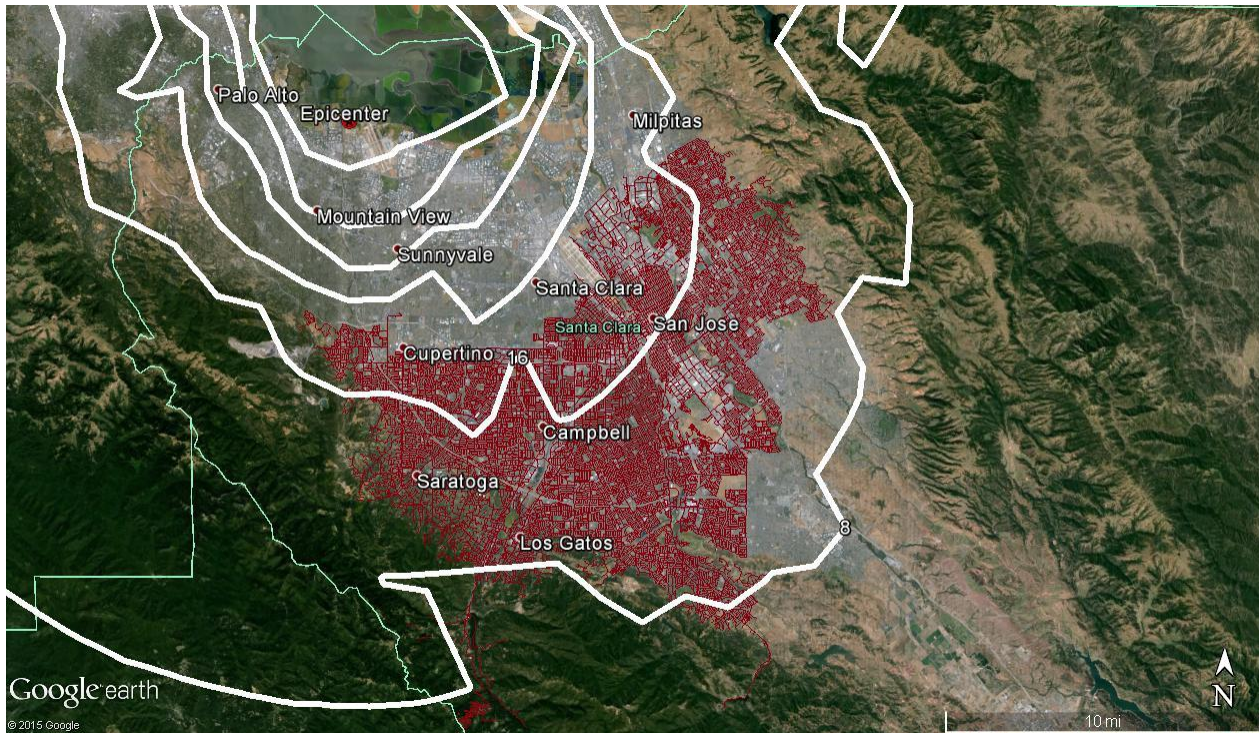
Figure 18. SJWC system map with M 6.4 Mountain View aftershock PGV contours (increments of 0.08 m/sec)

4.3 San Jose Water Company damage analysis

Table 13 summarizes mean damage to San Jose Water Company buried pipeline in the mainshock (1,054 repairs). Aftershocks continue to aggravate damage, contributing 903 more repairs: 29 more in large-diameter pipe and 873 more in small-diameter pipe. See Table 14 for the expected value of number of pipe repairs by event in the sequence and Table 15 for subtotals by day. In those tables, "large diameter" means at least 20 inches. Table 16 summarizes the expected value of the number of repairs by material, summing damage over the entire earthquake sequence. The table shows that the plurality of repairs are in asbestos cement pipe (481 breaks), and although the next-largest contributor is ductile iron pipe (470 breaks), repairs are disproportionately from AC, with an expected value of 0.23 repairs per 1000 linear feet of pipe (0.75 per km), versus 0.11 per 1000 lf (0.37 per km) from ductile iron. The unsurprising implication is that it is better to have ductile iron pipe than asbestos cement water pipe.

Table 13. Mainshock mean damage estimate in San Jose Water Company buried pipeline

Mean number of repairs	1,054
Repairs/km pipe	0.27
Due to wave passage	665 (63%)
Due to liquefaction	345 (33%)
Due to landslide	44 (4%)
Large diameter ($\geq$ 20 in diam)	30 (3%)
Small diameter (< 20 in diam)	1024 (97%)
Breaks	294 (28%)
Leaks	760 (72%)

Table 14. Estimated number of leaks and breaks in SJWC buried pipeline in the Hayward Fault sequence

Name	Day	Epicenter	Mag	Leaks + breaks	Lg diam	Sm diam
Mainshock	1	Oakland	7.05	1,054	30	1024
uc523	1	Union City	5.23	34	1	33
sp504	1	San Pablo	5.04	6	0	6
ff558	12	Fairfield	5.58	2	0	2
fr51	15	Fremont	5.10	47	1	46
ok542	32	Oakland	5.42	30	1	29
pa62	40	Palo Alto	6.21	102	3	99
mp552	40	Menlo Park	5.52	30	1	29
pa569	41	Palo Alto	5.69	58	2	56
at511	41	Atherton	5.11	30	1	29
pa522	67	Palo Alto	5.22	47	2	45
pa526	74	Palo Alto	5.26	48	2	46
mv598	166	Mountain View	5.98	93	3	90
cu64	166	Cupertino	6.40	172	6	166
sv535	166	Sunnyvale	5.35	73	2	71
sc509	166	Santa Clara	5.09	102	3	98
pa501	492	Palo Alto	5.01	29	1	28
Total				**1,957**	**59**	**1,897**

Table 15. Total leaks and breaks by day

Day	Leaks + breaks	Lg diam	Sm diam
1 Total	1,094	31	1,063
12 Total	2	0	2
15 Total	47	1	46
32 Total	30	1	29
40 Total	132	4	127
41 Total	88	3	85
67 Total	47	2	45
74 Total	48	2	46
166 Total	440	14	426
492 Total	29	1	28
Grand Total	1,957	59	1,897

Table 16. Repair rate in Hayward Fault sequence in San Jose Water Company buried pipeline, by material

Material	Repairs/1000 lf	Repairs/km
AC	0.23	0.75
BCL	0.13	0.42
CCCL	0.19	0.62
CI	0.19	0.62
CL	0.12	0.40
CU	0.31	1.00
DCCL	0.14	0.45
DCIL	0.09	0.29
DFK	0.23	0.74
DICL	0.11	0.37
DIMCL	0.25	0.81
DS	0.07	0.21
FKCL	0.13	0.41
GALV	0.08	0.26
GG	0.23	0.74
HDPE	0.05	0.16
PB	0.08	0.27
PE	0.06	0.20
PP	0.05	0.17
PVC	0.09	0.29
RCP	0.08	0.26
S	0.13	0.42
SB	0.15	0.50
SG	0.12	0.39
SI	0.14	0.45
SOMCL	0.16	0.53
SS	0.19	0.63
TBD	0.18	0.60
WI	0.22	0.71
WS	0.12	0.39
WSCL	0.13	0.43
ZCCL	0.07	0.24
Grand total	0.15	0.50

The estimates in Table 14 and Table 15 ignore the potential for liquefaction outside the area with estimated liquefaction probability. They also ignore damage from ground failure in aftershocks, for which I have not estimated liquefaction or landslide probability. However, since liquefaction requires long duration as well as strong shaking, and since aftershocks would tend to have short duration because of their moderate and small magnitude, they would tend to produce relatively few pipeline breaks as a result of liquefaction. Note that after the mainshock, the M 6.4 aftershock near Mountain View (Figure 18) adds the largest number of aftershock-related breaks in buried pipelines, likely setting SJWC back substantially in restoring service.

Figure 19 presents a heat map of break rate in the Hayward Fault mainshock. Colors indicate mean breaks per km². A warmer color indicates greater concentration of damage.

To be clear, if any additional emphasis is needed, this heatmap shows estimated break rates in one scenario earthquake—the Hayward Fault mainshock—not all possible earthquakes, not even all possible M 7.0 earthquakes on the Hayward fault. Different earthquakes produce different damage patterns. However, the point of a scenario is to understand what might realistically happen, and a heatmap makes a possible outcome more tangible, more useful for planning purposes. By planning for one scenario, one becomes more prepared for what actually happens, which will invariably differ from the scenario.

To return to the map: it unsurprisingly shows greater damage near the fault and on soil with high liquefaction probability, with maximum values approaching 12 breaks per km². Figure 20 shows an analogous map for the M 6.4 Cupertino aftershock. The color scale is shifted to be informative. Damage rates just exceed 1 break per km² in the aftershock in the neighborhoods along the northern edge of the SJWC service area. Figure 21 shows the heatmap for the entire sequence, with damage rates of approximately 15 per km² in the northeastern portion of the service area.
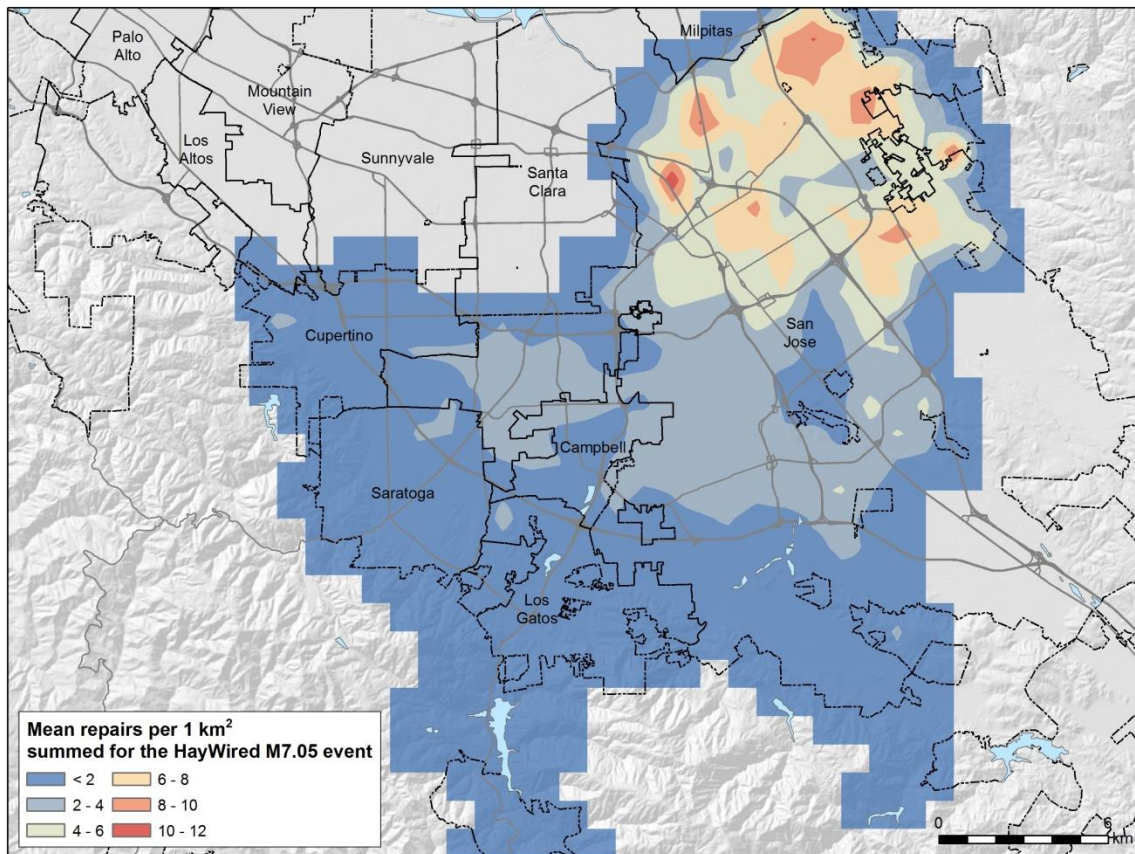
Figure 19. Buried water pipeline damage heatmap for the Hayward Fault mainshock in SJWC's service area
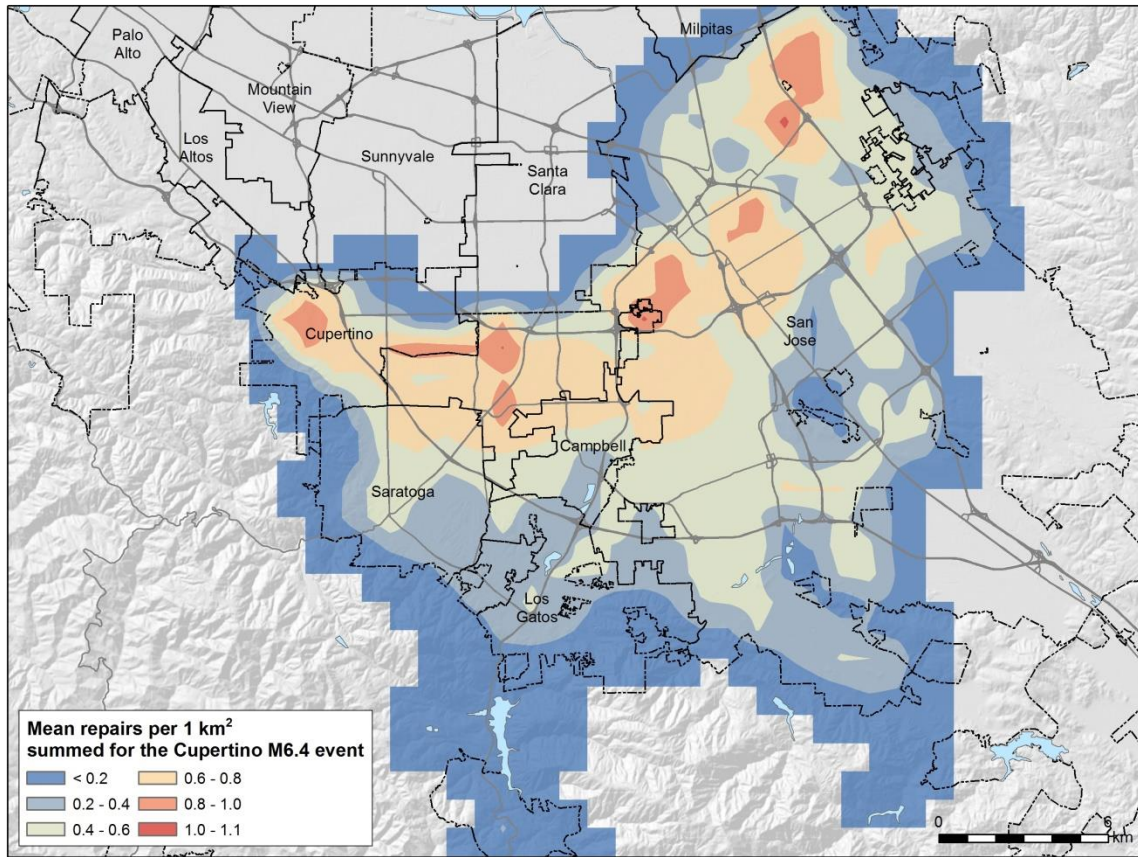
Figure 20. Buried water pipeline damage heatmap for Cupertino M 6.4 aftershock in SJWC's service area
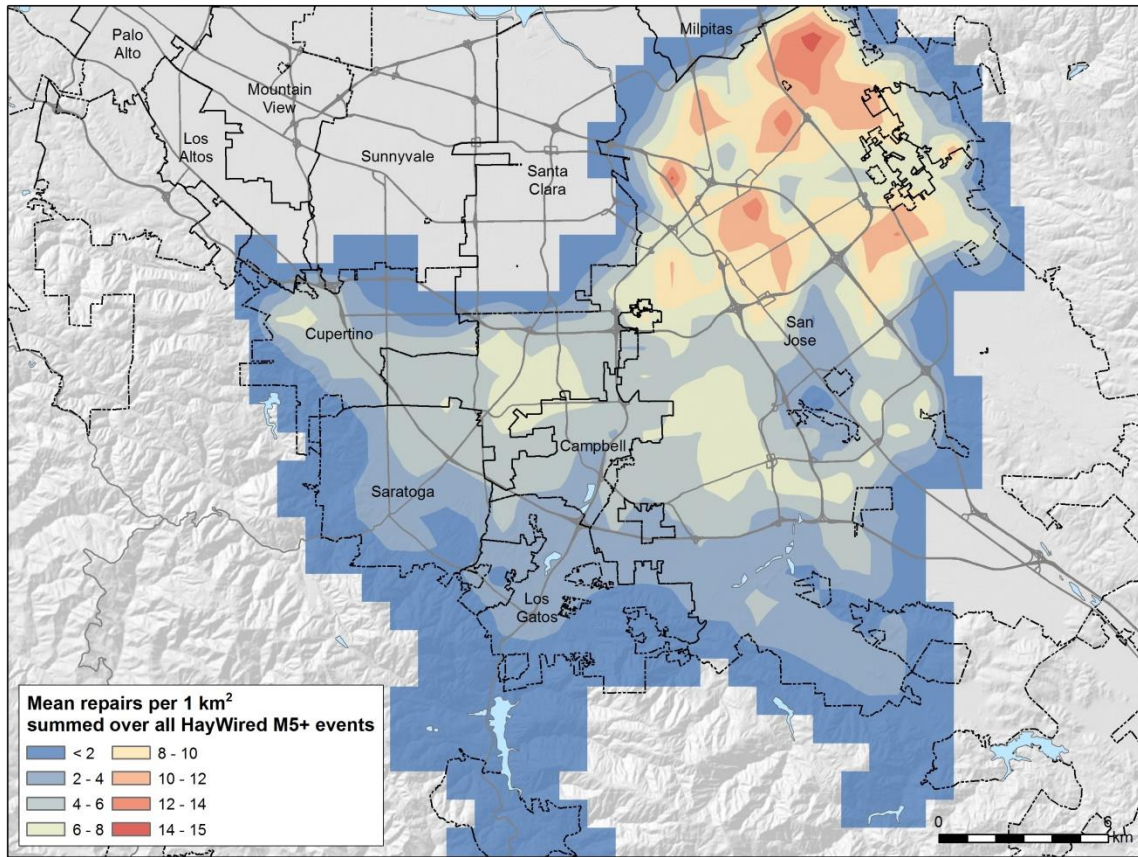
Figure 21. Buried water pipeline damage heatmap for entire the Hayward Fault earthquake sequence in SJWC's service area

I simulated damage locations by applying Equation (42) once for the mainshock and each aftershock. Figure 22 shows pipeline segments with at least one repair in the Hayward Fault mainshock. Figure 23 shows segments with at least one repair in the M 6.4 Cupertino aftershock. Figure 24 shows locations are those with at least one repair in the entire earthquake sequence.
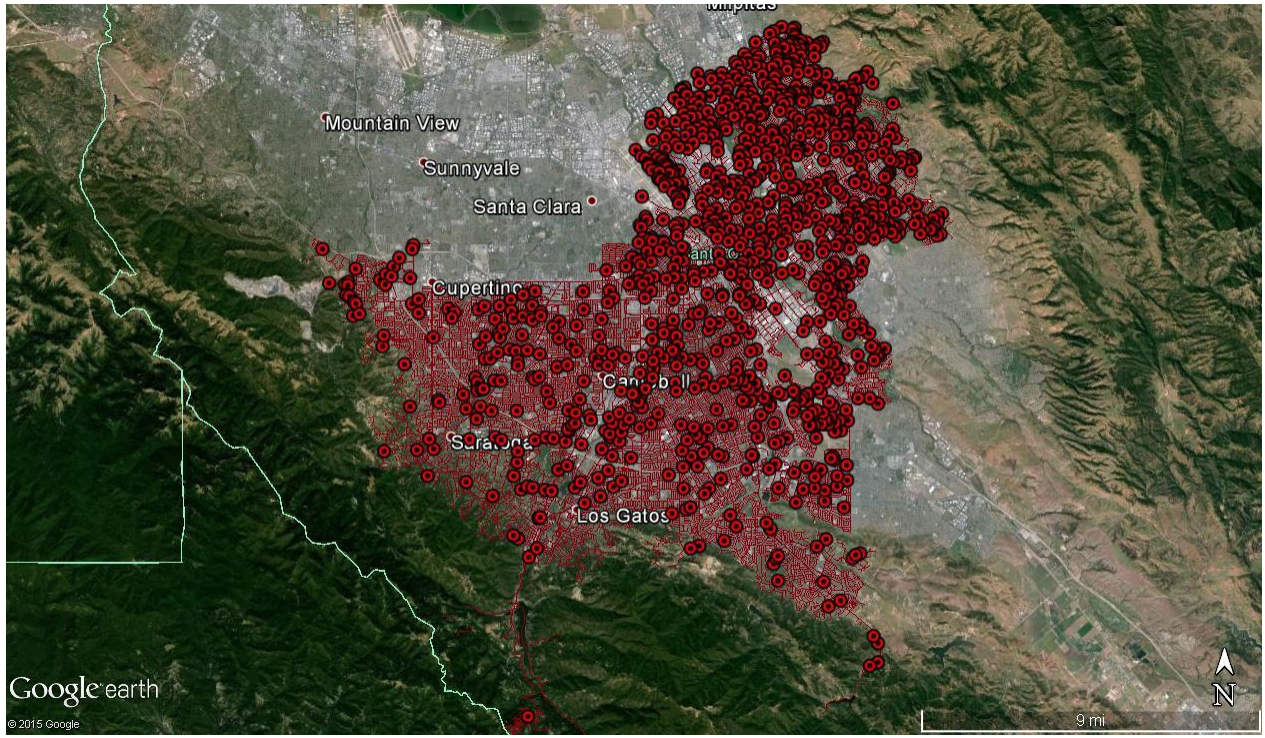
Figure 22. Simulated repairs in SJWC buried pipelines in Hayward Fault mainshock
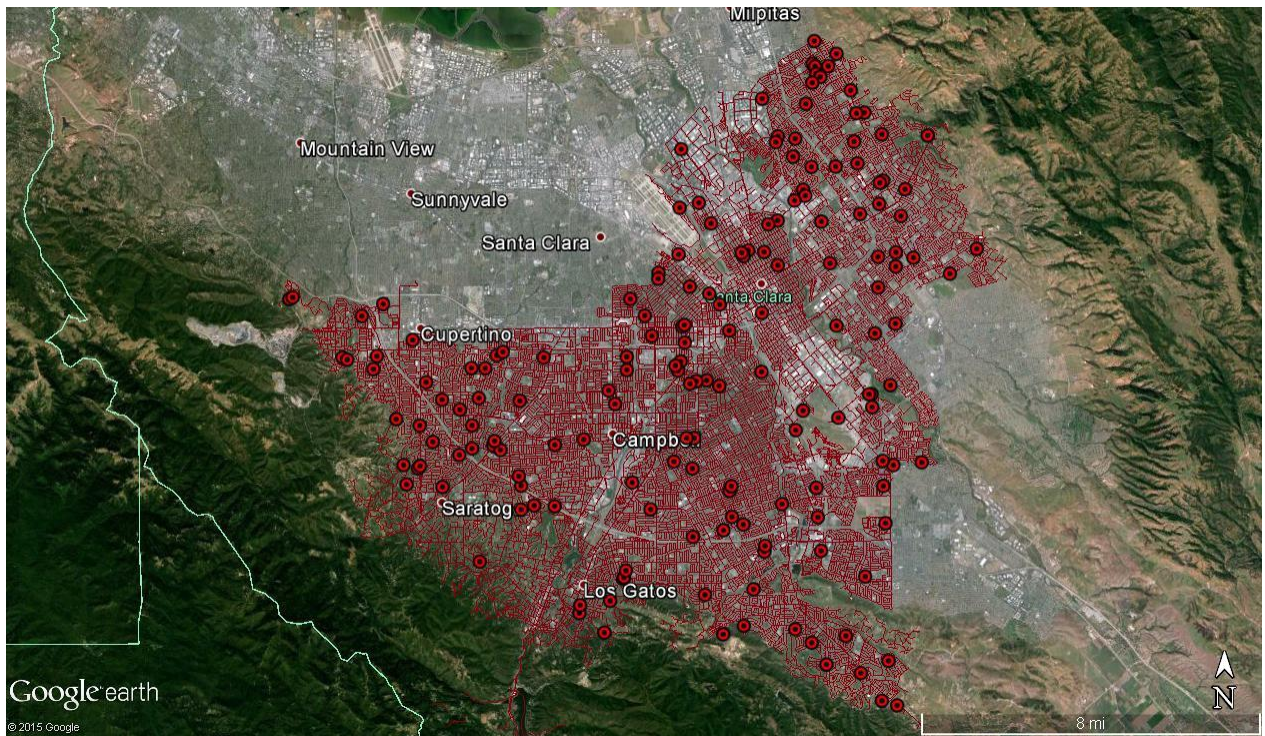
Figure 23. Simulated repairs in SJWC buried pipelines in Cupertino M 6.4 aftershock
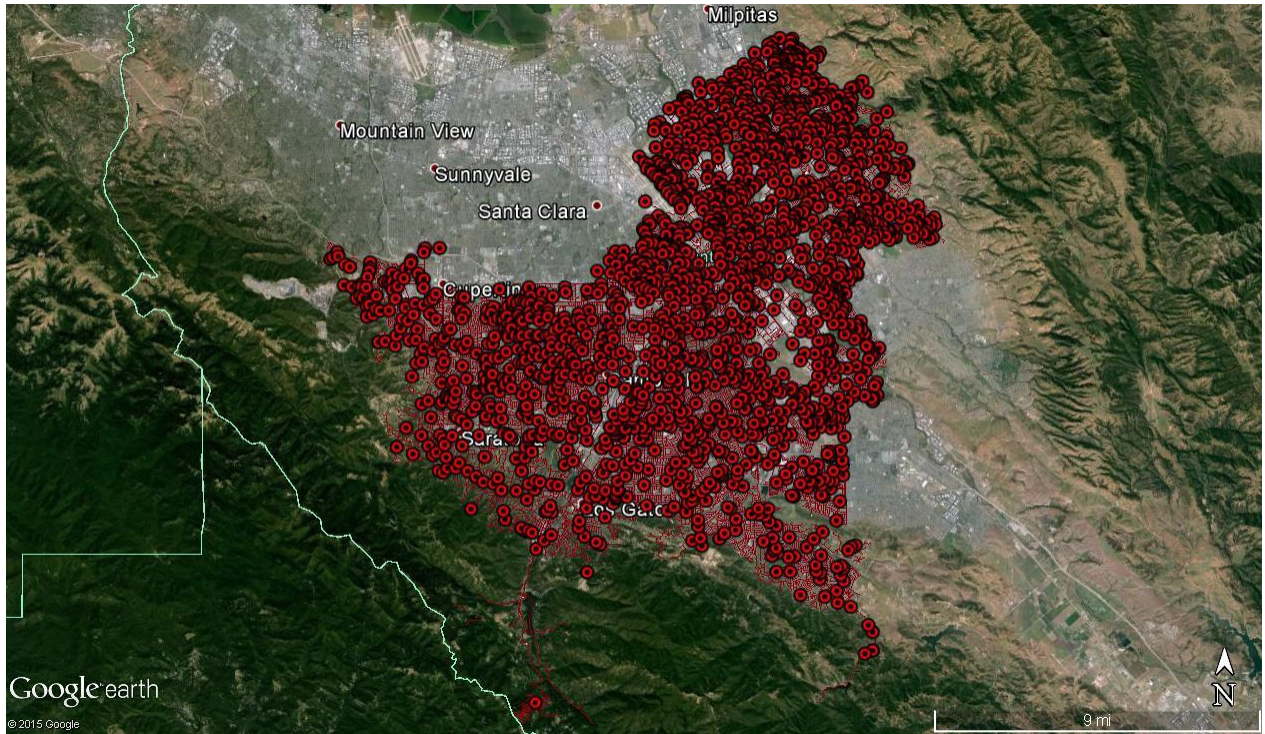
Figure 24. Simulated repairs in SJWC buried pipelines in Hayward Fault sequence

4.4 San Jose Water Company restoration analysis

Let us take the following *g*-value time series for lifelines upstream of water, and iterate later if necessary:

Consumables. SJWC has one of the best stock of repair materials in the Bay Area (J. Wollbrinck, oral commun., 14 Oct 2015). Let us assume sufficient repair consumable materials (pipe, clamps, etc.) are on hand or can be acquired as they are needed, i.e.,

$g(t) = 1.0$ for all t

Fuel. As of this writing, SJWC is in the process of preparing its fuel plan (J. Wollbrinck, oral commun., 14 Oct 2015). Let us treat two possible outcomes: (1) the earthquake happens before the plan is implemented, and (2) it happens afterwards. If afterwards, let us assume that the fuel plan is sufficient to ensure adequate supplies throughout the repair and restoration process, in which case $g(t) = 1.0$ for all t.

Without the fuel plan, let us assume that there is sufficient fuel initially, but that shortages would impair restoration for a few days until emergency supplies were secured. Quantitatively, let us assume:

Before implementing fuel plan:

$g(t) = 1.0$ for $0 \leq t < 3$ days
$g(t) = 0.25$ for $3 \leq t < 7$ days
$g(t) = 1.0$ for $t > 7$ days

After implementing fuel plan:

$g(t) = 1.0$

Electricity. PG&E expects to restore power throughout the Bay Area within 1 week. Let us assume therefore that in practice that means 999 out of 1000 customers are receiving power by the end of day 7 in a M 7 earthquake, or 2 days after a M 6+ aftershock. Quantitatively, let us therefore take

$g(t) = 1 - \exp(-0.987 \cdot t)$, t measured in days after the mainshock
$g(t) = 1 - \exp(-3.45 \cdot t)$, t in days after the aftershocks on days 40 and 166

Communication. SJWC has battery powered radios for its repair crews that reach almost its entire service area. Let us assume that communication to facilitate coordination between utilities will be such a high priority that coordination will not be a constraint. Let us therefore assume

$g(t) = 1.0$

Crews. SJWC personnel estimated that they could realistically field between 20 and 25 crews on a work basis of 12 hours on and 12 hours off. Let us therefore take $a(t) = 0.5$ and $c(t) = 22$ for purposes of Equation (35).

Figure 25 shows the repair timeline for San Jose Water Company before and after implementing the fuel-management plan. Figure 26 illustrates the simulated restoration curve. If the Hazus-MH serviceability index realistically measures the fraction of services receiving any water, as its reports suggest, then "services available" in Figure 26 measures the fraction of service connections receiving even small flows. If it means the post-earthquake flow as a fraction of pre-earthquake flow, then the chart underestimates the number of service connections receiving at least some water.
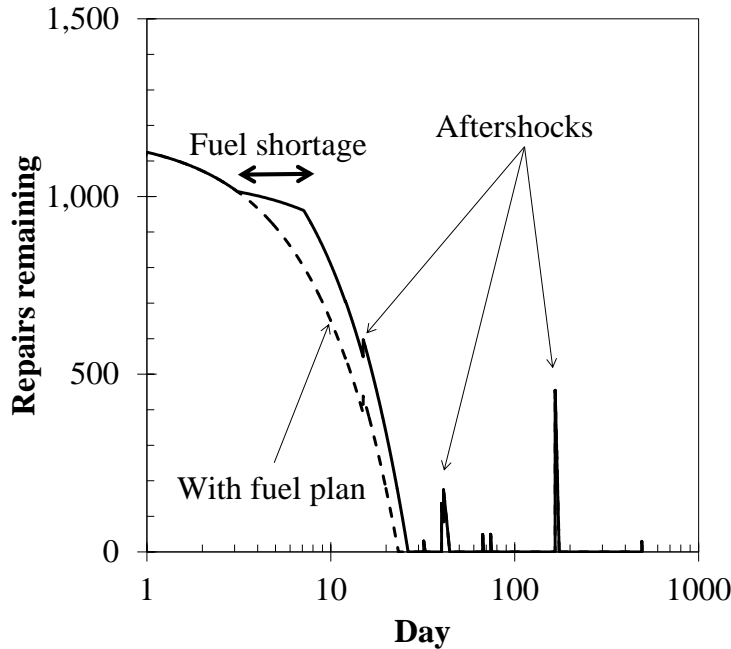
Figure 25. Simulated repair timeline of San Jose Water Company, with and without fuel management plan
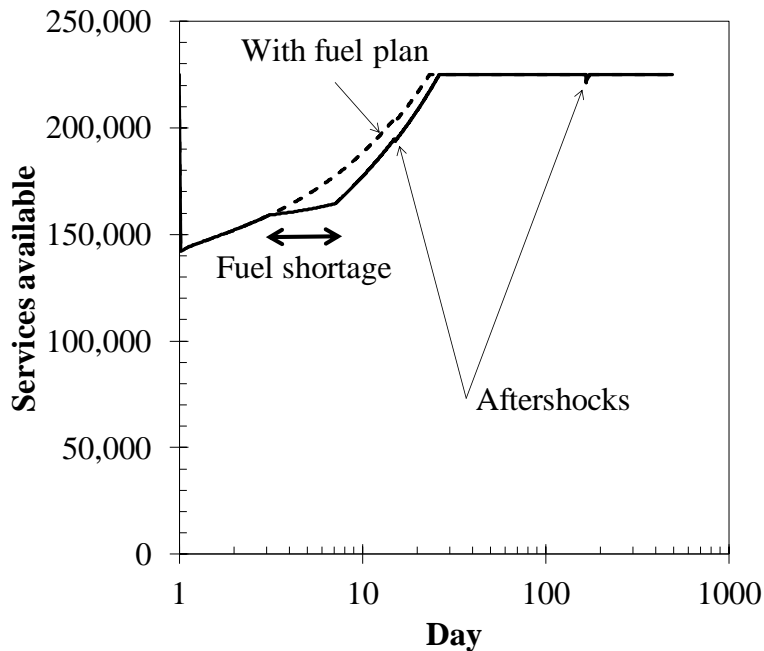
Figure 26. Simulated service availability of San Jose Water Company, with and without fuel management plan

As discussed earlier, one views the area above the curves in Figure 26 as a measure of resilience: less area means less impact, faster recovery, or both. The areas above the three curves are measured in units of service-days. That is, each day of lost water supply to a service connection equates with one service-day. The areas above the three curves are shown in Table 24: lost service-days under as-is conditions, with a fuel plan, and under ideal-world conditions, i.e., assuming that all brittle pipe is replaced before the earthquake. The table shows the lost service-days as a multiple of number of services, i.e., the average number of days that each service connection is without potable

water under as-is conditions, with the fuel plan, and under ideal-world conditions. The difference between lost service days under as-is and what-if conditions (fuel plan or ideal world) measures the resilience benefit of the what-if condition: with a fuel plan and if all brittle pipe were replaced before the earthquake occurred. Figures have been rounded to reduce the impression of excessive precision.

Table 17. SJWC lost service-days

Condition	Lost service-days $R \cdot M$	Resilience benefit $\Delta(R \cdot M)$	Average lost days R
As-is	940,000	0	4
Fuel plan	750,000	190,000	3
Ideal world	470,000	470,000	2

4.5 Validation of San Jose Water Company restoration analysis

4.5.1 Cross validation with SJWC's internal damage estimate

By scaling up the number of breaks in the 2014 Napa earthquake, San Jose Water Company personnel estimated that the Hayward Fault mainshock would cause 1,200 water main breaks to their own system (J. Wollbrinck written commun. 19 Oct 2015). The estimate follows this logic: Napa has 370 miles of water main and experienced 120 leaks the first week, and over 170 for the 1st 6 months. Scaling up by system size, SJWC estimates that Napa's 120 leaks would equate with 850 leaks for SJWC, and 170 would equate with 1200. The South Napa earthquake was weaker than what is expected for the mainshock imagined here, so that would make a difference. The similarity between SJWC's estimates of 850 increasing to 1200 and the ones produced here (1,054 increasing to 1,956) suggests that either both are reasonable or neither is. That the two set of figures used two different approaches to arrive at basically the same set of numbers tends to support both being reasonable, rather than neither. In either case, SJWC engineers found the results presented here to be reasonable (J. Walsh, written commun., 19 Oct 2015), with the exception that Wollbrinck (written commun. 4 Dec 2015) expected more damage to wrapped steel pipe because of its age and corrosion susceptibility.

4.5.2 Validation against Northridge, Kobe, and South Napa earthquakes

Jeon and O'Rourke (2005) report that the 1994 Northridge earthquake caused 1,095 breaks or leaks to buried pipeline operated by the Los Angeles Department of Water and Power, most of the damage occurring in the San Fernando Valley. Lund et al. (2005) report that repairs took about 1 week. The present calculation suggests that SJWC would take 23 days to repair 1,176 repairs (mainshock plus 4 aftershocks through day 15), i.e., about 3 times as long for about the same number of repairs. Lund et al. (2005) do not report the number of crews required to perform those repairs. Presumably LADWP fielded more crews than SJWC has at its disposal.

Lund et al. (2005) report that, according to M. Matsushita of the Kobe Municipal Waterworks Bureau, 1,757 breaks and leaks occurred in buried water supply distribution pipe in Kobe after the 1995 Kobe earthquake and that repairs took 10 weeks. The present estimate of 3 weeks to repair

1,176 breaks and leaks suggests 1/3rd the time to repair 2/3rds the breaks and leaks. Thus, in a sense, Northridge and Kobe bracket the restoration estimates for SJWC presented here.

The City of Napa repaired approximately 120 leaks and breaks in 5 days with approximately 10 crews working 12-hour shifts (Scawthorn 2014), for a repair productivity of approximately 2.4 repairs per crew-day. The present model suggests that, before its fuel plan is implemented, San Jose Water Company would repair 1,176 breaks and leaks in 26 days with 22 crews working 12-hour shifts, or 2.1 repairs per crew day, suggesting fairly good agreement.

4.5.4 Cross validation with Hazus-MH

Using Hazus-MH, Seligson estimated restoration of water supply in Santa Clara County. Results are shown in Table 18. The estimates are for the mainshock only and do not reflect lifeline interaction. Applying the percentages to the number of SJWC's customers, one can compare the two models, as shown in Figure 27.

The present model and Hazus-MH disagree wildly in terms of initial level of service and restoration time, with the Hazus-MH model estimating a 6 times increase in time to restore service compared with the present model. Considering the validation against the Napa repair timeline, the present restoration model seems more plausible than the Hazus-MH restoration model. Why would Hazus-MH's restoration model differ so markedly from the present one? The difference can be partly explained by the user-specified number of repair crews.

Table 18. Hazus-MH estimate of Santa Clara County loss of water supply

Total households		Households without potable water				
		Day 1	Day 3	Day 7	Day 30	Day 90
565,853	#	504,596	502,302	497,394	458,220	137,185
	%	89.20%	88.80%	87.90%	81.00%	24.20%
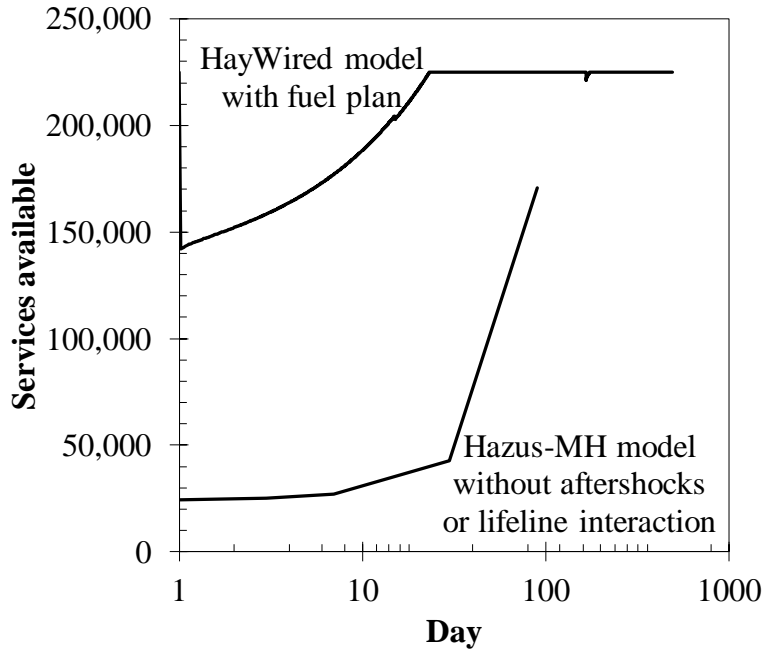
Figure 27. Comparison of the present model with that of Hazus-MH, as applied to SJWC

4.6 San Jose Water Company under ideal-world conditions

Suppose all of the more-vulnerable SJWC buried pipe (e.g., asbestos cement and cast iron) could be replaced with less-vulnerable pipe (e.g., ductile iron). What would be the benefit in terms of damage reduction and accelerated recovery? To explore this question, let us assume that all asbestos cement and cast iron pipe is replaced with ductile iron before the Hayward Fault sequence occurs. Let us refer to this as the ideal world assumption. Figure 28 plots the restoration curves for San Jose Water Company's buried water supply pipelines under the ideal-world assumption.

An SJWC engineer informs SAFRR that SJWC replaces 1%, or 24 miles, of existing water mains every year. He does not imagine this study being used to change that percentage of replacement, but they might change their mix of pipes. Their replacement program is based on both consequences of failure and probability of failure. They consider a multitude of factors and then apply genetic algorithm software to predict leaks. They will likely add additional weighting to AC and CI pipe in close proximity to fault lines based on the present work.
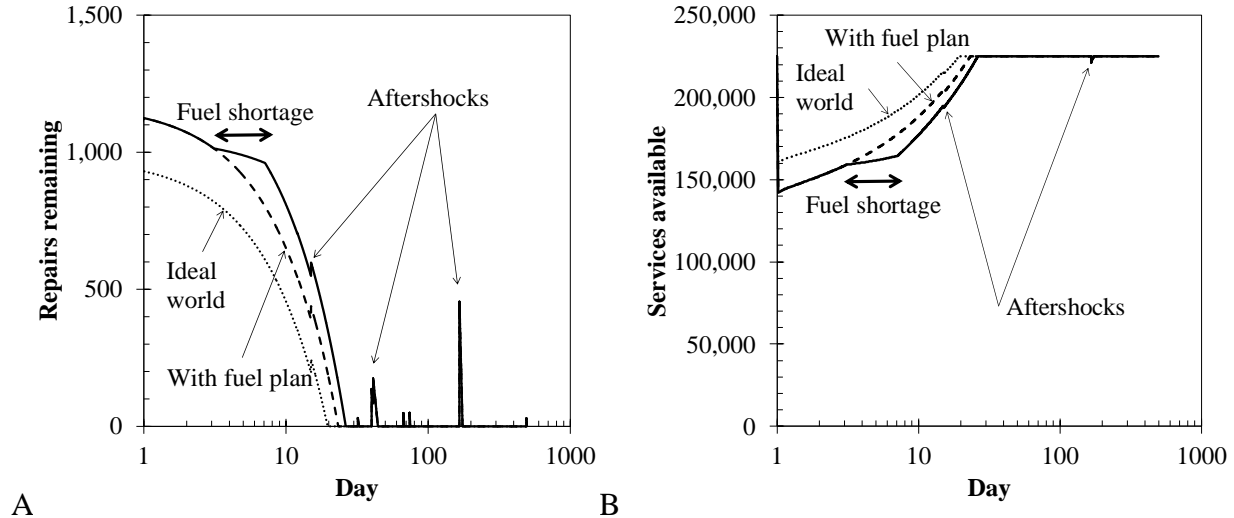
Figure 28. Benefit of replacing AC and CI pipe with ductile iron: A) repairs remaining versus time and B) services available versus time

4.7 Effect of lifeline interaction and consumable limits

Suppose one ignored limitations in fuel and other consumables, and ignored impairment of electricity, telecommunications, and so on. How much difference do lifeline interaction and consumable limits make? Without these effects, damage is unaffected, but repairs could potentially proceed faster. Recall that Equation (34) gives the time $\tau(n,t)$ required to perform the nth repair, which occurs at time t. It can be expressed as a baseline productivity increased by a factor $S(t)$ that accounts for how lifeline interaction and consumable limits slow repairs, i.e.,

$$\tau(n,t) = \frac{d_0}{w(t) \cdot c(t)} \cdot S(t) \tag{64}$$

where

$$S(t) = \frac{1}{\left(\prod_i \left(1 - u_i \cdot \left(1 - g_i(t)\right)\right) \right)} \tag{65}$$

The first multiplicand in Equation (64) is the baseline productivity, i.e., the time required to perform the nth repair, without lifeline interaction and consumable limits. The factor $S(t)$, which is always at least 1.0, increases the repair time to account for lifeline interaction and consumable limits. Repeating the calculations for San Jose Water Company under as-is conditions but with $S(t)$ = 1 produces an estimated 740,000 lost service days, about 80 percent of the value estimated considering lifeline interaction. Viewed another way, lifeline interaction and consumable limits decrease the calculated water supply resilience in the area served by San Jose Water Company by 25 percent in the Hayward Fault scenario. The factor would vary in other earthquakes, generally being larger the dependent the utility is on other lifelines and consumables, and the more these lifelines and consumables are impaired.

5. Case study 2: East Bay Municipal Utility District

5.1 East Bay Municipal Utility District asset definition

We can examine a second system subjected to the same hypothetical earthquake sequence, to see whether the model can produce plausible results twice. This section considers the East Bay Municipal Utility District's water supply buried pipeline network.

The following description is largely quoted from Contra Costa Local Agency Formation Commission (2008) and from conversations with EBMUD. East Bay Municipal Utility District (EBMUD) provides water and sewage treatment services for an area of approximately 331 square miles in the eastern side of the San Francisco Bay. EBMUD serves approximately 1.3 million people in portions of Alameda County and Contra Costa County in California. EBMUD currently has an average annual growth rate of 0.8% and is projected to serve 1.6 million people by 2030. As of 2015 it provides water to approximately 390,000 service connections. Approximately 100,000 are located east of the East Bay Hills, the other 290,000, west.

EBMUD's administrative offices, located in Oakland, own and maintain 2 water storage reservoirs on the Mokelumne River, 5 terminal reservoirs, 91 miles of three separate water transmission aqueducts, 4,100 miles of water mains (the only part of the system modeled here), 6 water treatment plants, 29 miles of wastewater interceptor sewer lines and a regional wastewater treatment facility rated at a maximum treatment capacity of 320 MGD.

EBMUD provided an ArcGIS map of its water supply system. The system map is shown in Figure 29. The map shows 6,698 km (4,162 mi) of pipe of various types and lengths, of which 2,091 km are located east of the East Bay Hills, the other 4607 km, west. Total quantities of pipe are summarized by material in Table 19 and by diameter in Table 20. I discretized EBMUD's system into segments with an average length of 64 m and a standard deviation of 79 m—short enough that shaking should vary little between ends of segments. In the tables, "Material" presents a code for pipe material, "Count" means the number of segments of that material in the system map, "Miles" refers to the total length of pipe of that material, "Material description" describes the pipe material, and "Eidinger type" and "ID" refer to the assumed corresponding vulnerability functions by Eidinger (2001) and their associated vulnerability factors K_1 and K_2 from Table 1. Some of EBMUD's pipe does not map well to an Eidinger type. One of the material codes do not appear in EBMUD's glossary of pipe types, and is probably a data-entry error. I have made a reasonable assumption about the intended meaning, but in any case the total quantity is small: 0.1 miles.

Terentieff et al. (2015) report that 176,000 of 390,000 water services are in pumped pressure zones. These pressure zones rely on 130 pumping stations, of which 117 (90 percent) have no emergency generators. Therefore, let us set the parameter z used in the lifeline interaction matrix for EBMUD to be 0.9·176,000/390,000 = 0.41, and $u_{electr.} = 0.41 + 0.03 = 0.44$. The factor 0.9 reflects the 90 percent of pumping stations that have no generator. Conceivably EBMUD could install emergency generators with large fuel tanks at all its pumping stations, in which case we can take $u_{electr.} = 0.03$. Let us take the former as the real-world scenario and the latter as an ideal-world scenario. Let us also assume that fuel limitations affect EBMUD the same as SJWC, and like SJWC, EBMUD can optionally develop a fuel plan and storage to ensure that fuel does not limit its ability to perform pipeline repairs.
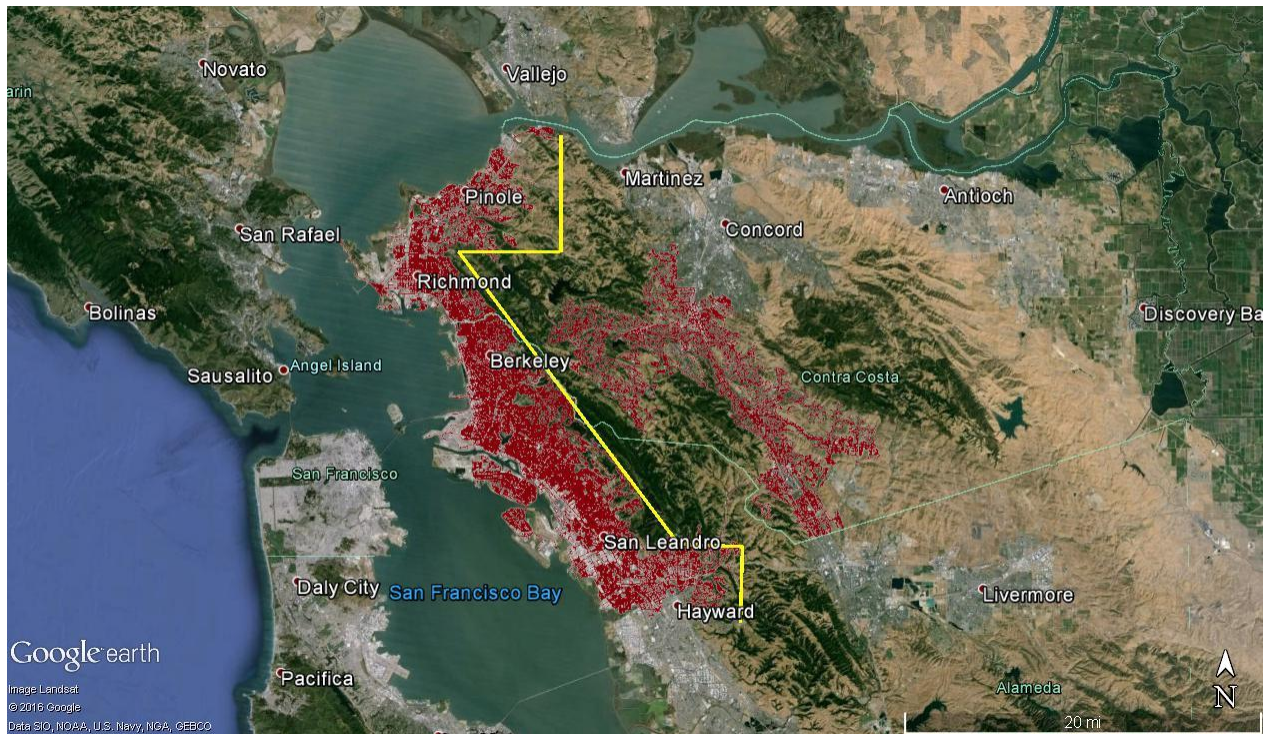
Figure 29. EBMUD system map (red) with dividing line (yellow) to approximately separate pipe and services east and west of the East Bay Hills

Table 19. EBMUD pipe construction, associated with Eidinger (2001) vulnerability functions

Code	Material, joint[1]	Count	Miles	Closest Eidinger (2001) type[2]	ID[2]
A	Asbestos cement, unrestrained	24543	1136.4	Asbestos cement with cement joint	14
C	Cast iron, unrestrained	33747	1322.1	Cast iron with cement gasket	1
D	Ductile iron, unrestrained	43	2.1	Ductile iron with rubber gasket	19
F	Fusible PVC, welded	30	1.2	Welded steel lap arc welded joint	6
H	High density polyethylene, weld	167	8.8	PVC with rubber gasket	18
K	Copper, restrained	50	0.7	Welded stl lap arc weld jt sm diam	6
L	Reinf concrete cyl., unrestrained	197	14.3	Concrete w steel cylinder cement jt	16
N	PVC, unrestrained	8613	380.4	PVC with rubber gasket	18
P[3]	*Pre-tens. conc. cyl., restrained*	1	0.1	Concrete w steel cylinder cement jt	16
R	Reinf. conc. noncylinder	2	0.0	Concrete w steel cylinder cement jt	16
S	Steel, weld	37101	1282.4	Welded steel lap arc welded joint	6,9[4]
T	Pre-tens. conc. cyl., restrained	127	10.4	Conc w steel cylinder lap arc weld	15
W	Wrought iron	71	2.7	Cast iron with cement gasket	1
	Total	**104,692**	**4,162**		

[1] EBMUD pipe material and description of joint; descriptions in italics are assumptions

[2] Closest equivalent corresponding vulnerability function from Table 1

[3] One length of 48-inch diam 1927 pipe; P is probably a typo for T

[4] ID 6 = small diam (< 20 in), ID 9 = large diam (≥ 20 in)

Table 20. EBMUD pipe quantities by diameter

Diameter, in.	Length, mi.
0.00	0.4
0.75	0.2
1.00	1.0
2.00	18.6
3.00	0.7
4.00	294.6
6.00	1728.2
8.00	1105.7
10.00	38.0
12.00	475.8
14.00	1.4
16.00	157.6
18.00	1.4
20.00	78.1
24.00	74.4
25.00	0.5
30.00	36.5
36.00	66.8
42.00	18.5
48.00	38.3
54.00	8.8
60.00	2.6
66.00	6.8
69.00	4.6
72.00	0.0
78.00	0.2
84.00	1.8
90.00	0.2
96.00	0.1
108.00	0.0
Total	4161.7

5.2 EBMUD hazard analysis

Ground motion and coseismic slip are quantified by Aagaard et al. (2010a, b). Liquefaction, landslide, and afterslip were estimated by colleagues in as-yet-unpublished work. Figure 30 shows EBMUD's system and the mainshock peak ground velocity. See Figure 31 for liquefaction probabilities in the mainshock. I have not calculated liquefaction probability in Contra Costa County, but assume that liquefaction damage occurs in Contra Costa County in approximately the same proportion to shaking-induced damage as in Alameda County. Landslide probability in the EBMUD service area is mapped in Figure 32. See Figure 33 for a map of EBMUD's water supply buried pipeline system with a fence diagram showing coseismic slip. In the figure, the height of

the red fence represents the right-lateral surface slip occurring at the fault at the time of the earthquake. The tallest point on the fence, near the location with Interstate 80 crosses the fault between Richmond and Pinole, represents 2.1 meters of offset. At California Route 24 near Berkeley, the offset is 0.84 meters. At Interstate 238 near Castro Valley, the offset is approximately 1.68 meters. Figure 34 shows peak ground velocity in one of the more damaging aftershocks, namely a Mw 5.4 earthquake with an epicenter near Oakland.

Aagaard et al. (2010a, b) do not offer a map of afterslip, which progresses with time and varies spatially along the fault. For present purposes, let us assume that for most of the fault length, total slip (coseismic plus afterslip) equals 1.9 meters, except where coseismic slip exceeds that amount. Afterslip evolves over time following Equations 6-9 in Aagaard et al. (2012), with C = 0.09845, calculated using their Fig 11 and Mw = 7.05.
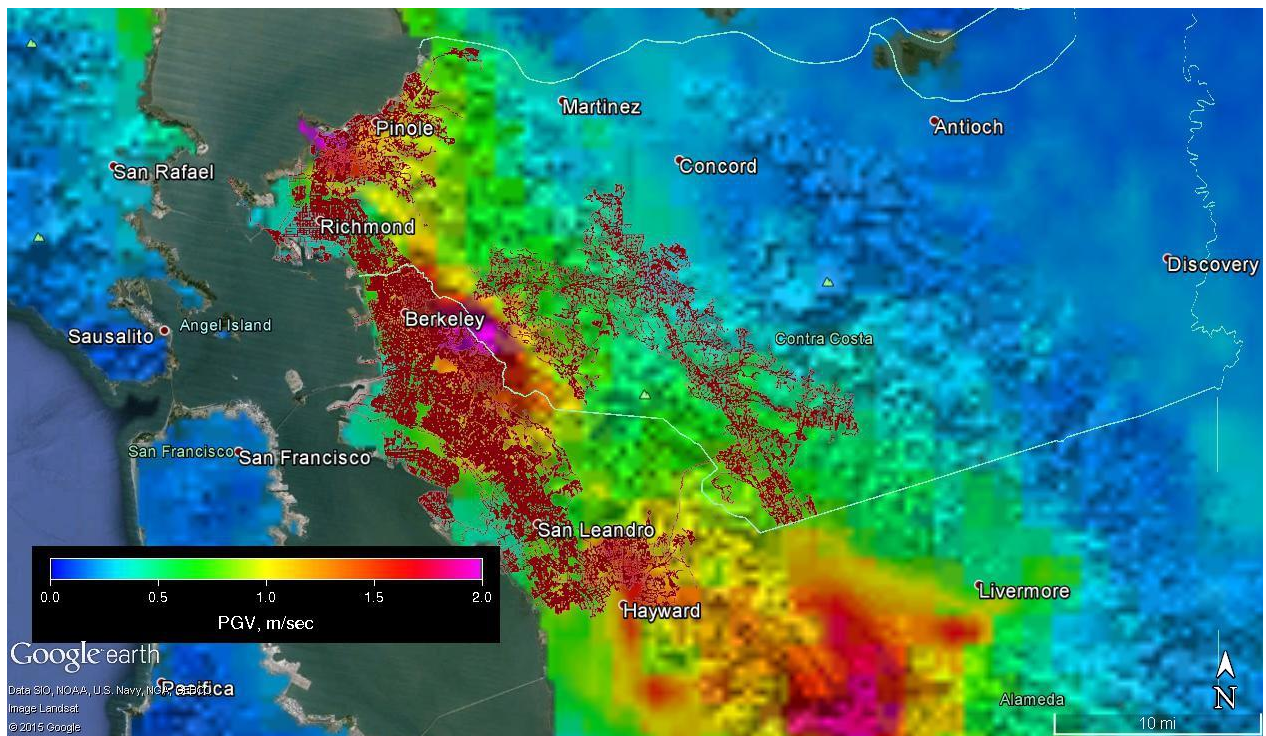

Figure 30. EBMUD water supply system with mainshock peak ground velocities

**Figure 31. EBMUD water supply system with mainshock liquefaction probability**

**Figure 32. Mainshock landslide probability near EBMUD service area**
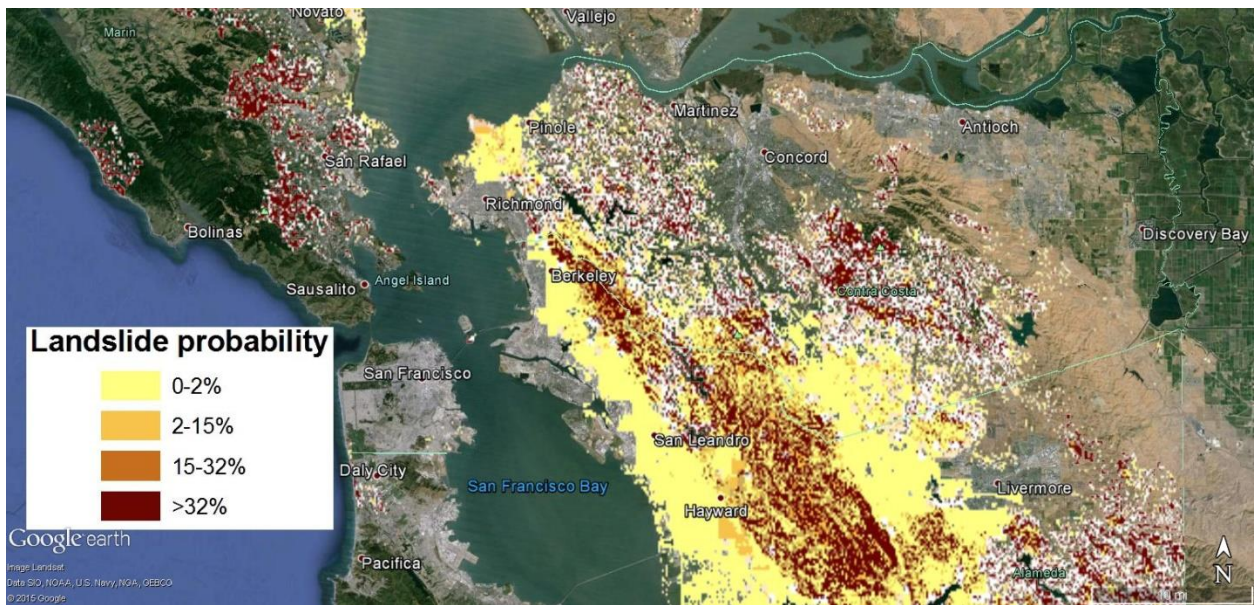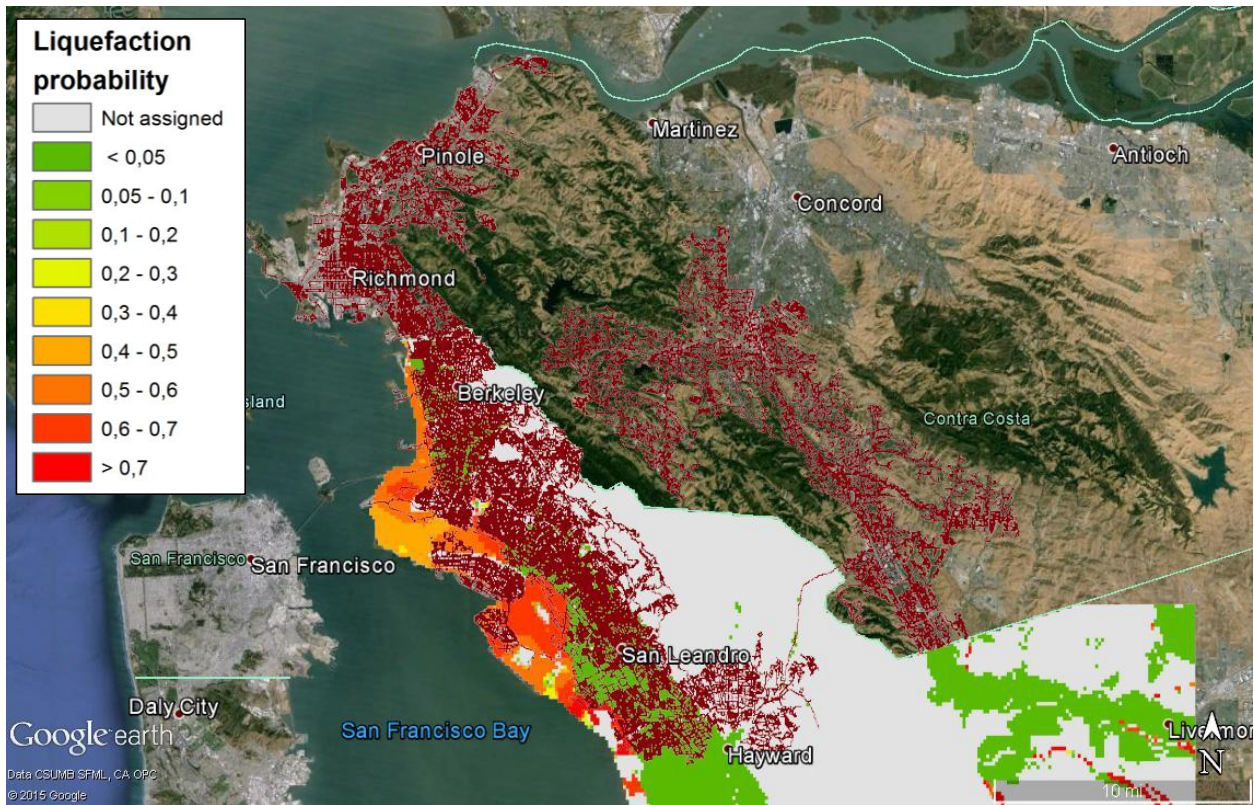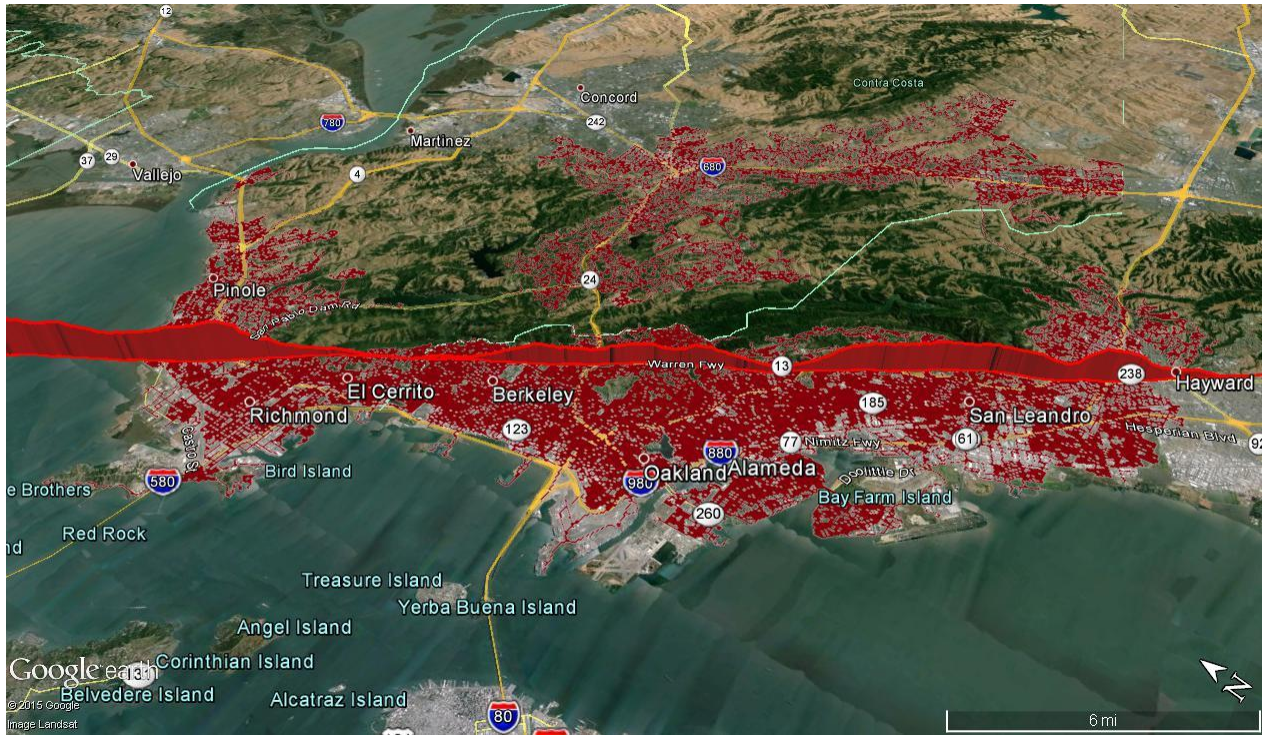
Figure 33. EBMUD system with fault

Figure 34. EBMUD water supply system with Oakland M 5.42 aftershock PGV contours

5.3 EBMUD damage analysis

Table 21 summarizes the estimated damage to EBMUD pipelines from the scenario mainshock and aftershocks. Damage in the mainshock includes ground shaking, liquefaction, landsliding, and surface rupture. Since the available liquefaction map does not include Contra Costa County, I assume that liquefaction damage in Contra Costa county is proportional to shaking damage in Contra Costa County, in the same proportions as in Alameda County. As the table illustrates, aftershock damage ignores landslides, liquefaction, and surface rupture. Note that the mainshock damage estimate for afterslip assumes that after pipes that are ruptured by fault slip are damaged a second time by afterslip, EBMUD may decide to either install earthquake-resistant pipe (e.g., HDPE pipe or steel pipe with flexible joints that can tolerate extension, compression, and lateral deformation) or to temporarily install flexible hose until the damaged main can be repaired or earthquake-resistant pipe can be installed. The table shows that the mainshock produces the majority of the overall damage, but that after the mainshock, 36% more damage occurs in aftershocks. Half the mainshock damage is associated with wave passage, the other half to liquefaction, landsliding, and fault offset.

Table 22 presents the estimated number of leaks plus breaks in EBMUD buried pipeline in each earthquake of the Hayward Fault sequence. After the mainshock, 6 of 16 aftershocks each produces at least 100 breaks or leaks, and one produces more than 300, with significant numbers of breaks and leaks occurring almost 6 months after the mainshock, a point that is made somewhat clearer by Table 23, which summarizes damage by day after the mainshock. Table 24 details repair rate over the entire sequence by pipe material. Unsurprisingly, it shows that most damage is in brittle cast iron and asbestos cement pipe, with damage rates approaching 0.3 per 1,000 lf. Table 25 presents repair rate over the entire sequence by pipe diameter, with most repairs required in 6-inch and 8-inch diameter pipe, which together represents the majority of pipe in the system.

Figure 35, Figure 36, and Figure 37 present damage heatmaps for EBMUD's system: they map mean repairs (estimated per the present methodology) per square kilometer in the mainshock, most-damaging aftershock (a M 5.4 event with an Oakland epicenter), and the entire sequence. Damage rates reach 50 repairs per square kilometer along the fault and in zones of high liquefaction probability. The heatmap for the mainshock shows 20 to 50 breaks per km^2 in large areas west of the fault, and no levels so high east of the fault, consistent with older pipe and higher liquefaction probability west of the fault. As a further sanity check of the mainshock heatmap, notice that it shows on the order of 10 leaks or breaks per km^2 over an area of about 500 km^2, or about the 5,200 leaks and breaks estimated here.

As with the first case study, the heatmaps show estimated break rates in the Hayward Fault sequence. Different earthquakes would produce different damage patterns. The EBMUD heatmaps depict a single realistic damage pattern in order to make the scenario more tangible. EBMUD and its customers, by planning for this scenario, could better prepare for what actually happens, which will invariably differ in total quantities, spatial distribution of damage, and over time.

Table 21. Hayward Fault mean damage estimate in EBMUD buried pipeline

	Mainshock	Aftershocks	Total
Mean number of repairs	3,916	1,395	5,311
Repairs/km pipe	0.58	0.21	0.79
Due to wave passage	2,063 (53%)	1,395 (100%)	3,458 (65%)
Due to liquefaction	949 (24%)	Not calculated	949 (18%)
Due to landslide	179 (5%)	Not calculated	179 (3%)
Due to coseismic slip	214 (5%)	Not calculated	214 (4%)
Due to afterslip	214 (5%)	Not calculated	214 (4%)
Large diameter ($\geq$ 20 in diam)	215 (5%)	84 (6%)	299 (6%)
Small diameter (< 20 in diam)	3,701 (95%)	1,311 (94%)	5,011 (94%)
Breaks	1,235 (32%)	209 (15%)	1,444 (27%)
Leaks	2,681 (68%)	1,185 (85%)	3,866 (73%)

Table 22. Estimated number of leaks plus breaks in EBMUD buried pipeline in the Hayward Fault sequence

Name	Day	Epicenter	Mag	Leaks + breaks	Diam $\geq$ 20 in	Diam < 20 in
Mainshock	1	Oakland	7.05	3,916	215	3,701
sp504	1	San Pablo	5.04	102	6	96
uc523	1	Union City	5.23	101	6	95
ff558	12	Fairfield	5.58	49	3	46
fr510	15	Fremont	5.1	37	2	35
ok542	32	Oakland	5.42	323	20	304
mp552	40	Menlo Park	5.52	44	3	41
pa62_	40	Palo Alto	6.2	141	8	133
pa569	41	Atherton	5.11	61	4	57
at511	41	Palo Alto	5.69	44	3	42
pa522	67	Palo Alto	5.22	54	3	51
pa526	74	Palo Alto	5.26	59	4	55
sc509	166	Cupertino	6.4	25	2	24
cu640	166	Mountain View	5.98	173	10	162
sv535	166	Santa Clara	5.09	52	3	49
mv598	166	Sunnyvale	5.35	102	6	96
pa501	492	Palo Alto	5.01	28	2	26
Total				5,311	299	5,011

Table 23. Total EBMUD leaks plus breaks by day

Day	Leaks + breaks*	Diam ≥ 20 in	Diam < 20 in
1	4,118	227	3,891
12	49	3	46
15	37	2	35
32	323	20	304
40	185	11	174
41	105	6	98
67	54	3	51
74	59	4	55
166	352	21	330
492	28	2	26
Grand Total	5,311	299	5,011

* Slight differences from Table 22 and summation differences are due to rounding

Table 24. Repair rate in Hayward Fault sequence in EBMUD buried pipeline, by material

Material	Description	Length, ft	Repairs*	Repairs/1000 lf
A	Asbestos cement, unrestrained	6,000,452	1,558	0.260
C	Cast iron, unrestrained	6,980,888	1,977	0.283
D	Ductile iron, unrestrained	10,841	4	0.332
F	Fusible PVC, welded	6,478	1	0.142
H	High density polyethylene, weld	46,472	8	0.169
K	Copper, restrained	3,646	0	0.133
L	Reinf concrete cyl., unrestrained	75,622	19	0.250
N	PVC, unrestrained	2,008,486	363	0.181
P	Reinf concrete cylinder	372	0	0.084
R	Reinf. conc. noncylinder	174	0	0.155
S	Steel, weld	6,771,086	1,074	0.159
T	Pre-tens. conc. cyl., restrained	55,106	7	0.124
W	Wrought iron	14,319	4	0.249
Grand Total		21,973,942	5,014	0.228

*Excludes damage estimated to occur in zones of liquefaction in Contra Costa County

Table 25. Repair rate in Hayward Fault sequence in EBMUD buried pipeline, by diameter

Diameter, in.	Length, ft	Repairs*	Repairs/1000 lf*
0	2,201	0	0.000
0.75	834	0	0.000
1	5,342	3	0.562
2	98,006	25	0.255
3	3,665	1	0.273
4	1,555,655	420	0.270
6	9,124,837	2,231	0.244
8	5,838,048	1,352	0.232
10	200,527	60	0.299
12	2,512,027	466	0.186
14	7,502	2	0.267
16	831,998	171	0.206
18	7,394	1	0.135
20	412,261	78	0.189
24	393,015	63	0.160
25	2,581	0	0.000
30	192,540	29	0.151
36	352,938	50	0.142
42	97,882	13	0.133
48	202,222	32	0.158
54	46,248	10	0.216
60	13,778	2	0.145
66	35,784	3	0.084
69	24,207	2	0.083
72	70	0	0.000
78	978	0	0.000
84	9,598	1	0.104
90	994	0	0.000
96	689	0	0.000
108	122	0	0.000
Grand Total	21,973,942	5,014	0.228

* Where expected number of repairs < 0.5, number of repairs and repair rate per 1,000 are rounded to 0. Table excludes damage assumed to occur in zones of liquefaction in Contra Costa County.
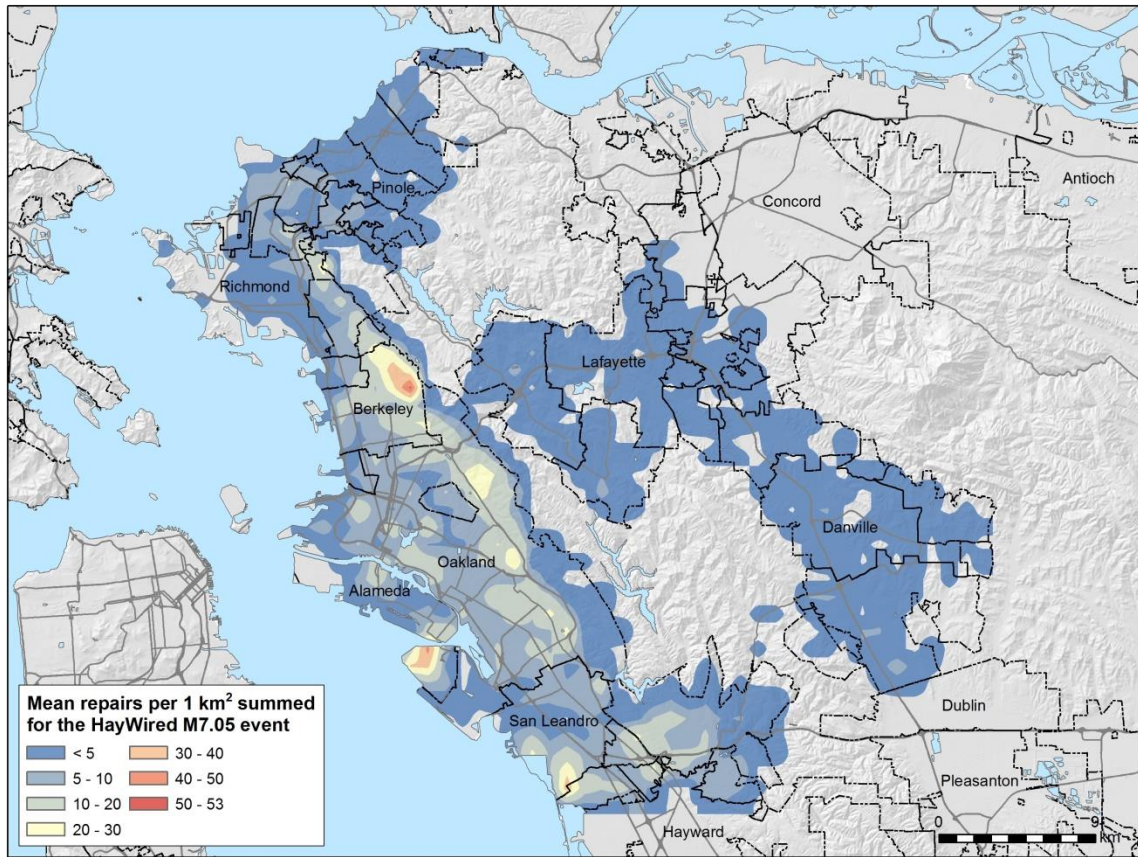
Figure 35. Buried water pipeline damage heatmap for the Hayward Fault mainshock in EBMUD's service area
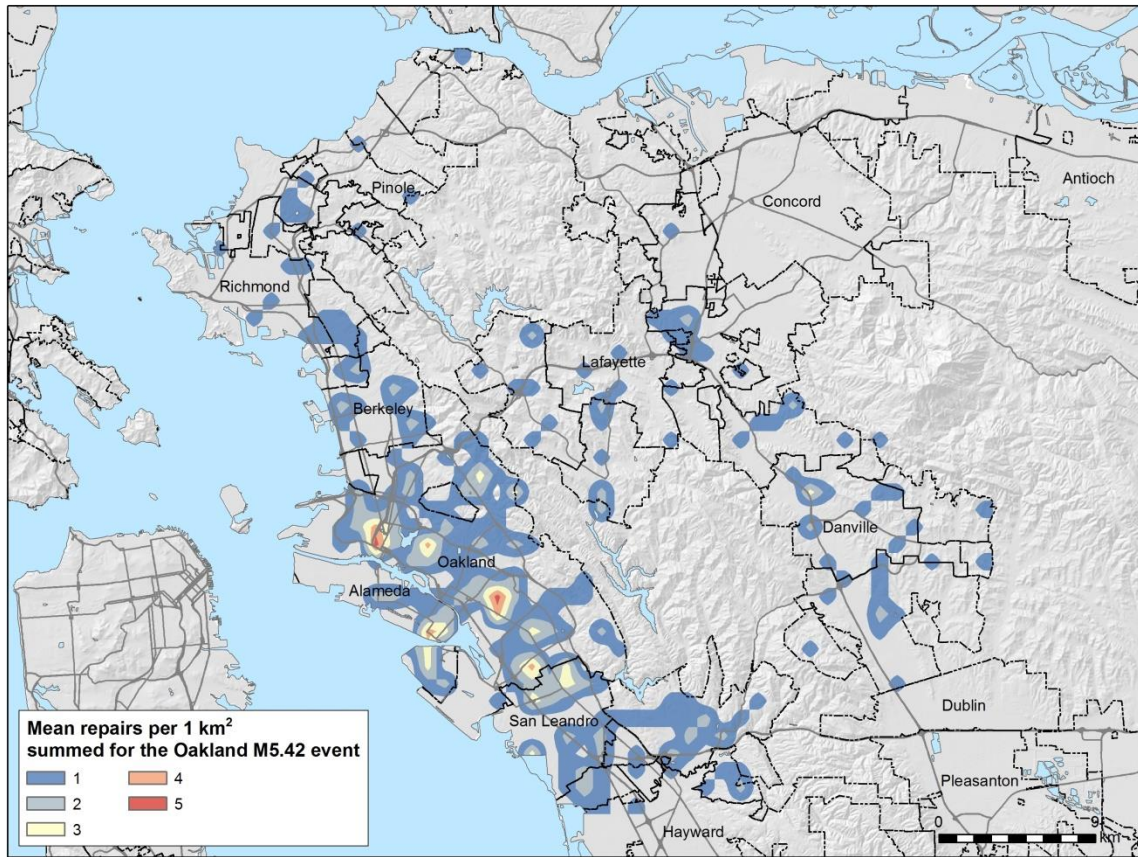
Figure 36. Buried water pipeline damage heatmap for the most-damaging aftershock in EBMUD's service area
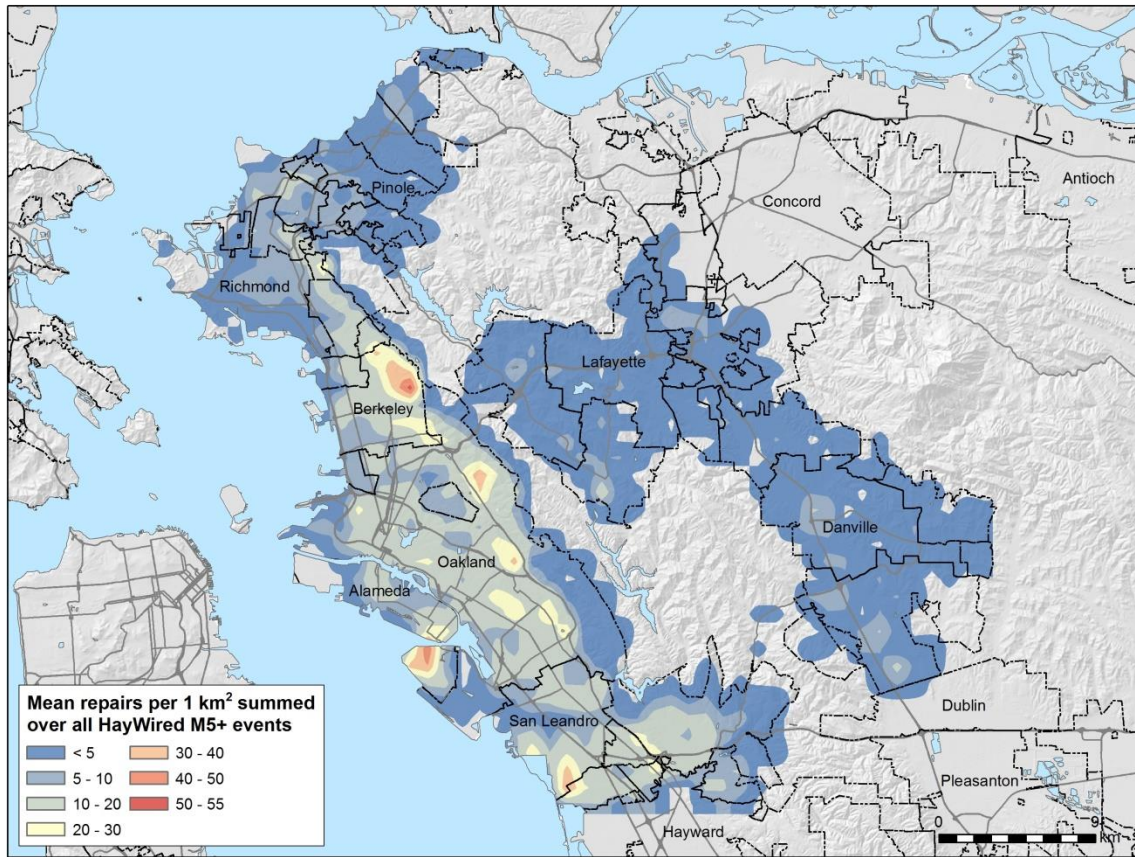
Figure 37. Buried water pipeline damage heatmap for the entire Hayward Fault sequence in EBMUD's service area

5.4 EBMUD restoration analysis

See Section 4.4 for the scenario's assumptions about electricity, fuel, and communication. Let us further assume that EBMUD can acquire consumables—pipe, clamps, replacement valves, etc.—as quickly as needed. Regarding crews, EBMUD agrees with the scenario assumption that it would take up to a week to assess the extent of damage and locate leaks before before repairs can be initiated on a larger scale, and that repair efforts would likely need to initially focus on larger diameter mains. EBMUD staff also estimated that they may be able to field 20 of their own repair crews plus 15 crews provided through mutual aid, for a total of on the order of 35 repair crews. Of these, ¼ are deployed east of the East Bay Hills, the other ¾, west. Let us assume that repairs begin 5 days after the mainshock (the mainshock occurs on day 1), and that $c(t)$ ramps up from 20 to 35 crews over the following 14 days, and that crews work 8 hour days until repairs are completed. Figure 38 illustrates repair crew availability, which is expressed mathematically here:

$a(t) = 0.33$
$c(t) = 2 \qquad t < 6$

– 90 –

$$\begin{aligned}&= \lfloor 2t - 5 \rfloor && 6 \le t < 20 \\ &= 35 && 20 \le t < 41 \\ &= 20 && 41 \le t\end{aligned}$$

The notation $\lfloor x \rfloor$ means the integer part of the quantity x, used here because there are no such things as fractional crews.
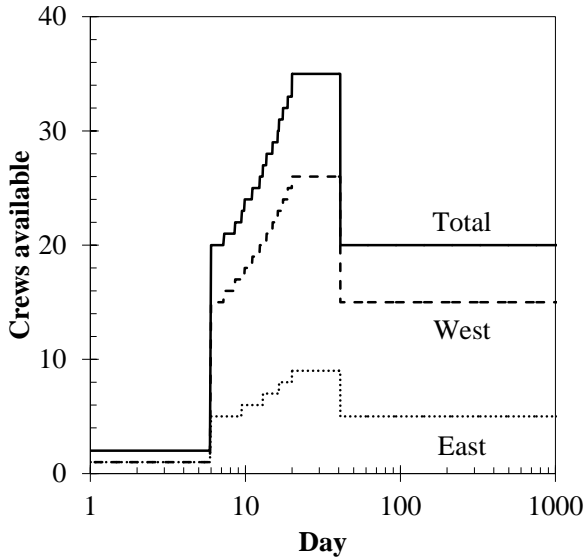
Figure 38. EBMUD repair-crew availability

Figure 39 illustrates the initial level of service according to Equation (27): the loss of system pressure results in approximately 87% of services east of the hills receiving water shortly after the mainshock, 13% of those west of the hills.
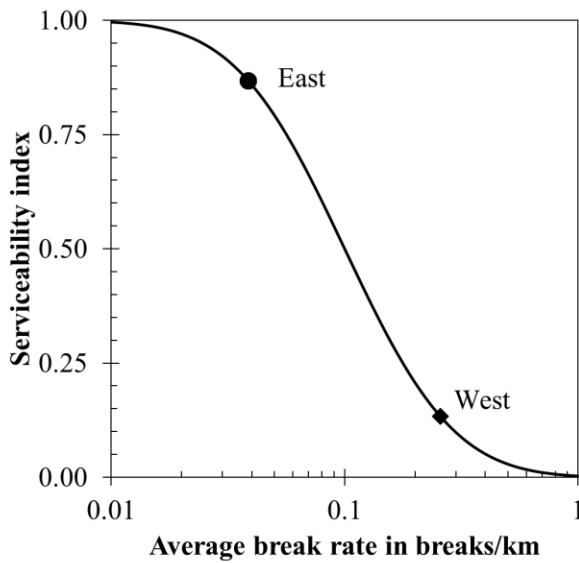
Figure 39. Initial serviceability east and west of the East Bay Hills

Since PG&E expects electricity to be almost completed restored by day 7 and under the present scenario fuel is only impaired from day 3 to day 7, loss of electricity and a fuel shortage have little effect on EBMUD's restoration curve. (It seems realistic that restoring electricity might take longer than PG&E expects, at least in small areas, but nonetheless I am guided by PG&E's assertion that they will meet their restoration objective.) Figure 40 presents the estimated service restoration curve for EBMUD under three conditions: (1) as is, (2) assuming the EBMUD develops a fuel plan to ensure that repair crews are never slowed or idled from lack of fuel, and (3) under ideal conditions. If the Hazus-MH serviceability index realistically measures the fraction of services receiving any water, as its reports suggest, then "services available" means the fraction of service connections receiving even small flows. If it means the post-earthquake flow as a fraction of pre-earthquake flow, then the charts underestimate the number of service connections receiving at least some water. Note that "ideal conditions" refers to the case in which the mainshock occurs after all of EBMUD's brittle pipe is replaced, and where the pumping stations are all supplied with emergency generators and fuel. The curves show that under as-is conditions, full restoration takes 23 weeks (just over 5 months). Under ideal-world conditions, full service is restored in 14 weeks (just over 3 months), roughly 2 months earlier than under as-is conditions.
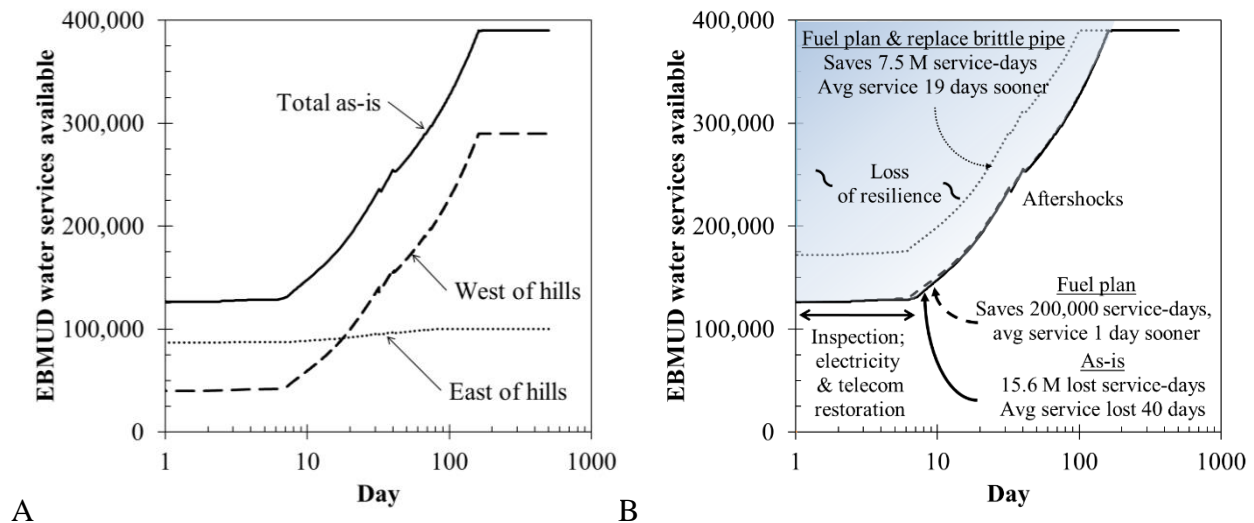
Figure 40. EBMUD restoration curves in the Hayward Fault sequence: (A) under as-is conditions, showing service east and west of East Bay Hills, and (B) under several conditions, total for the system

Figure 41 shows the progress of repairs, again illustrating the possible effects of a fuel shortage, an estimate of the benefit of a fuel plan, and the potential benefit of replacing brittle pipe quickly.
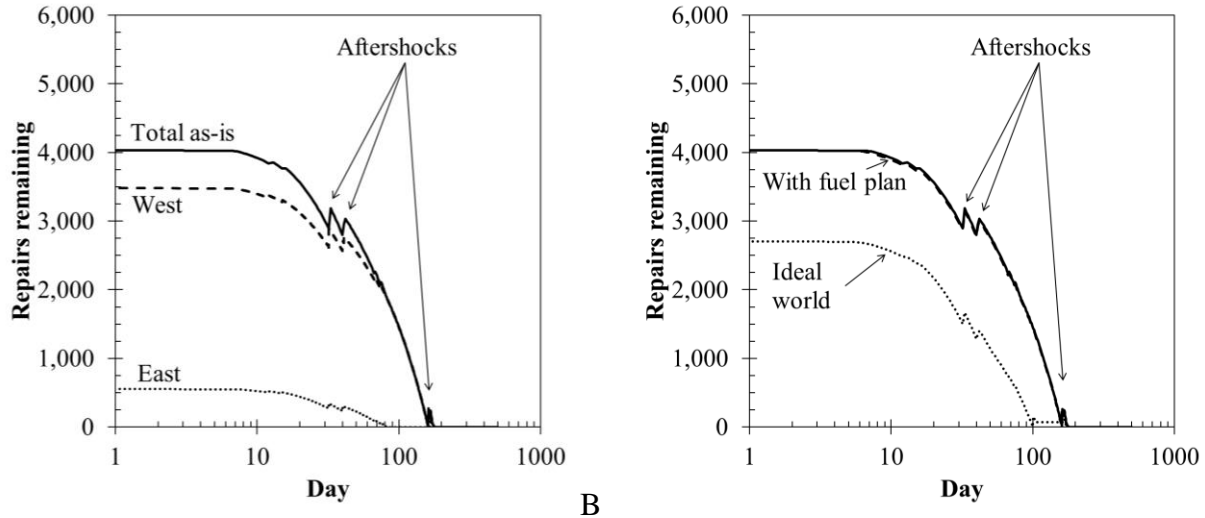
**Figure 41. EBMUD repair progress in the Hayward Fault sequence (A) under as-is conditions, showing repair progress east and west of East Bay Hills, and (B) under several conditions, total for the system**

One can view the area above the curves in Figure 40 as a measure of resilience: less area means less impact, faster recovery, or both. The areas above the three curves are measured in units of service-days. That is, each day of lost water supply to a service connection equates with one service-day. The areas above the three curves are shown in Table 26. The table shows lost service-days under as-is conditions, with a fuel plan, and under ideal-world conditions, i.e., in which all cast iron and asbestos cement pipe is replaced before the earthquake. The difference between lost service days under as-is and what-if conditions (fuel plan or ideal world) measures the resilience benefit of the what-if condition: with a fuel plan and if all brittle pipe were replaced before the hypothetical earthquake occurred. Although full restoration takes much longer, the table also shows average number of days that each service connection goes without potable water under as-is conditions, with the fuel plan, and under ideal-world conditions. Figures have been rounded to reduce the impression of excessive precision.

Table 26. EBMUD lost service-days

Condition	Lost service-days $R \cdot M$	Resilience benefit $\Delta(R \cdot M)$	Average lost days R
As-is	15,600,000		40
Fuel plan	15,400,000	200,000	39
Ideal world	8,100,000	7,500,000	21

5.5 Validation of EBMUD damage and recovery estimates

5.5.1 Cross validation with EBMUD internal damage estimates

EBMUD commissioned a private study that estimated, among other things, the damage potential for water supply pipeline damage resulting from a M 7.0 earthquake on the Hayward Fault. As described by Terentieff et al. (2015), that 1997 study estimated 4,054 pipe breaks and leaks, most of which occur in cast iron and asbestos cement pipe. EBMUD performed an internal study recently of large-diameter pipe (at least 16- to 24-inch diameter, depending on pipe material) and

estimated 334 breaks and leaks. The authors report that EBMUD has initiated an infrastructure renewal program with a goal of replacing approximately 1% of its pipe per year, focusing first on cast iron and asbestos cement.

The 1997 estimate of 4,054 breaks and leaks is very close to the 3,916 breaks and leaks estimated here for the mainshock and somewhat smaller than the present estimate of 5,311 breaks and leaks in the entire sequence. The recent estimate of 334 breaks and leaks among large diameter pipe is somewhat higher than the present estimate of 209 breaks and leaks in pipe of at least 20-inch diameter in the mainshock, though similar to the present estimate of 299 large-diameter breaks and leaks in the entire sequence.

It seems realistic that EBMUD will complete much of its replacement of the 61% of its pipe that are constructed of cast iron or asbestos cement before a large earthquake occurs on the Hayward Fault. Although the issue is more complicated than just whether a M 7.0 or larger earthquake occurs on the Hayward Fault, according to the UCERF 3 fault section data (Field et al. 2013), the chance that one does occur in the next 61 years is approximately 16% on the northern segment, 12% on the southern segment, and 26% on one or the other—significant, but nowhere near certain.

5.5.2 Comparison with EBMUD judgment, Northridge, Kobe, and Napa restoration

As previously noted, Jeon and O'Rourke (2005) report that the 1994 Northridge earthquake caused 1,095 breaks or leaks to buried pipeline operated by the Los Angeles Department of Water and Power, while Lund et al. (2005) report that repairs took about 1 week. The present calculation suggests that EBMUD would take 23 weeks to repair 5,311 breaks and leaks. While the estimate of just over 5 months' restoration agrees with EBMUD judgment, it is about 23 times as long for about 5 times the number of repairs, or about 1/5th as fast as LADWP's repairs.

Also as previously noted, the Kobe Municipal Waterworks Bureau experienced 1,757 breaks and leaks after the 1995 Kobe earthquake and that repairs took 10 weeks, i.e., 176 repairs per week. The present estimate of 23 weeks to repair 5,311 breaks and leaks (230 repairs per week) is roughly on par with Kobe.

The City of Napa repaired approximately 120 leaks and breaks in 5 days (170 repairs per week) after the 2014 South Napa earthquake, approximately equal to the 200 repairs per week estimated here.

5.5.3 Cross validation with Hazus-MH

Table 27 presents the Hazus-MH estimate of water supply restoration in Contra Costa and Alameda Counties, where EBMUD operates. As before, the estimates are for the mainshock only and do not reflect lifeline interaction. Applying the percentages to the number of EBMUD's customers, one can compare the two models, as shown in Figure 42. The two models substantially disagree in terms of initial service availability and in terms of restoration time.

Table 27. Hazus-MH estimate of Contra Costa and Alameda County loss of water supply

Analysis		Households without water				
		Day 1	Day 3	Day 7	Day 30	Day 90
Hazus-MH[a]	#	855,207	854,738	853,731	845,534	762,299
	%	98.58%	98.53%	98.41%	97.47%	87.87%
This analysis[b]	%	68%	67%	66%	41%	19%

[a] Hazus-MH figures as reported by the software, with its estimate of 867,495 total households.
[b] Estimates rounded to the nearest percent to reduce the appearance of excessive accuracy. Hazus-MH figures are as reported by the
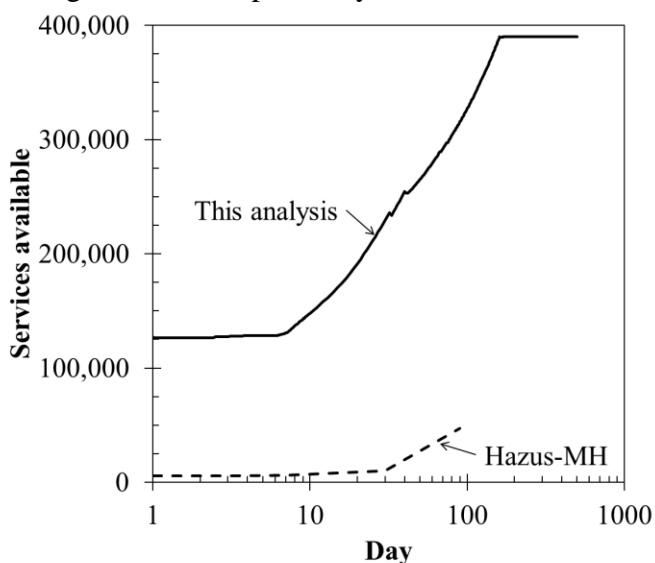
Figure 42. Cross validation of EBMUD restoration with Hazus-MH

5.6 Effect of lifeline interaction and consumable limits on EBMUD

EBMUD does not expect to begin repairs until about day 7, after power and telecommunications have been mostly restored, so lifeline interaction will have little effect on EBMUD in the scenario.

6 Performance of other water utilities based on Hazus-MH

It is time consuming to acquire the necessary data and to perform the analysis of a water supply system. The Bay Area has on the order of 30 of them. To estimate the effects of the earthquake sequence on the metropolitan area, let us apply the proposed modification of the Hazus-MH methodology to the analysis of the Bay Area's water supply system performed by Bausch (2014) and Seligson (2014). First, let us adjust restoration to account for the differences between Hazus' default assumptions of repair crew availability.

San Jose Water Company estimates it can field 22 repair crews to respond to damage in its service area of 225,000 service connections, or approximately 1 crew per 10,000 service connections. Hazus-MH seems to equate households with service connections. Using a building inventory that FEMA enhanced for the San Francisco Bay Area prior to this study, Hazus estimates that Santa Clara County has 565,863 households, which it seems to equate with the number of service

connections. For purposes of adjusting Hazus' default number of pipeline repair crews, for purposes of Equation (56), let us take

$$\frac{q}{q_0} = \frac{1}{100} \cdot \left(\frac{565,863}{10,000} \cdot 4 \right)$$
$$= 2.26$$

EBMUD engineers agree with the scenario assumption that EBMUD can field 35 crews to respond to damage in its system that provides water to 390,000 service connections. Those figures indicate approximately 1 crew per 11,000 service connections, versus SJWC's estimate of up to 1 crew per 9,000 service connections. Let us assume therefore that Alameda and Contra Costa counties (EBMUD's service area), have approximately 1 crew (4 workers) per 11,000 households, Santa Clara County (SJWC's service area) has 1 crew per 9,000 households, and other counties have one crew per 10,000 households (an approximate mean of EBMUD and SJWC, in round numbers). Table 28 presents the restoration-rate adjustment factors for repair-crew availability. The household-weighted average value of the repair-crew factor q/q_0 is 1.37, although it is higher in the strongly shaken counties of Alameda and Santa Clara.

Table 28. Repair-crew adjustment factors $q/q0$ for Bay Area buried water supply pipeline restoration

County	Households	Crews	Workers	$q/q0$
Alameda	523,366	48	190	1.90
Contra Costa	344,129	31	125	1.25
Marin	100,650	10	40	0.40
Merced	63,815	6	26	0.26
Monterey	121,236	12	48	0.48
Napa	45,402	5	18	0.18
Sacramento	453,602	45	181	1.81
San Benito	15,885	2	6	0.06
San Francisco	329,700	33	132	1.32
San Joaquin	181,629	18	73	0.73
San Mateo	254,103	25	102	1.02
Santa Clara	565,863	63	251	2.51
Santa Cruz	91,139	9	36	0.36
Solano	130,403	13	52	0.52
Sonoma	172,403	17	69	0.69
Stanislaus	145,146	15	58	0.58
Yolo	59,375	6	24	0.24

To address lifeline interaction for the purposes of Equation (62)—the product term inside the summation—let us take rate-limiting factors u and the flow of rate-limiting factors g as those proposed for EBMUD. That is, let us assume that approximately half of services are in pumped pressure districts that require electricity, that electricity is restored within one week, and that there is a temporary fuel shortage between days 3 and 7.

Hazus' estimates of the number of service connections with water service at time t_j (normalized by the number of households) are recapped in Table 29. The assumption of complete restoration

at day 540 is mine. Hazus-MH does not report level of service beyond 90 days, but I suggest that full restoration would likely be completed within 18 months. The table reports values of $\hat{V}(t)$ in the sense of Equation (56). Table 30 shows the restoration curves adjusted for repair-crew availability and lifeline interaction, but using the restoration curves for Alameda, Contra Costa, and Santa Clara counties as those calculated in the case studies under as-is conditions. Table 31 shows the restoration curves adjusted with a fuel plan in place in all counties. Alameda, Contra Costa, and Santa Clara counties as those calculated in the case studies with a fuel plan. Table 32 shows the restoration curves with emergency generators and fuel in all counties. Alameda, Contra Costa, and Santa Clara counties as those calculated in the case studies under ideal-world conditions. The tables are illustrated in Figure 43 A through D. Note that, since Hazus-MH analyses were unavailable for lifelines subjected to aftershocks, the restoration curves for counties other than Santa Clara, Alameda, and Contra Costa counties do not reflect aftershock damage.

Table 29. Hazus-MH unadjusted estimate of water service restoration

County	Day					
	1	3	7	30	90	540
Alameda	1%	1%	1%	1%	2%	100%
Contra Costa	3%	3%	3%	5%	28%	100%
Marin	91%	98%	100%	100%	100%	100%
Merced	98%	99%	100%	100%	100%	100%
Monterey	100%	100%	100%	100%	100%	100%
Napa	100%	100%	100%	100%	100%	100%
Sacramento	100%	100%	100%	100%	100%	100%
San Benito	98%	100%	100%	100%	100%	100%
San Francisco	40%	52%	87%	100%	100%	100%
San Joaquin	100%	100%	100%	100%	100%	100%
San Mateo	30%	34%	41%	100%	100%	100%
Santa Clara	11%	11%	12%	19%	76%	100%
Santa Cruz	100%	100%	100%	100%	100%	100%
Solano	98%	100%	100%	100%	100%	100%
Sonoma	100%	100%	100%	100%	100%	100%
Stanislaus	100%	100%	100%	100%	100%	100%
Yolo	100%	100%	100%	100%	100%	100%

Table 30. Hazus-MH-based estimate of water service restoration after adjusting for repair crew availability, lifeline interaction, but with no fuel plan. Santa Clara, Alameda, and Contra Costa Counties are as calculated in case studies without a fuel plan.

County	Day					
	1	3	7	30	90	540
Alameda	32%	33%	34%	61%	81%	100%
Contra Costa	32%	33%	34%	61%	81%	100%
Marin	91%	94%	95%	100%	100%	100%
Merced	98%	98%	98%	100%	100%	100%
Monterey	100%	100%	100%	100%	100%	100%
Napa	100%	100%	100%	100%	100%	100%
Sacramento	100%	100%	100%	100%	100%	100%
San Benito	98%	98%	100%	100%	100%	100%
San Francisco	40%	55%	67%	100%	100%	100%
San Joaquin	100%	100%	100%	100%	100%	100%
San Mateo	30%	34%	35%	80%	100%	100%
Santa Clara	63%	70%	73%	100%	100%	100%
Santa Cruz	100%	100%	100%	100%	100%	100%
Solano	98%	99%	99%	100%	100%	100%
Sonoma	100%	100%	100%	100%	100%	100%
Stanislaus	100%	100%	100%	100%	100%	100%
Yolo	100%	100%	100%	100%	100%	100%

Table 31. Hazus-MH-based estimate of water service restoration after adjusting for repair crew availability, lifeline interaction, and with a fuel plan. Santa Clara, Alameda, and Contra Costa Counties are as calculated in case studies.

County	Day					
	1	3	7	30	90	540
Alameda	32%	33%	35%	59%	81%	100%
Contra Costa	32%	33%	35%	59%	81%	100%
Marin	91%	94%	100%	100%	100%	100%
Merced	98%	98%	99%	100%	100%	100%
Monterey	100%	100%	100%	100%	100%	100%
Napa	100%	100%	100%	100%	100%	100%
Sacramento	100%	100%	100%	100%	100%	100%
San Benito	98%	98%	100%	100%	100%	100%
San Francisco	40%	55%	100%	100%	100%	100%
San Joaquin	100%	100%	100%	100%	100%	100%
San Mateo	30%	34%	41%	86%	100%	100%
Santa Clara	63%	70%	79%	100%	100%	100%
Santa Cruz	100%	100%	100%	100%	100%	100%
Solano	98%	99%	100%	100%	100%	100%
Sonoma	100%	100%	100%	100%	100%	100%
Stanislaus	100%	100%	100%	100%	100%	100%
Yolo	100%	100%	100%	100%	100%	100%

Table 32. Hazus-MH-based estimate of water service restoration after adjusting for repair crew availability, lifeline interaction, with a fuel plan and emergency generators and fuel at all pumping stations. Santa Clara, Alameda, and Contra Costa Counties are as calculated in case studies under ideal-world conditions.

| County	Day					
	1	3	7	30	90	540
Alameda	44%	44%	47%	73%	97%	100%
Contra Costa	44%	44%	47%	73%	97%	100%
Marin	91%	94%	100%	100%	100%	100%
Merced	98%	98%	99%	100%	100%	100%
Monterey	100%	100%	100%	100%	100%	100%
Napa	100%	100%	100%	100%	100%	100%
Sacramento	100%	100%	100%	100%	100%	100%
San Benito	98%	98%	100%	100%	100%	100%
San Francisco	40%	55%	100%	100%	100%	100%
San Joaquin	100%	100%	100%	100%	100%	100%
San Mateo	30%	34%	41%	86%	100%	100%
Santa Clara	71%	78%	85%	100%	100%	100%
Santa Cruz	100%	100%	100%	100%	100%	100%
Solano	98%	99%	100%	100%	100%	100%
Sonoma	100%	100%	100%	100%	100%	100%
Stanislaus	100%	100%	100%	100%	100%	100%
Yolo	100%	100%	100%	100%	100%	100%
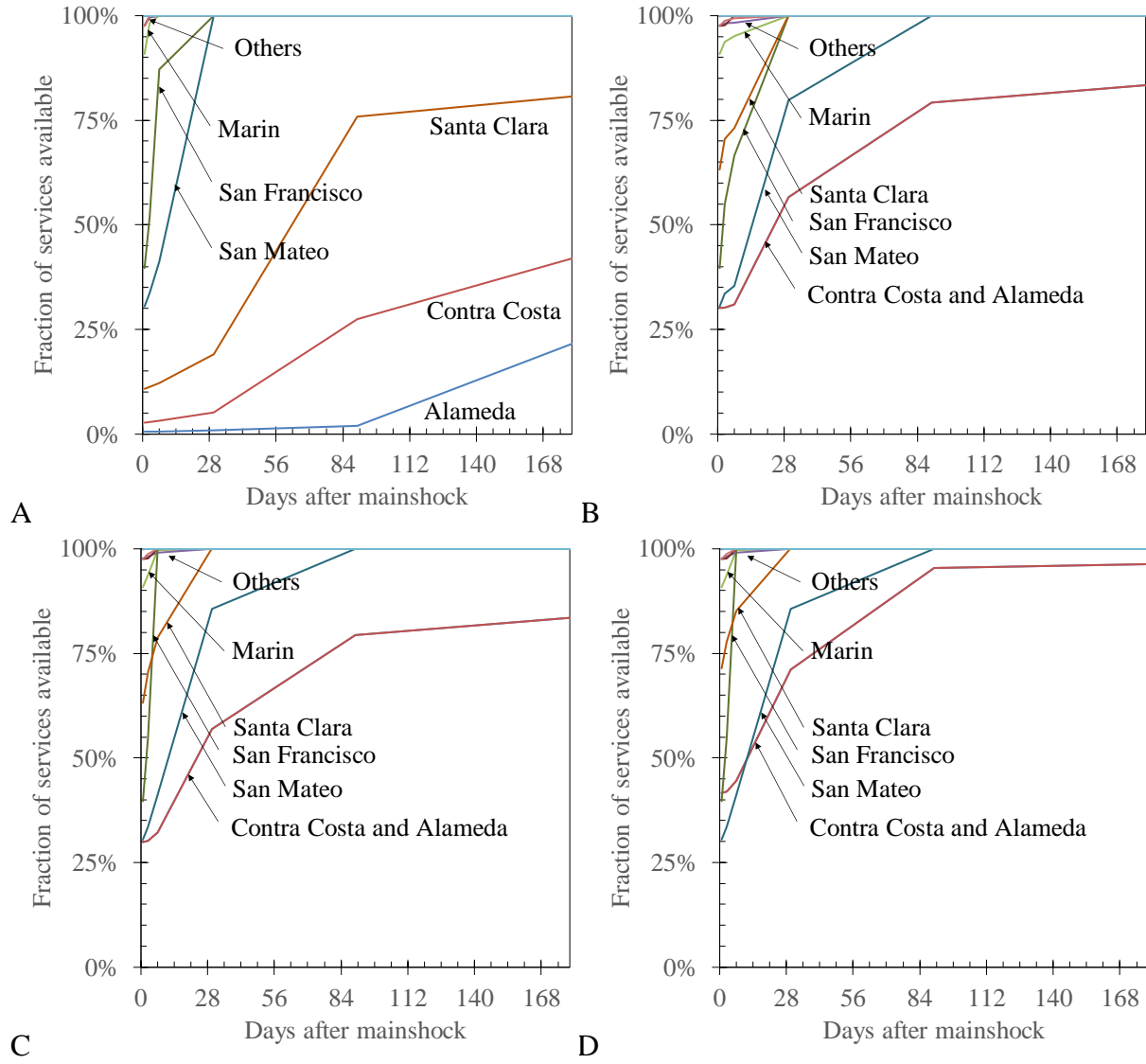
Figure 43. Water restoration (A) according to initial Hazus-MH calculations (B) after adjusting for repair-crew availability and lifeline interaction, (C) after all utilties have implemented a fuel plan, and (D) ideal-world conditions. Curves in B, C, and D use the more-detailed case-study calculations for Contra Costa, Alameda, and Santa Clara counties instead of Hazus-MH.

7. Conclusions

7.1 Summary

The methodology proposed here models damage and restoration of buried pipelines subject to earthquake shaking (called wave passage) and ground failure (liquefaction, landslide and surface rupture of the fault). The methodology assumes that the analyst already has maps of the earthquake excitation (especially peak ground velocity and ground-failure probability) and of the pipeline system in question. Many authors have proposed such models in the past. The present model may be unique in combining some unusual features:

(1) It treats lifeline interaction and limited consumables by reducing the speed with which repairs are completed in relation to how important those upstream lifelines and other resources are to repair productivity. In the example of San Jose Water Company, it was estimated that lifeline interaction and limited consumables increase the loss of resilience (measured in terms of lost service-days) by 25 percent.

(2) The model treats aftershocks.

(3) It can be evaluated either deterministically (with no uncertainty) or as stochastic model (accounting for major sources of uncertainty).

(4) It can be carried out with a GIS system and a spreadsheet and does not require other special software such as Hazus-MH. Doing so provides the analyst more insight into the reasonableness of model results and underlying sources of damage and restoration delay.

(5) It offers an approximate method to modify Hazus-MH lifeline damage and restoration-time estimates to account for lifeline interaction.

(6) It does not require hydraulic analysis of the damaged system or the system as repairs proceed. That simplification necessarily involves a common but questionable assumption relating break rate to loss of service, and it prevents the analyst from gaining important insight into

(7) It mostly avoids reliance on expert opinion and unpublished data. Expert opinion seems to be required to quantify the rate-limiting factors u and the service time series $g(t)$ for damage to other lifelines that have not been modeled.

The methodology is applied here to examine the effect of a large hypothetical but not exceedingly rare earthquake in the San Francisco Bay Area on the buried pipeline network of the San Jose Water Company and East Bay Municipal Utility District. Results tend to agree with operator judgment, various restoration measures observed in past earthquakes, and comparable aspects of other models.

Like all other aspects of any earthquake scenario, the outcomes presented here will invariably differ in quantity, spatial distribution, and over time from whatever actually happens when (not if) a large earthquake happens next on the Hayward Fault or other Bay Area fault. By preparing for the water-supply impacts of this hypothetical earthquake sequence, the reader can be better prepared for whatever real earthquake actually occurs.

7.2 Research needs

The methodology proposed here mostly avoids reliance on opinion and judgment, but it would be practical to eliminate reliance on much of what remains. Presumably the u-factors based on expert opinion could be replaced by compiling sufficient earthquake experience from utilities, perhaps by some survey analogous to that of Lund and Schiff (1991). The time series $g(t)$ could be replaced by explicit modeling. It would be interesting to know if there were some theoretical justification for service restoration following a power law as in Equation (30), and whether or why the power should be approximately 2/3. It would be also desirable:

- To examine more closely or replace the Hazus-MH formulation of the serviceability index. Can one relate break rate to the fraction of customers receiving various thresholds of flow, such as minimal flows for cooking and basic sanitary needs?

- To know whether and how a large mainshock degrades the seismic resistance of apparently undamaged pipe;
- To add treatment of earthquake damage to other elements in the water-supply system, including tanks, tunnels, canals, valves, and reservoirs;
- Regarding the Lund and Schiff (1991) database, it would be desirable for water utilities to adopt a standard database for recording leaks and breaks, especially in earthquakes, so as to inform future improvements in pipe fragility functions; and
- To model the damage to Napa-area water supply systems subjected to the August 24, 2014 South Napa earthquake to see how well it agrees with experience.

8. References cited

Aagaard, B.T., R.W. Graves, D.P. Schwartz, D.A. Ponce, and R.W. Graymer, 2010. Ground-motion modeling of Hayward Fault scenario earthquakes, part I: construction of the suite of scenarios. *Bulletin of the Seismological Society of America*, 100 (6) 2927–2944

Aagaard, B.T., R.W. Graves, A. Rodgers, T.M. Brocher, R.W. Simpson, D. Dreger, N.A. Petersson, S.C. Larsen, S. Ma, and R.C. Jachens, 2010. Ground-motion modeling of Hayward Fault scenario earthquakes, part II: simulation of long-period and broadband ground motions. *Bulletin of the Seismological Society of America*, 100 (6) 2945–2977

American Water Works Association, 2008. *AWWA Small Systems Pipe Repair Checklist, as published in July 2008 Opflow Question of the Month*. 7 pp.

Ang, A.H.S. and W.H. Tang, 1975. *Probability Concepts in Engineering Planning and Design, Vol 1—Basic Principles*, John Wiley & Sons, New York, 409 pp.

Bruneau, M., S.E. Chang, R.T. Eguchi, G.C. Lee, T.D. O'Rourke, A,M. Reinhorn, M. Shinozuka, K. Tierney, W.A. Wallace, and D. von Winterfeldt, 2003. A Framework to Quantitatively Assess and Enhance the Seismic Resilience of Communities, *Earthquake Spectra*, 19 (4): 733–752

Committee on Gas and Liquid Fuel Lifelines, 1984. *Guidelines for the Seismic Design of Oil and Gas Pipeline Systems*. American Society of Civil Engineers, Technical Council on Lifeline Earthquake Engineering, Reston, VA, 473 pp.

(ATC) Applied Technology Council, 1991. *Seismic Vulnerability and Impact of Disruption of Lifelines in the Conterminous United States* (FEMA 224, ATC-25). Federal Emergency Management Agency, Washington, DC. http://www.fema.gov/plan/prevent/earthquake/pdf/fema-224.pdf [viewed 6 June 2006]

Ballantyne, D., E. Berg, J. Kennedy, R. Reneau, and D. Wu, 1990. Earthquake Loss Estimation Modeling of Seattle Water System, Kennedy/Jenks Inc., Seattle WA, Report to USGS, Grant No. 14-08-000 I-G 1526.

Ballantyne, D., and C. Crouse, 1997. *Reliability and Restoration of Water Supply Systems for Fire Suppression and Drinking Following Earthquakes*, prepared for National Institute of Standards and Technology, NIST GCR 97-730

Benjamin J.R. and C.A. Cornell, 1970. *Probability, Statistics, and Decision for Civil Engineers*. Dover Books on Engineering. 704 pp.

Boore, D.M., J.P. Stewart, E. Seyhan, and G.M. Atkinson, 2014. NGA-West2 equations for predicting PGA, PGV, and 5% damped PSA for shallow crustal earthquakes. *Earthquake Spectra* 30 (3), 1057-1085.

Byers, W.G., 2008. *The ShakeOut Scenario Supplemental Study: Railway Network*. SPA Risk LLC, Denver CO

(CalWARN) California Water/Wastewater Agency Response Network, 2009. *Mutual Aid/Assistance Operational Plan*. https://goo.gl/kyT8qE

(CalWARN) California Water/Wastewater Agency Response Network, No date. *CalWARN Mutual Assistance Activated in Response to Napa Earthquake*. http://goo.gl/ldZ4jl

Bay City News, 2015. EBMUD Reports 9 Broken Water Pipes Following Quake. August 18, 2015. http://abc7news.com/news/ebmud-reports-9-broken-water-pipes-following-quake/943303/ [accessed 27 Dec 2015]

Chen W.F. and C.R. Scawthorn, 2003. *Earthquake Engineering Handbook*, CRC Press, New York, NY

Contra Costa Local Agency Formation Commission, 2008. Section 9.0, East Bay Municipal Utility District Water And Wastewater Service, In *West Contra Costa County Water and Wastewater MSR Adopted 8/13/08*, Martinez, CA. http://www.contracostalafco.org/municipal_service_reviews.htm [accessed 26 Oct 2015]

East Bay Municipal Utility District, 2014. Napa's neighbors to the rescue. *Customer Pipeline.* Nov-Dec 2014, p. 1, https://www.ebmud.com/files/1314/3197/7857/customer-pipeline_0.pdf [accessed 17 Oct 2015]

Eidinger, J., 2001. *Seismic Fragility Formulations for Water Systems*. American Lifelines Alliance, G&E Engineering Systems Inc., www.americanlifelinesalliance.com/pdf/Part_1_Guideline.pdf, 96 pp.

Field, E.H., Biasi, G.P., Bird, P., Dawson, T.E., Felzer, K.R., Jackson, D.D., Johnson, K.M., Jordan, T.H., Madden, C., Michael, A.J., Milner, K.R., Page, M.T., Parsons, T., Powers, P.M., Shaw, B.E., Thatcher, W.R., Weldon, R.J., II, and Zeng, Y., 2013. *Uniform California earthquake rupture forecast, version 3 (UCERF3)—The time-independent model*: U.S. Geological Survey Open-File Report 2013–1165, 97 p., California Geological Survey Special Report 228, and Southern California Earthquake Center Publication 1792, http://pubs.usgs.gov/of/2013/1165/.

Goodson, A., ND. Quantifying and Managing Mutual Aid. East Bay Municipal Utility District, Oakland CA, 38 pp, http://www.orwarn.org/files/Qualifying%20and%20Managing%20Mutual%20Aid.pdf [accessed 20 Oct 2015]

Heubach, W.F., 1995. Seismic damage estimation for buried pipeline systems. Proc., 4th U.S. Conference on Lifeline Earthquake Engineering, 312-319.

Honegger D.G. and Eguchi R.T., 1992. *Determination of Relative Vulnerabilities to Seismic Damage for San Diego County Water Authority (SDCWA) Water Transmission Pipelines*, October 1992.

Howard, R.A., 1990. From influence to relevance to knowledge. In R.M. Oliver and J.Q. Smith, eds., *Influence Diagrams, Belief Nets and Decision Analysis*, New York: John Wiley & Sons, pp. 3-23

Hudnut, K.W., Brocher, T.M., Prentice, C.S., Boatwright, J., Brooks, B.A., Aagaard, B.T., Blair, J.L., Fletcher, J.B., Erdem, J.E., Wicks, C.W., Murray, J.R., Pollitz, F.F., Langbein, J., Svarc, J., Schwartz, D.P., Ponti, D.J., Hecker, S., DeLong, S., Rosa, C., Jones, B., Lamb, R., Rosinski, A., McCrink, T.P., Dawson, T.E., Seitz, G., Rubin, R.S., Glennie, C., Hauser, D., Ericksen, T., Mardock, D., Hoirup, D.F., and Bray, J.D., 2014. *Key Recovery Factors for the August 24, 2014, South Napa Earthquake: U.S. Geological Survey Open-File Report 2014–1249*, 51 p., http://dx.doi.org/10.3133/ofr20141249.

Hwang, H., Lin, H., and Shinozuka, M. (1998). "Seismic Performance Assessment of Water Delivery Systems." J. Infrastruct. Syst., 4(3), 118–125.

Isoyama, R., and Katayama, T. (1982). *Reliability Evaluation of Water Supply Systems During Earthquakes*. Report of the Institute of Industrial Science, the University of Tokyo, 30 (1), 1-64

Javanbarg, M., and C. Scawthorn, 2012. UILLIS: Urban Infrastructure and Lifelines Interactions of Systems. *Proc, 15th World Conference on Earthquake Engineering, September 2012*, Lisbon Portugal

Jayaram, N., and J. Baker, 2009. Correlation model for spatially distributed ground-motion intensities. *Earthquake Engineering and Structural Dynamics* 38:1687-1708.

Jeon, S.S. and T.D. O'Rourke, 2005. Northridge earthquake effects on pipelines and residential buildings. *Bulletin of the Seismological Society of America*, 95 (1), 294-318

Jones, M.C., 2009. Kumaraswamy's distribution: a beta-type distribution with some tractability advantages. *Statistical Methodology,* 6: 70-81

Kennedy, R.P., Chow, A.W., and Williamson, R.A., 1977. Fault movement effects on buried oil pipeline, *J. Transport. Eng. Div.*, 103 (TE5), 617–633.

Khater, M., and M. Grigoriu, 1989. Graphical demonstration of serviceability analysis. *Structural Safety and Reliability*. ASCE, pp 525-532t

Kuramaswamy, P., 1980. A generalized probability density function for double-bounded random processes. *Journal of Hydrology*, 46: 79-88

LADWP, 2014. Westwood / Sunset Trunk Line Repair Update. Press release Sunday August 3, 2014. http://www.ladwpnews.com/go/doc/1475/2218222/

Lilliefors, H., 1967. On the Kolmogorov-Smirnov Test for Normality with Mean and Variance Unknown, *Journal of the American Statistical Association*, 62 (318). (June 1967), 399-402

Lund, L. and A. Schiff, 1991. *TCLEE Pipeline Failure Database*, Technical Council on Lifeline Earthquake Engineering, American Society of Civil Engineers, Reston, VA, 36 pp.

Lund, L. and C. Davis, 2005. Multihazard mitigation Los Angeles water system: A historical perspective. In C. Taylor and E. VanMarcke, eds., *Infrastructure Risk Management Processes: Natural, Accidental, and Deliberate Hazards*, American Society of Civil Engineers, Reston VA, 224-279.

Lund, L., C.A. Davis, and M.L. Adams, 2005. Water system seismic performance 1994 Northridge-1995 Kobe earthquakes. *Proc., Fourth Japan-US Workshop on Seismic Measures for Water Supply, AWWARF/FWWA, Kobe, Japan*, 19-30

Markov I., M. Grigoriu, and T. O'Rourke 1994. *An Evaluation of Seismic Serviceability of Water Supply Networks with Application to San Francisco Auxiliary Water Supply System.* NCEER Report No. 94-0001, National Center for Earthquake Engineering Research, Buffalo NY, 154 pp.

Mid-America Earthquake Center, 2006. *MAEviz Software.* Urbana, IL: MAE Center, University of Illinois at Urbana-Champaign.

(NIBS and FEMA) National Institute of Building Sciences and Federal Emergency Management Agency, 2012. *Multi-hazard Loss Estimation Methodology Earthquake Model Hazus®-MH 2.1 Technical Manual*. Federal Emergency Management Agency, Washington, DC, 718 pp.

Nojima, N., and H. Kameda, 1991. Cross-impact analysis for lifeline interaction. *Proceedings of the 3rd U.S. Conference on Lifeline Earthquake Engineering*, *August 22-23, 1991, Los Angeles, California*. American Society of Civil Engineering Technical Council on Lifeline Earthquake Engineering, pp. 629-638

Ogata, Y., 1998. Space-time point-process models for earthquake occurrences. *Annals of the Institute of Statistical Mathematics*, 50 (2): 379-402.

O'Rourke, M.J., 2003. Chapter 23, Buried pipelines. In Chen W.F. and C.R. Scawthorn, *Earthquake Engineering Handbook*, CRC Press, New York, NY

O'Rourke M.J., and Ayala G., 1993. Pipeline damage due to wave propagation. *Journal of Geotechnical Engineering*, ASCE 119 (9): 1490-1498

O'Rourke, T.D., and M.C. Palmer, 1996. Earthquake performance of gas transmission pipelines. *Earthquake Spectra*, 12 (3), 493-527

O'Rourke, T.D., S.S. Jeon, S. Toprak, M. Cubrinovski, M. Hughes, S. van Ballegooy, and D, Bouziou, 2014. Earthquake response of underground pipeline networks in Christchurch, NZ. *Earthquake Spectra* 30 (1) 183–204

O'Rourke, T.D. and Trautmann, C.H., 1980. *Analytical Modeling of Buried Pipeline Response to Permanent Earthquake Displacements, Report No. 80-4*, School of Civil Engineering and Environmental Engineering, Cornell University, Ithaca, NY.

Porter, K.A. C. Scawthorn, D.G. Honegger, T.D. O'Rourke, and F. Blackburn, 1992. Performance of water supply pipelines in liquefied soil. Proceedings of the 4th US-Japan Workshop on Earthquake Disaster Prevention for Lifeline Systems, Los Angeles, CA, USA, 08/19-21/91; pp. 3-17. 1992. http://www.sparisk.com/pubs/Porter-1992-water-pipe-liquefied-soil.pdf [accessed 3 Jul 2015]

Prashar, Y., R. McMullin, B. Cain, and X. Irias, 2012. Pilot Large Diameter Pipeline Seismic Fragility Assessment. *Pipelines Conference 2012, Miami Beach, Florida, August 19-22, 2012*, 396-407.

Rose, A., D. Wei, and A. Wein 2011. Economic impacts of the ShakeOut earthquake scenario, *Earthquake Spectra* 27, 521-538

San Francisco Bay Area Rapid Transit District, 2015. *Remembering Loma Prieta.* http://www.bart.gov/marketing/25-years-after-Loma-Prieta-quake [accessed 27 Dec 2015]

San Francisco Lifelines Council, 2014. *Lifelines Interdependency Study 1 Report.* San Francisco Office of the City Administrator, San Francisco, 56 pp.

Scawthorn, C., 1993. Lifeline interaction and post-earthquake functionality. *Proceedings of the 5th US-Japan Workshop on Earthquake Disaster Prevention for Lifeline Systems, Tsukuba Science City, Japan,* October 26-27, 1992, 441-450.

Scawthorn, C.R., 2008. *The ShakeOut Scenario Supplemental Study: Fire Following Earthquake*. SPA Risk LLC, Denver CO, http://books.google.com/books?id=mDGrFAw5zqYC&lpg=PA1&dq=shakeout%20fire%20follo wing&pg=PA1#v=onepage&q&f=false [viewed 26 Oct 2010]

Scawthorn, C., K. Porter, M. Khater, D. Seidel, D. Ballantyne, H.T. Taylor, R.D. Darragh, and C. Ng, 1992. Utility performance aspects, liquefaction study, Marina and Sullivan Marsh areas, San Francisco California. *National Center for Earthquake Engineering Research, Proceedings from the 4th Japan-U.S. Workshop on Earthquake Resistant Design of Lifeline Facilities and*

Countermeasures for Soil Liquefaction: Tokai University Pacific Center, Honolulu, Hawaii, May 27-29, 1992. Vol. 1., 1992, 317-333. http://www.sparisk.com/pubs/Scawthorn-1992-SF-Liquefaction-Study.pdf

Schiff, A., 1988. The Whittier Narrows, California earthquake of October 1, 1987—response of lifelines and their effect on emergency response. *Earthquake Spectra* 4 (2): 339-366

Seligson, H.A., R.T. Eguchi, L. Lund, and C.E. Taylor, 1991. *Survey of 15 Utility Agencies Serving the Areas Affected by the 1971 San Fernando and 1987 Whittier Narrows Earthquakes*. report prepared for the National Science Foundation. Dames & Moore, Los Angeles CA

Terentieff, S., A. Chen, R. McMullin, Y. Prashar, and X.J. Irias, 2015. Emergency planning and response damage prediction modeling to mitigate interdependency impacts on water service restoration. *Proc. 9th Water System Seismic Conference, Sendai, Japan October 14-16, 2015*.

Tierney, K.J., 1995. Impacts of recent U.S. disasters on businesses: the 1993 Midwest floods and the 1994 Northridge earthquake. *Proc. National Center for Earthquake Engineering Research Conference on the Economic Impacts of Catastrophic Earthquakes--Anticipating the Unexpected, New York NY, September 12 and 13, 1995*. 52 pp.

Treiman, J., and D. Ponti, 2011. Estimating surface faulting impacts from the ShakeOut scenario earthquake. *Earthquake Spectra*, 27 (2) 315–330

Winnipeg City, 2014. Water Main Breaks Frequent Asked Questions (FAQs). http://www.winnipeg.ca/waterandwaste/water/mainbreaks.stm [last accessed 6 Oct 2015]